Characterization of Parathyroid Hormone Receptor 1 in Periodontal Ligament Cells

Dissertation

zur

Erlangung des Doktorgrades (Dr. rer. nat.)

der

Mathematisch-Naturwissenschaftlichen Fakultät

der

Rheinischen Friedrich-Wilhelms-Universität Bonn

vorgelegt von

Nuersailike Abuduwali

aus

Xinjiang, China

Bonn 2012

Angefertigt mit Genehmigung der Mathematisch-Naturwissenschaftlichen Fakultät der Rheinischen Friedrich-Wilhelms-Universität Bonn

1. Referent: Prof. Dr. Andreas Jäger

2. Referent: Prof. Dr. Klaus Mohr

Tag der mündlichen Prüfung: 13.06.2012

Erscheinungsjahr: 2012

Danksagung

Mein besonderer Dank gilt Herrn Prof. Dr. Andreas Jäger und PD Dr. Stefan Lossdörfer für die Überlassung des Themas und die Betreuung und Förderung der Arbeit.
Außerdem danke ich Herrn Prof. Dr. Klaus Mohr für die Begutachtung sowie Unterstützung meiner Arbeit.
Mein besonderer Dank geht an Herrn Dr. Jochen Winter, Herrn Dr. Dominik Kraus und PD Dr. Rainer Probstmeier für die vielen hilfreichen Diskussionen und praktischen Ratschlägen während meiner Promotion.
Dann danke ich Herrn PD Dr. Stefan Guhlke und Prof. Dr. Stephan Baader für die Unterstützung bei den Bindungsassays und der Immunofluoreszenzmikroskopie.
Ich bedanke mich auch herzlich bei der Flow Cytometry Core Facility Group für die methodische Unterstützung.
Auch möchte ich mich bei meinen Laborkollegen und allen, die mir bei der Erstellung meiner Arbeit geholfen haben, ganz herzlich bedanken.

Verfassererklärung

Hiermit erkläre ich, dass ich die vorliegende Arbeit in allen Teilen selbständig verfasst und keine anderen als die angegebenen Quellen und Hilfsmittel benutzt habe.
Die Stellen der Doktorarbeit, die anderen Quellen im Wortlaut oder dem Sinn nach entnommen wurden, sind durch Angaben der Herkunft kenntlich gemacht. Dies gilt auch für Zeichnungen, Skizzen, bildliche Darstellungen sowie für Quellen aus dem Internet.

Bonn, 2012

Nuersailike Abuduwali

To my parents

Table of Contents

SUMMARY

In addition to the classic catabolic effects, it is now widely accepted that parathyroid hormone (PTH) exerts anabolic effects on bone, when administered intermittently. As a result of the regenerative characteristic, Teriparatide (Forsteo® Europe, Forteo® U.S.A., Eli Lilly) which is a recombinant PTH (1-34), was recently approved for treatment of osteoporosis in the USA and the Europe. The dual actions of PTH are mediated primarily through PTH receptor 1 (PTH1R), which is a class II G protein-coupled receptor. PTH1R can activate diverse signaling pathways, including cAMP/PKA and PLC/PKC pathways (Vilardaga et al., 2011).

Periodontitis is an inflammatory disease, which manifests clinically as loss of supporting periodontal tissues. Accumulating evidences *in vivo* and *vitro* indicate that the intermittent PTH administration exerts anabolic effects on periodontal ligament (PDL) tissue and alveolar bone (Nohutcu et al., 1995; Ouyang et al., 2000; Barros et al., 2003; Lossdörfer et al., 2005, 2006b). Understanding the physiology of PTH1R is crucial to promote the regenerative effect of PTH. PTH1R has been exclusively studied in kidney and bone cells. However, the knowledge on PTH1R characteristics and physiology in PDL cells is still in its infancy.

In this study, we characterized the PTH1R in PDL cells, in terms of its cellular localization, binding affinity, density, signal transduction and gene regulation, and compared these characteristics with those of PTH1R in human osteosarcoma cell line (MG63) and Human Embryonic Kidney 293 cells (HEK293). In the second part, we transplanted human PDL cells into immunodeficient nude mice *and evaluated in vivo* the regenerative capacity of PDL cells upon intermittent hPTH (1-34) administration.

PTH1R mRNA and protein were detected in PDL, MG63 and HEK293 cells. Like other GPCRs, PTH1R was found on the plasma membrane and in the cytoplasm of the three cell lines, while they were to some extent also present in the nuclei of PDL and MG63 cells. Binding characteristics of PTH1R were cell type specific in the examined three cell lines, with PDL cells demonstrating a low binding affinity (K_d=1030±10 nM) and a relative high number of receptors (3.03±0.57 million receptors/cell). Dexamethason and 1,25-dihydroxyvitamin D_3 increased the expression level of PTH1 mRNA in PDL cells (12-fold and 14-fold of the corresponding control group, respectively), whereas the effect of hPTH (1-34) on

receptor mRNA expression was depended on the mode of its administration. The response of cAMP in MG63 and HEK293 cells was additive with growing concentration of hPTH (1-34), while it was concentration dependent in PDL cells. However, in all three cell lines, we observed a cross-talk between the cAMP/PKA and PLC/PKC signaling pathways, which were regulated oppositely at a given concentration of hPTH (1-34). The results of the *in vivo* experiments proved that the implanted human PDL cells not only survived, but also were able to develop a bone/cementum like tissue which closely resembles natural bone or cementum and this capacity was significantly enhanced by intermittent PTH administration.

ZUSAMMENFASSUNG

Neben dem klassischen katabolen Effekt von Parathormon (PTH), wurde aktuell auch eine anabole Wirkung von intermittierend appliziertem PTH auf den Knochen erkannt. Aufgrund seiner regenerativen Wirkung wurde Teriparatide (Forsteo® Europa, Forteo® U.S.A., Eli Lilly) ein rekombinantes PTH (1-34), in den USA und Europa zur Therapie von Osteoporose zugelassen. Die dualen Wirkungen von PTH werden primär über den PTH Rezeptor 1 (PTH1R) vermittelt, der der Klasse II der G-Protein gekoppelten Rezeptoren angehört. Durch Ligand-induzierte Aktivierung des PTH1R werden verschiedene intrazelluläre Signalwege, wie z.B der cAMP/PKA - und der PLC/PKC-Signalweg, reguliert (Vilardaga et al., 2011).

Parodontitis ist eine entzündliche Erkrankung, die zur irreversiblen Zerstörung des Zahnhalteappartes führt. Ergebnisse von Untersuchungen *in vitro* und *in vivo* deuten darauf hin, dass intermittierendes PTH eine anabole Wirkung auf das Parodontalligament (PDL) Gewebe und den Alveolarknochen hat (Nohutcu et al., 1995; Ouyang et al., 2000; Barros et al., 2003; Lossdörfer et al., 2005, 2006b). Die Aufklärung der Physiologie dieses Rezeptors ist äußerst wichtig für die Optimierung der regenerativen Wirkung von PTH. PTH1R wurde exklusiv in den Zellen der Nieren und des Knochens untersucht. Allerdings stecken unsere Kenntnisse über die Physiologie des PTH1R in PDL Zellen noch in den Kinderschuhen.

In der vorliegenden Arbeit wurde der PTH1R in PDL-, MG63- und HEK293-Zellen bezüglich seiner zellulären Lokalisation, Bindungsaffinität, Rezeptordichte, Signalvermittelung und Genregulation charakterisiert, beziehungsweise wurden diese Charakteristika mit denen des PTH1Rs in MG63- und HEK293-Zellen verglichen. Der zweite Teil der Arbeit beschäftigte sich mit der Untersuchung der regenerativen Kapazität von transplantierten humanen PDL Zellen durch intermittierend angewandtes hPTH (1-34).

PTH1R-mRNA und-Protein konnten in PDL-, MG63- und HEK293-Zellen nachgewiesen werden. Wie andere GPCR, zeigte PTH1R in allen untersuchten Zelllinien eine Zellmembran-ständige und cytoplasmatische Lokalisierung, während die Präsenz des Rezeptors zum Teil auch in den Zellkernen der PDL- und MG63-Zellen gezeigt werden konnte. Die Bindungeigenschaften von PTH1R scheinen zelltypspezifisch zu sein, wobei in PDL-Zellen eine geringere Affinität bei hoher Anzahl des Rezeptors festgestellt wurde (K_d=1030±10 nM, 3.03±0.57 Millionen

Rezeptoren/Zelle). Eine Stimulation der Zellen mit Dexamethason oder 1,25-Dihydroxyvitamin D_3 steigerte die mRNA Expression von PTH1R (12 - und 14 - fach jeweils im Vergleich zu der Kontrollgruppe), während der Effekt des hPTH (1-34) von der Art der Administration abhängig war. Die cAMP-Akkumulation in MG63- und HEK293-Zellen stieg mit aufsteigender Konzentration des hPTH (1-34), während sie in PDL-Zellen von der Konzentration des Hormons abhängig war. Interessanterweise wurde eine “cross-talk’’-Interaktion zwischen den cAMP/PKA- und PLC/PKC-Signalwege festgestellt, wobei die beiden Signalwege durch die jeweilige PTH-Konzentration gegenläufig reguliert wurden. Die Ergebnisse der Tierversuche belegten, dass die transplantierten humanen PDL-Zellen nicht nur überlebten, sondern auch ein Knochen/Zementum ähnliches Gewebe bilden konnten, und dass diese Differenzierung durch intermittierend zugeführtes hPTH (1-34) gesteigert werden konnte.

1 INTRODUCTION

1.1 Periodontitis

Periodontitis, also known as periodontal disease, is a bacterially induced chronic inflammation of the periodontium. The periodontal diseases range from the relatively benign form of gingivitis to aggressive periodontitis, depending on the severeness of the infection and the response of the host. Gingivitis, the most common form of periodontal disease, is characterized by inflammation, swelling, and bleeding of the gums and results most often from bacterial plaque. It is non-destructive and reversible with professional treatments. However, if not treated adequately, gingivitis can advance to periodontitis, which is a destructive form of the periodontal disease. In severe form, it triggers the degradation of periodontal connective tissue and alveolar bone, resulting in the most common cause of tooth loss in the world.

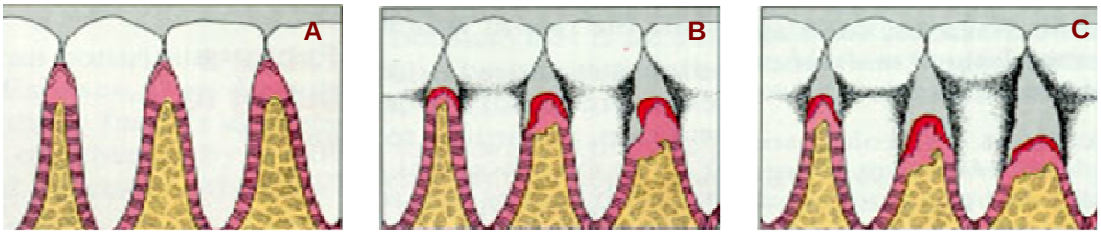

Figure 1.1 Schematic illustrations of Periodontitis (Taken from: Periodontitis Types: Periapical and Apical, Chronic and Aggressive Periodontitis, http://periodontitis.dentalbuzz.org). **A:** Healthy periodontium **B:** Moderate periodontitis. **C:** Severe periodontitis.

Periodontitis is a very common disease worldwide and associated with diverse physiological disorders such as cardiovascular disease (Kebschull et al., 2010), dyslipidemia (King, 2008), Type 2 diabetes (Seymour et al., 2007), low birth weight (Offenbacher et al., 1996) in otherwise healthy individuals and metabolic syndrome in hemodialysis patients (Chen et al., 2011).

Besides bacterial plaque, genetic as well as environmental factors have been proven to cause periodontal disease, especially tobacco use (Pihlstrom et al., 2005). Additionally, several physiological disorders, such as dermatological, haematological, granulomatous, immunosuppressive, and neoplastic diseases can exert an effect on periodontitis (Pihlstrom et al., 2005).

1.2 Periodontal ligament

The periodontium is a topographically complex organ that surrounds and supports the teeth. The structures comprising the periodontium include two soft tissues: gingiva, periodontal ligament and two hard tissues: cementum and alveolar bone. While each of the periodontal components has a specialized tissue architecture and characteristic biochemical composition, they interact dynamically and influence the cellular activities of each other (Bartold, 2006).

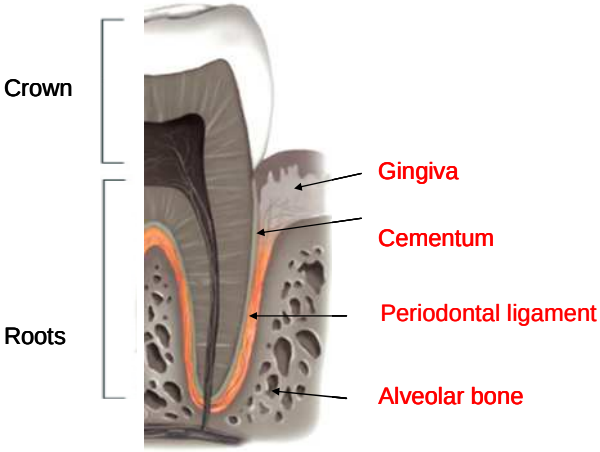

Figure 1.2 Components of the periodontium (Modified after: Periodontal Ligament - Studio Dentaire, http://www.studiodentaire.com). The four structural components of the periodotium, two soft connective tissues: gingival and periodontal ligament and two hard tissues cementum and alveolar bone are indicated in red. They interact with each other and together support and maintain the physiological activity of teeth.

The periodontal ligament, abbreviated as the PDL, is a highly specialized soft connective tissue embedded between the cementum covering the tooth root and alveolar bone. Thus, forming a link between the tooth and the bone, the ligament supports not only teeth, but also contributes to tooth nutrition, homeostasis, and repair of damaged tissue (Bartold et al., 2000). It ranges in width from 0.15 to 0.38 mm, reaching the thinnest portion around the middle third of the root (Nanci and Bosshardt, 2006). Upon aging, the thickness of this ligament decreases progressively.

This tissue is characterized by rapid turnover and high remodeling rates, which are essential for maintaining the width and integrity of the PDL as the teeth assume new positions in the jaws in response to changing forces such as mastication, speech and

orthodontic tooth movement (Beertsen, 1975; Berkovitz and Shore, 1995). Both turnover and remodeling are precisely regulated by the complex interplay between breakdown and synthesis of extracellular matrix components, specifically the collagenous meshwork (Beertsen et al., 1997). The collagen degradation is thought to be a result of collagen phagocytosis by fibroblasts without the involvement of collagenases (Beertsen et al., 1997). Moreover, the PDL is considered to be involved in repair, remodeling, and regeneration of the adjacent tissues, cementum and alveolar bone (Boyko et al., 1981; Nyman et al., 1982).

Similar to all soft fibrous connective tissues, the PDL consists of a fibrous matrix embedded in a gel of ground substance containing cells, blood vessels and nerves (Berkovitz, 1990). Its fibrous elements consist of mostly bundles of collagen fibers, which are distributed throughout the space of the periodontal ligament to join the tooth to the alveolar bone. The predominant collagens of the PDL are type I and III (Berkovitz, 1990; Takayama et al., 1997), which traverse the ligament space and insert into the cementum and bone surface as Sharpey's fibers. Additionally, the presence of collagen type V (Becker et al., 1991), type VI (Becker et al., 1991), XII (Dublet et al., 1988) and Oxytalan (Fullmer, 1958) in the PDL have been also reported. Aside from these fibrous elements, several matrix proteins are found in the periodontal ligament, including proteoglycans (Häkkinen et al., 1993) and glycoproteins such as undulin, tenascin, and fibronectin (Zhang et al., 1993). The ground substance of the PDL is structure-less and has been estimated to be 70% water. It is thought to have a pivotal role on the tooth's ability to withstand mechanical stress loads (Nanci and Bosshardt, 2006).

The PDL consists of a heterogeneous cell population that includes fibroblasts, cementoblasts, osteoblasts, endothelial progenitor cells, epithelial cell rests of Malassez, macrophages, osteoclasts and progenitor/stem cells (Ten Cate, 1998). While fibroblasts, macrophages, undifferentiated progenitor/stem cells, neural elements, and endothelial cells are found throughout the PDL, osteoblasts and osteoclasts reside on the alveolar bone side. Epithelial rests of Malassez cells and cementoblasts are localized close to the root surface of the tooth (Marchesan et al., 2011) whereas progenitor/stem cells are observed adjacent to blood vessels in the PDL (Gould et al., 1977).

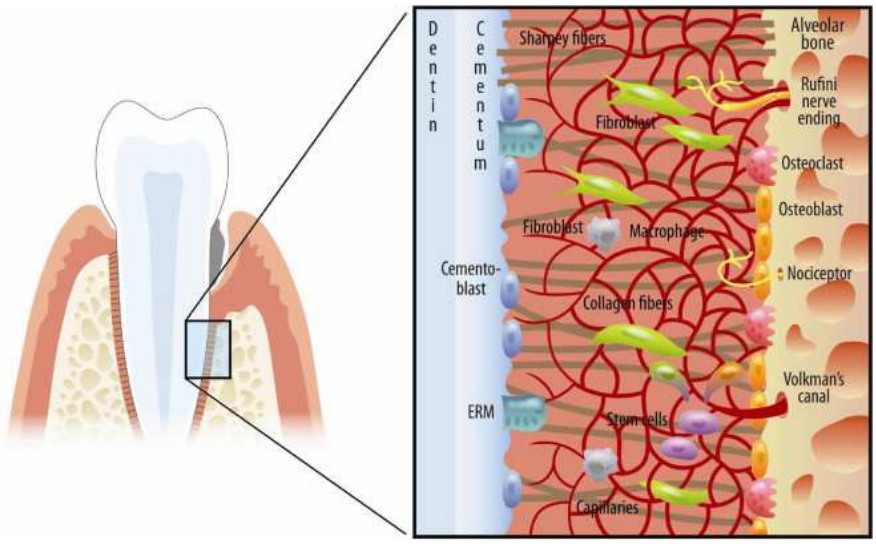

Figure 1.3 Overview of the structure and components of the periodontal ligament tissue (PDL) (Taken from: Marchesan et al., 2011)**.** The structure and heterogeneous cell population of periodontal ligament, along with its vascular and extracellular matrix elements are illustrated. The different cells are depicted in different colors: osteoblasts (orange), osteoclasts (pink), fibroblasts (green), stem cells (purple), cementoblasts (blue), epithelial cells rest of Malassez (ERM) (aqua), macrophages (grey). Blood vessels emerge from the alveolar bone, along with nerve fibres.

1.3 PDL fibroblasts

PDL fibroblasts, referred to as PDL cells, are the predominant cell type (Beertsen et al., 1997) and are thought to be mainly responsible for PDL homeostasis and regeneration (Lekic and McCulloch, 1996). The fibroblasts of the ligament are thought to originate in part from the ectomesenchyme of the investing layer of the dental papilla (Ten Cate et al., 1971), which may impart these cells specialized characteristics. The rapid turnover rate and remodelling of collagen in the PDL is considered to be the result of the phagocytosis by the periodontal fibroblasts. Moreover, they may provide a reservoir for mineral-forming cementoblasts or bone-forming osteoblasts (McCulloch et al., 2000).

Apart from theses unique properties, PDL fibroblasts exhibit osteoblastic properties such as alkaline phosphatase activity (Yamashita et al., 1987), production of bone sialoprotein in response to 1,25-dihydroxyvitamin D_3 (Nojima et al., 1990) and responsiveness to parathyroid hormone (Nojima et al., 1990). Furthermore, they have been shown to express not only proteins with osteoblastic properties such as

the runt-related transcription factor-2 (RUNX-2), osterix (Kato et al., 2004), osteocalcin (OSC) (Li et al., 2001), osteopontin (OPN) (Lekic et al., 2001; Li et al., 2001), periostin (Horiuchi et al., 1999), osteonectin (OSN) and type I collagen (Col I) (Lukinmaa and Waltimo, 1992), but also receptor activator of NF-kappa B ligand (RANKL) and osteoprotegerin (OPG), which play a pivotal role in the regulation of bone metabolism (Wada et al., 2001). PDL cells from rat were able to form mineralized nodules *in vitro*, although the mineralized nodules appeared to be different from those produced by osteoblasts (Cho et al., 1992). Other reports have shown the presence of type XII collagen (Col XII) (Karimbux et al., 1992), alpha-smooth muscle actin (a-SMA) (Arora and McCulloch, 1994) and scleraxis (Seo et al., 2004) in PDL fibroblasts.

In addition to their fibroblastic and osteoblastic properties, PDL cells demonstrate also functional characteristics of leucocytes and leucocyte-derived cells (e.g. macrophages) involved in classical innate immunity (Jönsson et al., 2011). It has been shown that ligament fibroblast cells up-regulated transcript and protein levels of several cytokines and chemokines upon stimulation with inflammatory promoters such as bacterial lipopolysaccharides (Jönsson et al., 2011).

These findings suggest that PDL fibroblasts contain a variety of subpopulations with different functional characteristics, although morphologically they look alike. However, whether these subsets are derived from a single type of progenitor cell is still unknown. Phenotypically stable but functionally different fibroblast subpopulations have been reported also in skin and other tissues (Hassell, 1993).

PDL fibroblasts are large cells with a spindle-shaped, elongated appearance in vitro, which is characteristic of fibroblast-like cells (Somerman et al., 1988). However, *in vivo*, they show an irregular disc-shape with a mean diameter of about 30 µm (Shore and Berkovitz, 1979). These cells have a prominent nucleus with approximately 25 % of the cell by volume (Berkovitz, 1990), and an extensive cytoplasm containing an abundance of organelles such as rough endoplasmic reticulum (5-10 % of the volume of the cytoplasm), mitochondria, golgi complex and vesicles. They possess a well-developed cytoskeleton and show frequent adherens and gap junctions (Nanci and Bosshardt, 2006). In the ligament, the fibroblasts are oriented parallel to the collagen fiber bundles and extend cytoplasmic processes that wrap around them (Beertsen et al., 1997).

1.4 Periodontal regeneration

Traditional treatment modalities of periodontitis include nonsurgical debridement of root surfaces or root canals, as well as resective surgery that provide better access to reshape the surrounding bone or root apex (Bashutski and Wang, 2009). Although these therapies have been established as effective treatment regimens in periodontal disease, the destruction of the attachment apparatus or bone is often the outcome and healing is always by repair (Bashutski and Wang, 2009). Since repair does not fully restore the function or structure of the destroyed tissue, new approaches such as regenerative therapies that aim to restore lost tissue through the regeneration of cementum, PDL, and alveolar bone have been introduced. These methods include bone replacement grafts, guided tissue regeneration and growth factors / cytokines / host modulating agents.

In bone replacement grafts, a ‘‘filler’’ bone graft material is introduced into the periodontal defect in the hope of inducing bone regeneration (Bartold et al., 2000). In guided tissue regeneration, occlusive barrier membranes are employed to inhibit the rapid downgrowth of epithelial cells and gingiva fibroblasts from a periodontal wound, which allows other regenerative cells (osteoblasts, PDL cells, cementoblasts) to repopulate the area and promote periodontal regeneration (Bashutski and Wang, 2009). Platelet-rich plasma (PRP) and growth factors such as bone morphogenic proteins (BMPs), platelet-derived growth factor (PDGF), and enamel matrix proteins (EMD) are the most commonly used agents to promote the healing and regeneration potential of periodontal destructed tissue (Heijl et al., 1997; Giannobile and Somerman, 2003; Jung et al., 2003; Nevins et al., 2005). Other therapeutics including collagen fragments bound to bone grafts, parathyroid hormone (Liu et al., 2009), and transforming growth factor beta 3 (Teare et al., 2008) have also been shown to promote the regenerative potential on the damaged tissue. Additionally, the application of cell-based, protein-based and genetic engineering approaches in periodontal tissue regeneration are currently under investigation (Rios et al., 2011).

1.5 Parathyroid hormone in PDL regeneration

Progressive periodontitis often results in alveolar bone resorption, and ultimately leads to the loss of teeth. Accordingly, the arrest of bone resorption and regeneration of alveolar bone are of significant importance.

Parathyroid hormone (PTH), an endogenous hormone, is involved in bone remodelling by exerting its catabolic effects (bone resorption) and anabolic effects (bone formation), depending on its administration mode (Neer et al., 2001). The prevailing view of catabolic effects of PTH suggests that PTH enhances production of receptor activator of nuclear factor- κB ligand, macrophage colony-stimulating factor and possibly other cytokines (i.e., IL-1, IL-6, and TNF-α) and downregulates the production of osteoprotegerin (Murray et al., 2005).

The anabolic activity of PTH on osteoblasts has been studied intensively both *in vivo* and *vitro*. Preclinical studies and small clinical trials have proven distinct anabolic effects of intermittent PTH administration on bone (Rubin et al., 2002; Turner, 2002). In another study, both full length PTH (1–84) and teriparatide (PTH 1–34) administration resulted in a rapid up-regulation of markers of bone formation, but a down-regulation of markers of resorption (Hodsman et al., 2003, 1993). Daily injections of PTH (1–84) or PTH (1–34) increase bone mass and reduce the incidence of fracture in postmenopausal women, in elderly men, and in women with glucocorticoid-induced osteoporosis (Jilka, 2007). The anabolic effect of intermittent PTH has also been extensively demonstrated in mice and rats (Hodsman et al., 2002). These findings finally resulted in an approval of the PTH therapy for osteoporosis by the US Food & Drug Administration (FDA) for FORTEO® (PTH).

Although the exact underlying mechanism accounting for the anabolic effect of intermittent PTH remains to be elucidated, emerging evidence indicates that the increase in bone formation is largely due to an increase in the number of osteoblasts, which is mediated by repeated delays of osteoblast apoptosis (Jilka et al., 1999), enhancing the recruitment of preosteoblasts from marrow stromal cells and stimulating the maturation of lining cells (Jilka, 2007).

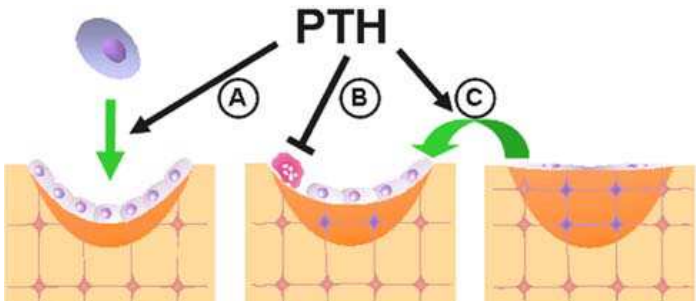

Figure 1.4 Proposed cellular mechanisms accounting for the anabolic effect of intermittent PTH (Taken from: Jilka, 2007). Intermittent PTH has been proposed to increase osteoblast number by: (A) increasing the development of osteoblasts, (B) inhibiting osteoblast apoptosis, and (C) reactivating lining cells to resume their matrix synthesizing function.

The anti-apoptotic signaling pathways triggered by intermittent PTH involve cAMP-mediated activation of protein kinase A (PKA), subsequent phosphorylation and inactivation of the pro-apoptotic protein Bad, and increased transcription of survival genes like Bcl-2 (Bellido et al., 2003). On the other hand, intermittent PTH has been shown to decrease the expression of histone H4, a marker of the cell cycle (Onyia et al., 1995), and expression of the cell cycle inhibitors $p27^{KIP1}$ and $p21^{Cip1}$ (Qin et al., 2005), in metaphyseal bone of young rats, a site rich in replicating osteoblast progenitors. This fact together with the results of other *in vivo* and *in vitro* studies strongly suggests that intermittent exposure to PTH causes an exit of osteoblast progenitors from the cell cycle, which leads to the differentiation and suppression of proliferation of these cells (Jilka, 2007).

Based on the anabolic properties of PTH established in osteoblasts and the fact that the PDL cells show osteoblastic characteristics, there have been numerous studies conducted both *in vivo* and *vitro* to elucidated the effect of PTH on PDL cells. The results of these studies have indicated that periodontal ligament cells respond to PTH in a osteoblastic manner, both *in vitro* (Nohutcu et al., 1995; Ouyang et al., 2000; Lossdörfer et al., 2005, 2006b) as well as in *in vivo* models (Barros et al., 2003). The involvement of PTH in the regulation of periodontal activities is further supported by the fact that PTH and parathyroid gland extract enhance tooth eruption and orthodontic tooth movement (Schneider et al., 1972; Davidovitch et al., 1972). Moreover, PTH receptors were immunohistochemically detected in rat cementoblasts (Tenorio and Hughes, 1996). Recently, Bashutski et al. reported markedly improved clinical and radiographic outcomes in patients with severe, chronic periodontal

disease who underwent periodontal surgery and received daily injections of teriparatide (Bashutski et al., 2010). Taken together, these lines of evidence suggest that PTH, currently approved for use in osteoporosis therapy, might also contribute to treatment of periodontal disease. In addition, bisphosphonates, another category of drugs, approved for the treatment of osteoporosis, have been evaluated for their therapeutic benefit in periodontal diseases, with promising results (El-Shinnawi and El-Tantawy, 2003).

1.6 Parathyroid hormone

Parathyroid hormone (PTH) is a single-chain polypeptide of 84 amino acids, which is synthesized in and secreted by the parathyroid glands (Habener et al., 1978). PTH is formed as a 115-amino acid polypeptide precursor (pre-pro-PTH) which then undergoes two successive proteolytic cleavages (Habener et al., 1976). First, in the rough endoplasmic reticulum, the NH_2-terminal peptide of 25 amino acids is cleaved from pre-pro-PTH and yields pro-parathyroid hormone (pro-PTH), an intermediate precursor of 90 amino acids, which is subsequently transported to the golgi apparatus, where the NH_2-terminal hexapeptide of pro-PTH is removed, resulting in the formation of active PTH (84 amino acids) (Habener et al., 1978).

The primary amino acid sequence of PTH is highly conserved among mammalian species (Figure 1.4). While the strongest homology resides in the N terminus of the molecule (32 of the first 38 residues), the greatest evolutionary variation is evident in the middle region of the hormone (between residues 39 and 52). In the C-terminal region, from 53 to 84, several stretches of high homology can be found. A number of residues are conserved also in the chicken and zebrafish sequences. Furthermore, sequence from 65 to 78 varies at only three positions among mammals (Murray et al., 2005).

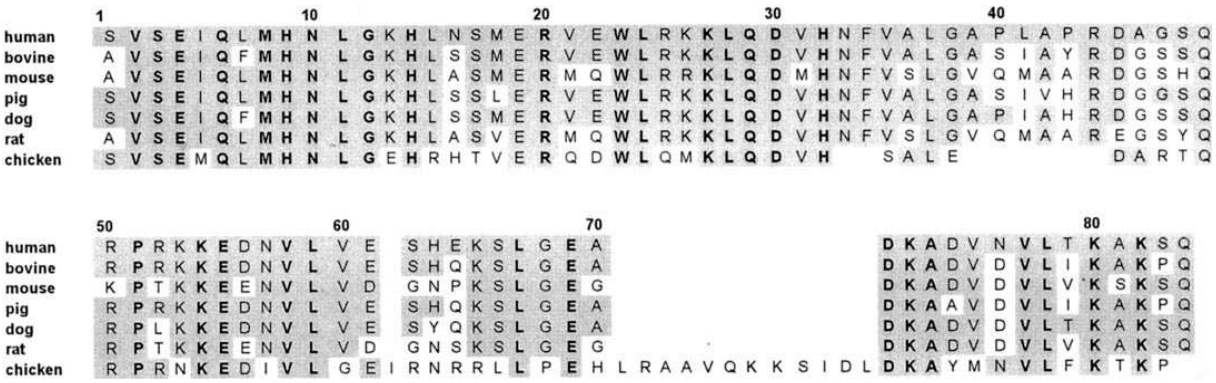

Figure 1.5 Amino acid sequences of intact PTH from several mammalian species (Taken from: Murray et al., 2005). Amino acids are denoted by the single-letter abbreviation for each of the indicated species. Shading indicates residues in hPTH that are conserved in other species, and those residues conserved in all species shown are indicated in bold.

In addition to intact PTH (1–84), parathyroids also secrete relatively high concentrations of heterogenous C-terminal fragments, which are thought to be inactive in classical terms (Murray et al., 2005). While another source of the C-terminal fragments is the proteolysis of intact PTH by Kupffer cells in liver, there is no direct evidence that N-terminal fragments are produced *in vivo* by metabolic cleavage or gland secretion under normal physiological conditions (Murray et al., 2005). Both the liver and kidney take part in the clearance of the circulating intact PTH and C-terminal fragments (Murray et al., 2005).

PTH regulates serum calcium concentration via acting directly on bone to increase calcium resorption and on kidney to increase calcium reabsorption in renal tubules (Potts et al., 1995). Additionally, PTH inhibits reabsorption of phosphate in kidney, stimulating its excretion (Pullman et al., 1960; Beutner and Munson, 1960). PTH has been also shown to act indirectly on intestine to promote absorption of calcium, which is mediated by 1,25-dihydroxyvitamin D_3 (Lawson et al., 1971). Apart from actions on calcium and bone metabolism, PTH has been also reported to have proliferative effects on blood and liver cells (Rixon et al., 1958; Whitfield et al., 1969; Rixon and Whitfield, 1972).

The secretion and synthesis of PTH is regulated by a number of factors such as calcium, phosphate and 1,25-dihydroxyvitamin D_3 level. A particular characteristic of the parathyroid gland is its sensitivity to small changes in serum calcium, which leads to large changes in PTH secretion, with a sigmoidal type response (Silver et al., 1999). Serum calcium is the chief regulatory signal for PTH secretion, and a

decrease in extracellular calcium enhances not only the PTH secretion but also increases PTH gene expression level and parathyroid cell proliferation (Silver et al., 1998). The parathyroid recognizes the changes in serum calcium via a G-protein receptor coupled on the cell membrane of parathyroid cells, the calcium sensing receptor (CaSR) (Brown et al., 1993). Conversely, CaSR activation by increased extracellular calcium induces the release of intracellular calcium, which in turn inhibits secretion of PTH (1–84) (Friedman and Goodman, 2006). Inhibition of PTH (1–84) secretion is accompanied by enhanced proteolysis of the NH_2 terminus of PTH, with the attendant secretion of PTH (7–84) and other NH_2-terminal truncated PTH peptide fragments (Friedman and Goodman, 2006).

A high serum phosphorus concentration has been shown to be associated with an increase in PTH secretion (Silver and Levi, 2005). The effect of phosphate is considered to be posttranscriptional and independent of 1,25-dihydroxyvitamin D_3 and calcium (Kilav et al., 1995). 1,25-dihydroxyvitamin D_3 dramatically decreased the levels of PTH mRNA in the parathyroids of normal rats at physiologically relevant doses without changing the levels of serum calcium (Shvil et al., 1990). Unlike phosphate, the effect of 1,25-dihydroxyvitamin D_3 on the PTH gene was shown to be transcriptional (Silver et al., 1986).

Studies on the structure and function of PTH have revealed that most of the biological activity of intact PTH (1–84) resides in the 1-34 N-terminal fragment of the hormone. It was found that a synthetic bovine (b)PTH(1–34) was able to generate the major biological actions of the full-length native bPTH (1-84), including activation of adenylyl cyclase in bone and kidney cells, increased urinary excretion of cAMP and phosphate in rats, and elevation of blood calcium in rats, dogs, and chickens (Murray et al., 2005). Moreover, Teriparatide has a similar binding affinity for PTH receptor 1 as PTH (1–84) (Brixen et al., 2004). Teriparatide (ForsteoA or ForteoA, Eli Lilly), a recombinant human PTH (1–34) (hPTH [1–34]), was first approved in the United States in November 2002 for the treatment of osteoporosis in men and women and became available in other countries, such as the United Kingdom and several other countries in the European Union, in April 2003 (Quattrocchi and Kourlas, 2004).

These facts, together with the practical difficulties in synthesizing large quantities of chemically pure PTH (1–84), led to the widespread use of recombinant PTH (1–34) as a surrogate for intact PTH in studies of hormone effect *in vitro* and *in vivo*.

While synthetic PTH (1–31), (1–34) and (1–38), seem to have the same anabolic effect on bone as PTH (1–84) (Brixen et al., 2004), PTH peptides lacking one or more amino acid residues such as PTH (2–34), N-terminal truncated peptides such as PTH(3–34) and PTH(7–34) bind with affinities considerably lower than that of PTH(1–34) (Friedman and Goodman, 2006; Murray et al., 2005). On the other hand, PTH (3–38), did not demonstrate an anabolic effect (Armamento-Villareal et al., 1997). Based on these observations, it appears that the first two amino acids are essential for biological activity, and the bone promoting properties are fully maintained in the 1–31 N-terminal domain of PTH. PTH (1–14) was shown to be the shortest native N-terminal PTH peptide for which some cAMP agonist activity could be detected (EC50 ~200 μM) (Luck et al., 1999). Studies on the structure and activity of the PTH (1–14) scaffold have shown that the first 9 amino acids are essential for receptor activation, and also that amino acid substitutions at several positions [Ala3,12,Gln10,Arg11,Trp14] in PTH(1–14) led to improved potency in stimulating cAMP accumulation, which was 250 times that of native PTH(1–14). By the same substitutions, the otherwise inactive PTH (1–11) could also be activated (Shimizu et al., 2000b). The modified PTH (1–14) has led to define the minimum N-terminal PTH agonist pharmacophore, which resides within the first 9 amino acids of the hormone, whereby the amino acids were covalently bound to the juxtamembranedomain using a tetraglycine linker (Shimizu et al., 2000a).

Although carboxyl fragments such as PTH (44–68), PTH (53–84), and PTH (39–84) did not compete for binding with PTH (1–34) radioligands, nor did they activate adenylyl cyclase in renal membranes or bone cells (Murray et al., 2005), both *in vitro* and *in vivo* studies indicate that the C-terminal part of PTH may have significant biological effects in bone (Hodsman et al., 2005). It has been reported that C-terminal PTH fragments may enhance osteocyte apoptosis (Divieti et al., 2001), and C-terminal fragments containing at least the last 30 or more amino acids of PTH increase production of alkaline phosphatase and other markers of osteoblast activity (Sutherland et al., 1994).

1.7 Parathyroid hormone related peptide

PTHrP was discovered in association with humoral hypercalcemia of malignancy syndrome and certain types of cancer in affected patients. The hypercalcemia, caused by the uncontrolled secretion of PTHrP, is a result of promoted Ca^{2+} resorption from bone and suppression of urinary Ca^{2+} loss (Guerreiro et al., 2007). PTHrP is widely expressed in a large variety of normal adult and fetal tissues, including cartilage, heart, kidney, hair follicles, placenta, breast, lungs, and many epithelial tissues (Schipani and Provot, 2003). This peptide has a pivotal role in regulating embryonic development of the skeleton and other tissues via intracellular, paracrine, and endocrine pathways (Gardella and Jüppner, 2001). Human PTHrP protein is encoded by a single gene, and generated by alternative splicing of the primary transcript as one of three variants of 139, 141 or 173 amino acids (Mannstadt et al., 1999). Both PTH and PTHrP bind to parathyroid hormone/parathyroid hormone related peptide receptor (PTH1R) (see section 1.6), and exert anabolic effects on bone (Stewart, 1996).

PTH and PTHrP share significant sequence homology within the first 13 amino acid residues, which underlines the functional importance of the N-terminal residues in receptor signaling. However, the sequence homology decreases siginficantly in the 14–34 region, showing no recognizable similarity beyond residue 34 (Mannstadt et al., 1999). For both PTH and PTHrP, the 15–34 region functions as the principal PTH1R binding domain

1.8 G-protein coupled receptors

GPCRs comprise the largest family of membrane proteins in the human genome, mediate most cellular responses to hormones and neurotransmitters, and are responsible for vision, olfaction and taste. Based on the similarity of their sequence and structure, GPCRs in vertebrates are commonly divided into five families: rhodopsin (family A), secretin (family B), glutamate (family C), adhesion and Frizzled/Taste2 (Fredriksson et al., 2003). These receptors are characterized by a common structural signature of seven hydrophobic transmembrane (TM) segments, with an intracellular carboxyl terminus and an extracellular amino terminus.

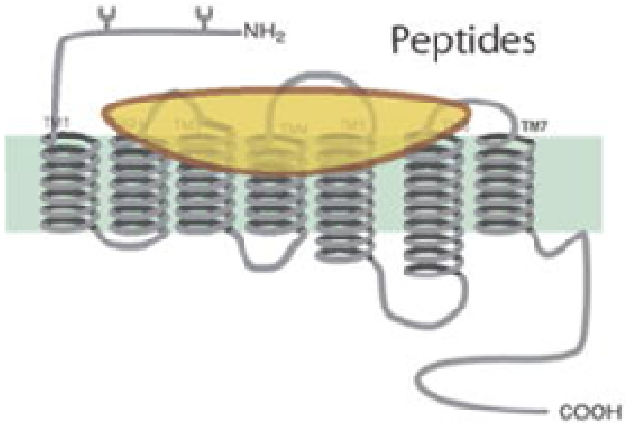

Figure 1.6 Seven transmembrane helix structure of GPCRs (Taken from: Kobilka, 2007). GPCRs contain an intracellular carboxyl terminus, an extracellular amino terminus and seven transmembrane helix segments. Cell membrane (green); Ligand peptide (yellow);

The G proteins comprise α, β and γ subunits. The α subunit is responsible for GTP and GDP binding for GTP hydrolysis, whereas the β and γ subunits are associated in a tightly linked βγ complex. GPCRs activate intracellular heterotrimeric G-proteins by stimulating the exchange of bound GDP in the α-subunit for GTP. Binding of GTP induces the dissociation of the α subunit from the βγ dimer, both being able to regulate the activity of target enzymes or channels responsible for the cellular response. There are at least 18 different human Gα proteins to which GPCRs can be coupled (Hermans, 2003; Wong, 2003). These Gα proteins form heterotrimeric complexes with Gβ subunits, of which there are at least 5 types, and Gγ subunits, of which there are at least 11 types (Hermans, 2003). Depending on the type of G protein to which the receptor is coupled, a variety of downstream signaling pathways can be activated. Consequently, the Gα- and Gβγ-subunits stimulate effector molecules, which include adenylyl and guanylyl cyclases (AC and GC), phosphodiesterases, phospholipase A2 (PLA2), phospholipase C (PLC) and phosphoinositide 3-kinases (PI3Ks), thereby activating or inhibiting the production of a variety of second messengers such as 3'-5'-cyclic adenosine monophosphate (cAMP), cyclic guanosine monophosphate (cGMP), diacylglycerol (DAG), inositol (1,4,5)-trisphosphate (IP3), phosphatidyl inositol (3,4,5)-trisphosphate, arachidonic acid and phosphatidic acid, in addition to promoting increases in the intracellular concentration of Ca^{2+} and the opening or closing of a variety of ion channels

(Marinissen and Gutkind, 2001). Furthermore, GPCRs may also activate intracellular pathways independently of G-proteins, possibly by the regulation of effector molecules through novel molecular mechanisms (Marinissen and Gutkind, 2001).

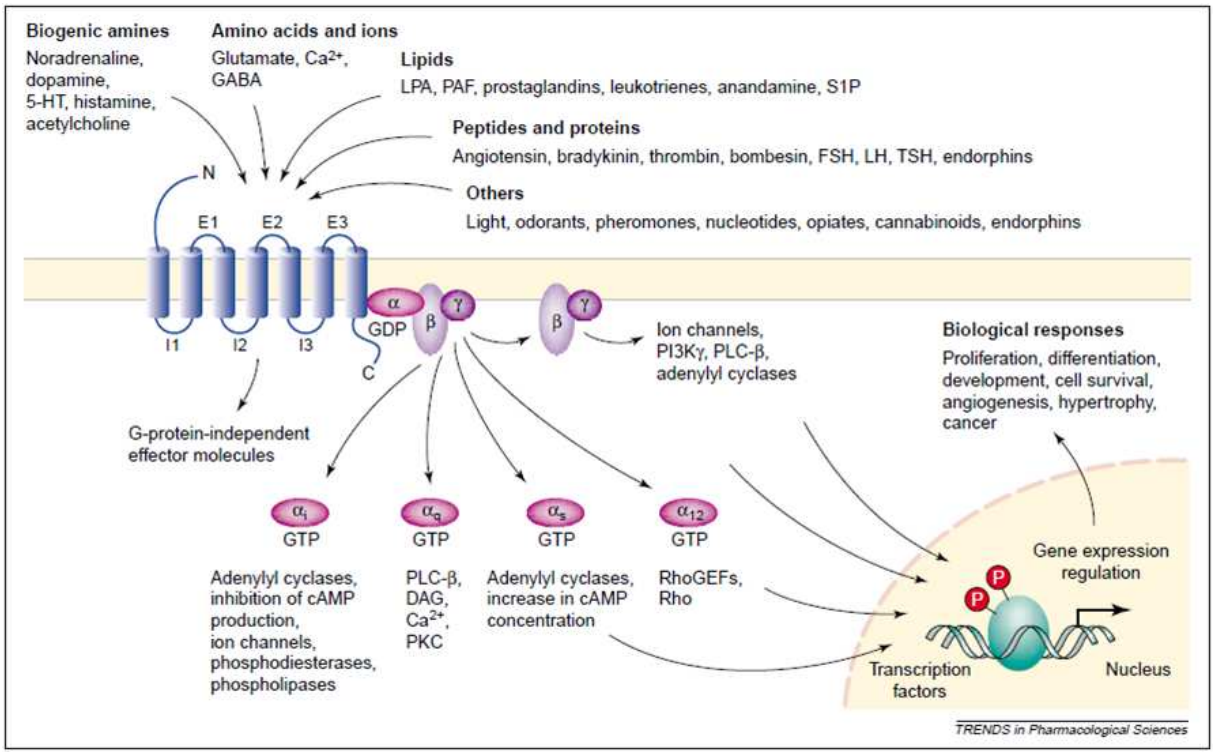

Figure 1.7 Diversity of GPCRs (Taken from: Marinissen and Gutkind, 2001). Various ligands, including biogenic amines, amino acids, ions, lipids, peptides and proteins, activate cytoplasmic and nuclear targets with or without heterotrimeric G-proteins, by binding GPCRs on cellular membrane. Such signaling pathways regulate key biological functions such as cell proliferation, cell survival and angiogenesis. Abbreviations: DAG, diacylglycerol; FSH, follicle-stimulating hormone; GEF, guanine nucleotide exchange factor; LH, leuteinizing hormone; LPA, lysophosphatidic acid; PAF, plateletactivating factor; PI3K, phosphoinositide 3-kinase; PKC, protein kinase C; PLC, phospholipase C; S1P, sphingosine-1-phosphate; TSH, thyroid-stimulating hormone.

The ligand efficacy is defined as the effect of a ligand on the structure and biophysical properties of a receptor. Based on their efficacy, natural and synthetic ligands are divided into four groups: full agonists – capable of maximal receptor stimulation; partial agonists – unable to elicit full activity even at saturating concentrations; neutral antagonists – with no effect on signaling activity; and inverse agonists – reduce the level of basal activity of the receptor.

The signal triggered by the exposure of GPCRs to agonists is attenuated by desensitization of the receptors, which is a combined consequence of several different mechanisms. These mechanisms include the uncoupling of the receptor

from heterotrimeric G proteins in response to receptor phosphorylation, the internalization of cell surface receptors to intracellular membranous compartments, the lysosomal and plasma membrane degradation of receptors, and the down-regulation of receptor mRNA and protein synthesis (Ferguson, 2001). The time course of these processes ranges from seconds (phosphorylation) to minutes (endocytosis) and even hours (down-regulation). The outcome of receptor desensitization varies from absolute termination of signaling to the attenuation of agonist potency and maximal responsiveness and is regulated by multiple factors, which include receptor structure and cellular environment (Ferguson, 2001).

1.9 PTH receptor 1

The pleiotropic actions of PTH are mediated primarily through the binding and activation of the PTH/PTH-related peptide (PTHrP) receptor (PTH1R), which is highly expressed in a variety of tissues, with highest expression in the kidney, bone, and cartilage (Langub et al., 2001). PTH binds also to a second receptor (PTH2R) with a distinct pharmacology (Gensure et al., 2005). Both PTH receptors are the class B G protein-coupled receptors (GPCRs), to which the receptors for secretin, calcitonin, glucagons and several other peptide hormones also belong. One prominent feature of these peptide hormone receptors, which can be distinguished from other classes of GPCRs, is their relatively large glycosylated N-terminal extracellular domain (~170 aa in PTH1R) containing six conserved cysteine residues, as well as by several other conserved amino acids that reside throughout the N-terminal domain, the membrane-embedded helixes, and the connecting loops (Gardella and Jüppner, 2001).

The complementary DNA (cDNA) encoding the PTH1R was first cloned in 1991 by COS-7 expression using an opossum kidney cell cDNA library (Juppner et al., 1991) Since then, PTHR1 has been cloned in a number of other species such as, rat (Abou-Samra et al., 1992), human (Schipani et al., 1993), mouse (McCuaig et al., 1994), pig (Smith et al., 1996), zebrafish (Rubin and Jüppner, 1999), as well as rabbit (Lu et al., 2001). Human PTH1R has 95% sequence homology with pig and dog, 90% with rat and mouse and 79% with opossum. The PTH1R gene consists of 2007 bp mRNA, which contains 14 exons and two transcript variants encoding the same protein with 593 amino acids (NCBI Reference Sequence: NM_001184744.1). In

addition to bone, kidney and cartilage, PTH1R expression was also found in heart and smooth muscle, skin, uterus, placenta, mammary gland, liver, ovary and testis (Ureña et al., 1993).

Like other members of class B GPCRs, PTH1R contains an extended N-terminal extracellular domain, a seven hydrophobic helical transmembrane domain (TMDs), and an intracellular cytoplasmic domain. The N-terminal domain is glycosylated at four asparagine residues clustered near the junction with the first TMD such as N151, N161, N166 and N176, at least one of which is required for the expression, ligand binding, and signal transduction of the PTH1R (Zhou et al., 2000). Additionally, the N-terminal domain contains three disulfide bonds involving six highly conserved cysteines, Cys48/Cys117, Cys108/Cys148, and Cys131/Cys170 (Grauschopf et al., 2000). The C-terminal domain contains several serine residues that undergo phosphorylation upon ligand binding (Hodsman et al., 2005).

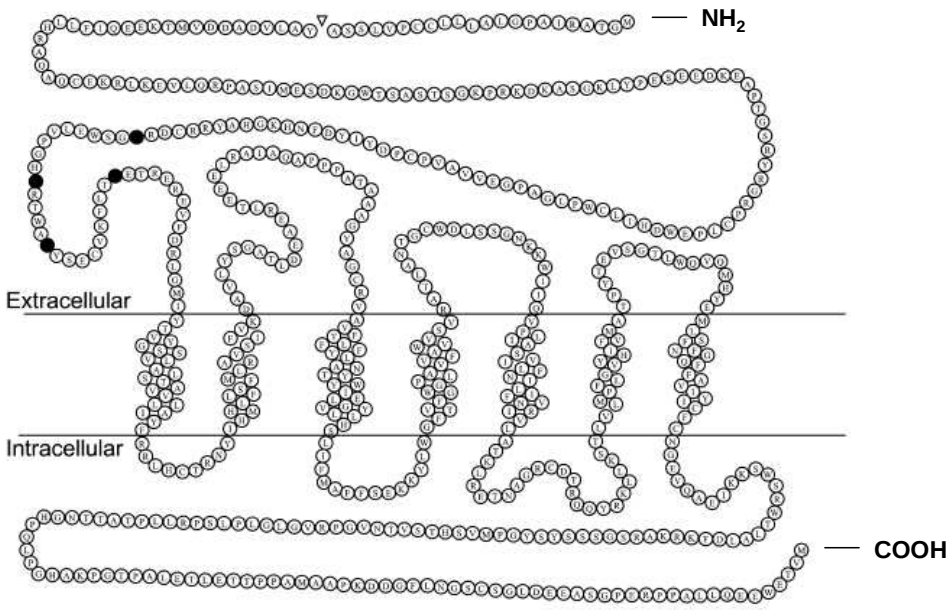

Figure 1.8 Schematic representation of the PTH1R (Taken from: Gensure et al., 2005)**.** The amino acid sequence of the PTH1R is represented in single-letter amino acid code in open circles, with the predicted locations of the transmembrane domains. Black circles represent amino acid positions for N-linked glycosylation, N151, N161, N166 and N176. The inverted triangle indicates the cleavage site for the 23-amino acid signal sequence.

The essential role of the PTH1R in endochondral bone development is underscored by the diseases such as Blomstrand's lethal chondrodysplasia, Jansen's

metaphyseal chondrodysplasia and enchondromatosis that are caused by mutations of this protein. Blomstrand's lethal chondrodysplasia is caused by inactivating mutations in the PTH1R and characterized by prenatal lethality, premature and abnormal bone mineralization and ossification, and shortened limbs. Defects in tooth and mammary gland development were also noted as a result of the disease. Jansen's metaphyseal chondrodysplasia is a rare autosomal dominant disorder characterized by short-limbed dwarfism secondary to severe abnormalities of the growth plate, and hypercalcemia. Three different heterozygous PTH1R mutations have been found to be responsible for the disease, which at cellular level lead to increases in basal cAMP. Enchondromas are common benign cartilage tumors of bone that can occur as solitary lesions or, in enchondromatosis, as multiple lesions. The heterozygous missense mutation identified in the PTH1R is responsible for the disorder (Schipani and Provot, 2003).

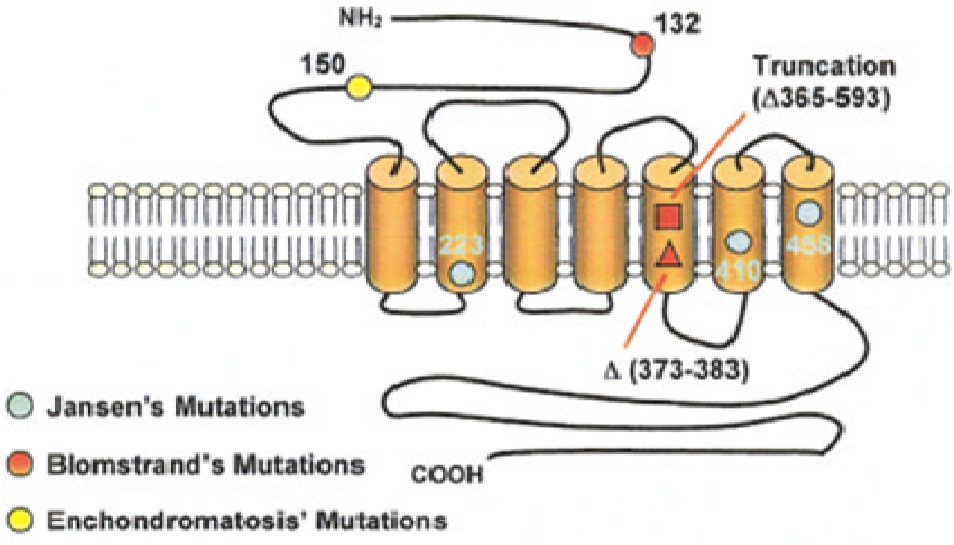

Figure 1.9 PTH1R related diseases (Taken from: Schipani and Provot, 2003). The PTH1R-mutations identified are represented in patients with Jansen's metaphyseal chondrodysplasia (in green), Blomstrand's lethal chondrodysplasia (in red), and enchondromatosis (in yellow).

1.10 PTH and PTH1R interactions

The general mechanism of PTH-PTH1R interaction has been deduced from an extensive series of studies including mutational analysis of both receptor and the ligand, use of ligand and/or receptors chimeras, as well photo-affinity cross-linking of ligands using photoreactive groups. These analyses suggested a simple “two-site model” of PTH-PTH1R interaction that involves two principal components: (1) an interaction between the C-terminal region of PTH (1–34) and the N-terminal domain of the receptor, which contributes predominantly to binding affinity; and (2) an interaction between the N-terminal domain of the ligand and the juxtamembrane region of the receptor comprised of the seven TMDs and their connecting intra- and extracellular loops, which contributes to receptor activation (Figure 1.8) (Gardella and Jüppner, 2001).

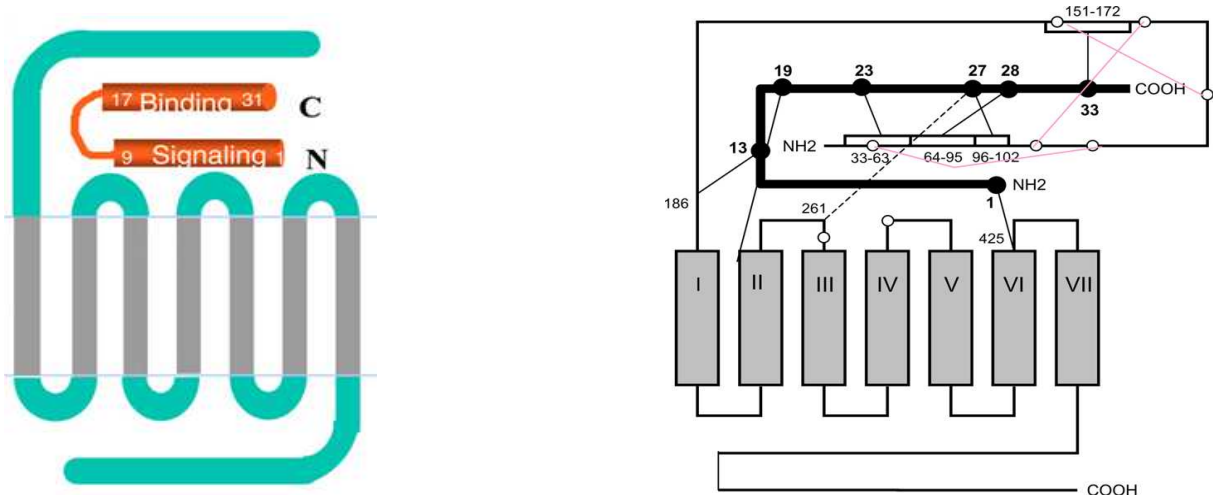

Figure 1.10 Representation of the “two-site model” and photoaffinity cross-linking of PTH to the PTH1R (Taken from: Gensure et al., 2005). **A:** The interaction between PTH (1–34) and PTH1R involves two principal mechanistic components: (1) an interaction between the C-terminal domain of PTH(1–34), represented by residues 17–31, and the N-terminal extracellular domain of the receptor; and (2) an interaction between the N-terminal domain of PTH, represented by residues 1–9, and the juxtamembrane region of the receptor. These two components of the interaction are postulated to contribute predominantly to binding affinity and receptor activation, respectively. **B:** A representation of the ligand-receptor through photoaffinity cross-linking is shown. The ligand is represented by the heavy filled bar. Segments and defined residues of contact in the receptor are indicated by open boxes and open circles, respectively.

1.11 PTH1R signaling

Like all members of the Family B receptors, the PTH1R is coupled to signal effector molecules by heterotrimeric G proteins. Studies of the signaling properties of clonal PTH1Rs expressed in heterologous cell lines, such as LLC-PK1, COS-7, or HEK 293 kidney cells or CHO cells, have revealed that this single receptor type is capable of activating multiple signaling pathways, including adenylyl cyclase (AC), phospholipase C (PLC), phospholipase D (PLD), protein kinase C (PKC), and mitogen-activated protein kinase (MAPK) as well as of increasing the concentration of cytoplasmic Ca^{2+} (Hodsman et al., 2005).

Following ligand binding, the PTH1R receptor can activate AC through the action of Gs (Gαs), and PLC through Gq (Gαq). Activated AC then stimulates the formation of 3,5-adenosine monophosphate (cAMP), which in turn binds to the regulatory subunit of the enzyme PKA that releases the active catalytic subunit of the enzyme. On the other hand, activated PLC cleaves phosphatidylinositol (4,5)-bisphosphate (PIP2) into diacylglycerol (DAG) and inositol (1,4,5)-trisphosphate (IP3). Subsequently, DAG activates PKC, and IP3 results in increased intracellular free Ca^{2+}, which then promotes PKC translocation to the plasma membrane, and then activation by DAG (Schipani and Provot, 2003).

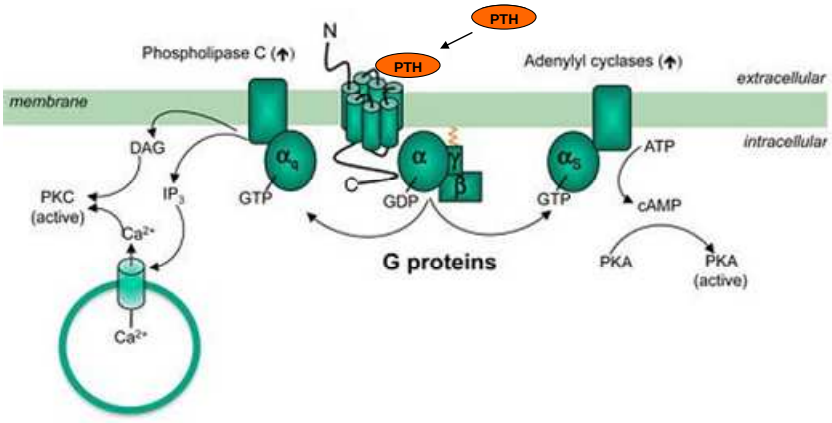

Figure 1.11 Gs (Gαs) and Gq (Gαq) transduction signaling pathways mediated by PTH1R (Taken from: Vilardaga et al., 2011). Up on ligand binding, PTH1R undergoes conformational changes, which induce its coupling with heterotrimeric G proteins (Gαβγ), and catalyzes the exchange of GDP for GTP on the a-subunit. This event triggers the dissociation the α unit from βγ dimer. G_s activates AC leading to cAMP synthesis, which in turn activates PKA. Gq activates PLC, which cleaves PIP2 into DAG and IP3. DAG then activates PKC and IP3 diffuses through the cytosol and activates IP3-gated Ca^{2+} channels in the membranes of the endoplasmic reticulum, causing the release of stored Ca^{2+} into the cytosol. The increase of cytosolic Ca^{2+} promotes PKC translocation to the plasma membrane, and then activation by DAG

The N-terminal truncated PTH peptides have been shown to activate PKC(s) in cells expressing endogenous or transfected recombinant PTH1Rs (Hodsman et al., 2005). On the other hand, studies of cells stably expressing the transfected PTH1R indicate that activation of PLC, which can lead to activation of PKC via generation of IP3 and DAG, requires the intact N terminus of the ligand (Takasu et al., 1999). These findings indicate that PTH1R can activate PKC(s) via a PLC-independent pathway, which is triggered by C-terminal ligand determinants, such as the residues 29–32 of PTH (Jouishomme et al., 1994). Indeed, PTH1R has been shown to activate PLD in the distal tubule cells of the kidney, whereas in proximal tubule cells it activated PLC (Friedman et al., 1999). Moreover, PTH (1–31) found unable to activate PKC in some systems, could nevertheless activate PKC in others (Hodsman et al., 2005). Thus, PTH1R might recognize different portions of the ligand as activation determinants for various phospholipases, depending on the cellular milieu (Whitfield et al., 2001).

Moreover, PTH1R can also couple to other subtypes of G proteins, including Gi/o, which can inhibit adenylyl cyclase (Mahon et al., 2006), and Ga12/13 which activates phospholipase D and RhoA in osteosarcoma cells challenged with PTH (Singh et al., 2005).

As with most GPCRs, the activation of PTH1R leads to the phosphorylation of its cytoplasmic tail by G protein-coupled receptor kinases (GRKs), which then facilitate the association with ß-arrestin proteins, resulting in internalization and desensitization of the receptor (Malecz et al., 1998; Tawfeek et al., 2002). Mapping of the phosphorylation acceptor sites of the opossum PTH1R receptor using mutagenesis approaches revealed that six serine residues at positions 483, 485, 486, 489, 495, and 498 are the sites for PTH-stimulated receptor phosphorylation, with the serine residue at position 489 being required for phosphorylation (Tawfeek et al., 2002). These residues correspond to S489, S491, S492, S495, S501, and S504 of the rat PTH1R (Tawfeek et al., 2002). Albeit the importance of the phosphorylation in PTH1R receptor internalization, it appears to be cell line and/or receptor species dependent, whether receptor internalization requires phosphorylation or not (Malecz et al., 1998; Tawfeek et al., 2002).

Arrestins are cytoplasmic proteins that bind to phosphorylated GPCRs and uncouple them from their cognate G proteins; thereby inactivate agonist-mediated G protein-signaling (Wang et al., 2009). ß-Arrestin1 and ß-arrestin2 are widely expressed and play a pivotal role in regulation of the functions of many GPCRs, including the

PTH1R (Malecz et al., 1998; Ferrari et al., 1999). The interaction of ß-arrestin1 or ß-arrestin2 with phosphorylated PTH1R is considered to be the likely mechanism of desensitization of the PTH1R-activated responses (Tawfeek et al., 2002). The ß-arrestins serve as an adaptor molecule that targets activated and phosphorylated receptors to clathrin-coated pits (Ferguson et al., 1996; Goodman et al., 1996).

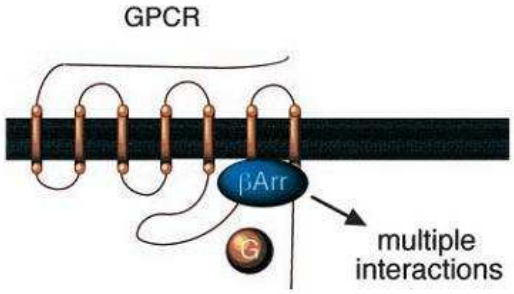

Figure 1.12 Schematic overview of ß-Arrestins associated with many GPCRs (Taken from: Hall and Lefkowitz, 2002). ß-Arrestins interact with GPCRs, uncoupling them from G-protein and also acting as scaffold proteins to facilitate multiple interactions between GPCRs and cytoplasmic proteins.

ß-Arrestin-PTH1R interactions lead to internalization (endocytosis) of the receptors which are either destined for degradation, resulting in receptor down-regulation (Tian et al., 1994; Ureña et al., 1994b; Massry and Smogorzewski, 1998), or recycled back to cell surface, leading to receptor resensitization (Chauvin et al., 2002).

In addition, ß-arrestin-associated GPCRs may also initiate activation of MAPK pathways, independent of classical G protein-mediated second messenger systems (Hall and Lefkowitz, 2002).

Na^+/H^+ exchange regulatory factor 1 (NHERF1), also known as ezrin-radixin-moesin-binding phosphoprotein-50 (EBP50), is a cytoplasmic scaffolding protein that recruits various cellular receptors, ion transporters, and other proteins to the plasma membrane of epithelia and other cells (Wang et al., 2009). NHERF1 contains 2 tandem N-terminal postsynaptic density 95/discs large/ zona occludens (PDZ) domains and a C-terminal merlin-ezrin-radixinmoesin (MERM) domain, through which it connects to actin bundles (Vilardaga et al., 2011). The PTHR harbors a C-terminal PDZ-like ligand domain that recognizes the PDZ1 domain of NHERF1 and the PDZ2 domain of NHERF2, leading to PTH1R binding to these domains (Songyang et al., 1997; Mahon et al., 2002; Mahon and Segre, 2004). NHERF1-null mice exhibited decreased phosphate reabsorption and elevated urinary phosphate excretion

because of reduced apical membrane tethering of the Npt2, the major hormone-regulated sodium-phosphate cotransporter in the renal proximal tubule. Although serum calcium level was unchanged, increased excretion secondary to complexation with phosphate was observed. Moreover, reduced bone mineralization was found (Shenolikar et al., 2002). On the other hand, humans with NHERF1 mutations present with renal stones or bone demineralization (Karim et al., 2008). These findings underscore the primary role of NHERF1 in associating with and modulating PTH1R activity.

NHERF1 promotes membrane retention of the PTH1R by inhibiting receptor endocytosis in several cell models both endogenously and exogenously expressing NHERF1, and for this effect both intact NHERF1 PDZ and MERM domains are essential (Wang et al., 2007). Moreover, the presence of NHERF1 suppresses PTH1R desensitization, and inhibiting NHERF1 restores receptor desensitization. This action appears to be due to preventing ß-arrestin2 from binding to the PTH1R, rather than altered receptor phosphorylation (Wang et al., 2009). Altogether, these actions may avert PTH resistance and downregulation of the PTH1R. In addition, NHERF2 can switch PTH1R signaling from AC to PLC by assembling a signaling complex that incorporates the PTHR, phospholipase C, and actin filaments (Mahon et al., 2002).

1.12 PTH2R

The PTH2R was first identified in 1995 through homology screening of a human brain cDNA library for other members of the class II GPCR family (Usdin et al., 1995). In humans, the PTH2 receptor is abundantly expressed in the brain, and found also in pancreas, testis, placenta, and lung. However, it was not detected on northern blots of human kidney mRNA or in bone-derived cell lines using RT-PCR (Hoare et al., 1999). In rats, PTH2 receptor expression was found in a number of discrete nuclei in the brain, vasculature, heart, scattered endocrine cells, as well as in pancreas. In the rat kidney, it is expressed by an extremely small number of cells, which are near the vascular pole of glomeruli (Usdin et al., 1996). Besides rat and human, zebrafish has also been reported to possess PTH2R, in addition to its PTH1R and a novel PTH3R with high homology to the PTH1R (Gensure et al., 2004).

The PTH2R shows 70% amino acid sequence homology and 52% identity to PTH1R. The highest amino acid sequence homology resides within the transmembrane domain, while it is as low as 14% within the C-terminal domain (Bisello et al., 2004). Like the PTH1R, the PTH2R exhibits dual signaling in response to PTH (1–34), coupling strongly to stimulation of cAMP accumulation, and more weakly, in a cell-specific manner to increases in intracellular calcium concentration (Usdin et al., 2002). In rats, PTH was reported to weakly stimulate cAMP accumulation via the PTH2R receptor, while no considerable increase in intracellular calcium was detectable (Goold et al., 2001).

The PTH2 receptor is also activated by tuberoinfundibular peptide of 39 residues (TIP39), a secreted peptide that is highly expressed in testis and, at lower levels, in various central nervous system cells, liver, and kidney (John et al., 2002). Conversely, in spite of a binding with moderate affinity, TIP 39 does not activate PTH1R (Hoare et al., 2000).

TIP39 appears to be distantly related to PTH and PTHrP. In most assays, the first 34 residues exhibit full activity, eight of which are identical in PTH and PTHrP from all species, and 11 are identical in mammalian peptides (Usdin, 2000). Residues at a number of additional positions are similar in size, charge, or hydrophobicity. TIP39 contains three of the residues shared by all mammalian PTH and PTHrP species and another five residues that are present in most of these peptides. If similar residues are considered, the homology between TIP39 and PTH or PTHrP increases to almost 50% (Usdin et al., 2000).

Figure 1.13 Sequence alignment of bTIP39 with PTH and PTHrP (Taken from: Usdin, 2000). The currently known sequence of bTIP39 is aligned to the N-terminal residues of PTH and PTHrP from several species. Colored backgrounds are used to indicate residues that are identical in TIP39 and PTH or PTHrP, and colored letters are used to indicate residues with similar properties. Numbering refers to residues of mature PTH.

The activation of human PTH2R via TIP39 triggers both cAMP and intracellular Ca^{2+} signaling, but in a different manner other than via PTH (Bisello et al., 2004). While PTH stimulation of cAMP formation is brief and rapidly resensitizes, the response to TIP39 is sustained and remains partly desensitized for a prolonged period (Bisello et al., 2004).

1.13 Aim of the study

PTH1R has been exclusively studied in bone and kidney cells, however not yet in PDL cells. In order to elevate the actions of PTH on PDL tissue regeneration, it is crucial to understand the physiology of PTH1R in PDL cells. In light of this, we aimed to clarify the characteristics of PTH1R in PDL cells and compare its characteristics to those of MG63 and HEK293 cells.

The objectives of the present study were to:

1. Detect and quantify PTH1R mRNA in PDL, MG63 and HEK293 cells
2. Detect and localize PTH1R in PDL tissue *in vivo* as well as in cultured PDL cells
3. Screen for a PTH1R-positive subpopulation in PDL, MG63 and HEK293cells
4. Study the effect of dexamethason, 1,25-dihydroxyvitamin D_3 and hPTH(1-34) on the expression level of PTH1R mRNA
5. Reveal the signaling pathways involved in mediating the actions of hPTH (1-34) on PDL, MG63 and HEK293 cells
6. Study the effect of intermittent hPTH (1-34) on human periodontal ligament cells transplanted into immunodeficient nude mice

2 MATERIALS AND METHODS

2.1 Materials

2.1.1 Equipment

Equipment	Supplier
Autoclave Model Varioklav 25T	H+P Labortechnik GmbH
Axioskope 2 Microscope	Carl Zeiss AG
Centrifuge 5804 R	Eppendorf
Centrifuge 5415 R	Eppendorf
ChemiDoc™ XRS	Bio-Rad Laboratories GmbH
TCS SP2 Laser Scanning Spectral Confocal Microscope	Leica Microsystems
Dounce Homogenizer 1 ml Tissue Grinder	Wheaton
Flow Cytometer LSR II	BD Bioscience
Freezer (-20℃)	Liebherr Premium
Freezer (-80℃)	Revco
Fridge (4℃)	Liebherr Premium
Fluorescence Microscope Axio Imager A1	Carl Zeiss AG
FugeOne™ Microcentrifuge	Starlab Groupe
Haemocytometer Neubauer improved	Brand GmbH + CO KG
iCycler iQ™ Real-Time PCR Detection System	Bio-Rad Laboratories GmbH
Incubator (cell culture)	Thermo Electronic
Laboport Vacuum Pump	KNF Neuberger GmbH
Light Microscope Axiovert 25	Carl Zeiss AG
Magnetic Stirrers MR 3001	Heidolph Instruments GmbH & Co. KG
Microwave	Siemens
MS2 Minishaker	IKA®-Werke GmbH & Co
Multi-channel Pipettes	Eppendorf
Multipette® plus	Eppendorf
Nanodrop ND-1000	Peqlab Biotechnologie GmbH
Paraffin Oven	Memmert GmbH & Co. KG

pH-meter	Wissenschaftlich-Technische Werkstätten GmbH
Pipetboy	Eppendorf
Pipetman	Gilson
PowerPac Basic™ Power Supply	Bio-Rad Laboratories GmbH
PowerPac HC™ Power Supply	Bio-Rad Laboratories GmbH
PowerWave X UV-Vis Plate Reader	BioTek Instruments, Inc.
Precision Weigher A 120 S	Sartorius AG
Mini-PROTEAN Tetra Cell,	Bio-Rad Laboratories GmbH
PTC-200 DNA Engine	GMI
Rocker PMR-30	Grant-bio Cambridgeshire
Sonopuls HD 2070	Bandelin Electronic GmbH & Co. KG
Sterile Workbench HeraSafe	Heraeus-Christ
Sub-Cell® GT Agarose Gel Electrophoresis Systems	Bio-Rad Laboratories GmbH
Thermo Block	Biometra Biomedizinische Analytik GmbH
Trans-Blot SD Semi-Dry Transfer Cell	Bio-Rad Laboratories GmbH
Wallac WIZARD γ-counter	PerkinElmer
Water Bath	Memmert GmbH & Co. KG

2.1.2 Plastic and glassware

Item	**Supplier**
96-well Flat Bottom Transparent Microplate	Greiner Bio-One GmbH
Adhesive Plate Seals	ABgene
Blot Absorbent Filter Paper	Bio-Rad Laboratories GmbH
Cell Culture Dishes	Greiner Bio-One GmbH
Cell Culture Flasks (T-75/175 cm^2)	Greiner Bio-One GmbH
Cell Culture Multiwell Plates (24,12 and 6-well plates)	Greiner Bio-One GmbH
Cover Slips	Carl Roth GmbH + Co. KG
Combitips Plus (2.5 mL/10 ml)	Eppendorf
Cryogenic Vials	Nalge Nunc
Filtertips	Starlab
Gelfoam®	Sullivan-Schein

Luer Slip Syringes (2 mL/5 ml)	Sartorious Stedim Biotech
Microcentrifuge Tubes (1.5 mL, 2 ml)	Eppendorf
Microscope Cover Glasses (15 mm Ø)	Marienfeld GmbH & Co. KG
Microscope Slides (75x25x1.0 mm)	Thermo Scientific
Filter Papers (Folded Filters)	Roth
Parafilm	Pechiney
PCR Tubes (0.2 ml)	Bio-Rad Laboratories GmbH
Pipette Tips	Sarsted AG & Co.
Polypropylene Tubes (15 ml and 50 ml)	Greiner Bio-One GmbH
Polystyrene Round-Bottom Tubes (5 ml,12x75 mm)	BD Bioscience
Serological Pipettes (5 ml, 10 ml, 25 ml)	Corning Incorporated
Single-Use Filter Unit (0.2 µm)	Sartorius Stedim Biotech
Sterile Filters	Millipore
Test Tube Soda Glass	VWR

2.1.3 Chemicals

Chemical	**Specification**	**Supplier**
0.01% Poly L-Lysine		Sigma-Aldrich Chemie GmbH Munich, Germany
0,05 % (w/v) Trypsin -EDTA		Invitrogen GmbH Karlsruhe, Germany
Forene®	2 vol% isoflurane	Abbott GmbH & Co. KG Wiesbaden, Germany
30% H_2O_2	Hydrogen peroxide	Merck KGaA Darmstadt, Germany
30% Acrylamid/Bis Solution 37.5:1 (2.6% C)		Bio-Rad Laboratories GmbH Munich, Germany
Accutase		PAA Laboratories GmbH Pasching, Austria
Acetone		Merck KGaA Darmstadt, Germany

Agarose		Promega Madison, WI, USA
Albumin Standard		Pierce Rockford, USA
Alizarin Red S	3,4-Dihydroxy-9,10-dioxo-2-anthracenesulfonic acid sodium salt	Sigma-Aldrich Chemie GmbH Munich, Germany
Aprotinin		Sigma-Aldrich Chemie GmbH Munich, Germany
APS	Ammonium persulfate	Sigma-Aldrich Chemie GmbH Munich, Germany
β-glycerolphosphate	β-glycerolphosphate disodium salt	Fulka Chemie GmbH Buchs, Switzerland
β-Mercaptoethanol		Sigma-Aldrich Chemie GmbH Munich, Germany
Boric acid		Sigma-Aldrich Chemie GmbH Munich, Germany
Bromphenol Blue		Roth GMBH Karlsruhe, Germany
BSA	Bovine Serum Albumin	Roche Diagnostics GmbH Mannheim, Germany
Citric Acid Monohydrate		Sigma-Aldrich Chemie GmbH Munich, Germany
Cruz Marker™ Molecular Weight Standards		Santa Cruz Biotechnology CA, USA
DAB	Diaminobenzidine	Pierce Rockford, USA
DABCO	Triethylendiamin, 1,4-Diazabicyclo[2.2.2]octan	Roth GMBH Karlsruhe, Germany
DAPI	4',6-diamidino-2-phenylindole	Sigma-Aldrich Chemie GmbH Munich, Germany
DePeX		Serva Electrophoresis GmbH Heidelberg, Germany
Dexamethason		Sigma-Aldrich Chemie GmbH Munich, Germany

DMEM	Dulbecco's Modified Eagle Media DMEM (1X), liquid - with GlutaMAX™ I, Sodium Pyruvate	Invitrogen GmbH Karlsruhe, Germany
DMSO	Dimethyl sulfoxide	Sigma-Aldrich Chemie GmbH Munich, Germany
DTT	Dithiothreitol	Sigma-Aldrich Chemie GmbH Munich, Germany
EDTA	Ethylenediamine tetraacetic acid Na_2-salt	CalBiochem San Diego, CA, USA
EGTA	Ethyleneglycol-O, O'-bis(2-aminoethyl)-N, N, N', N'-tetraacetic Acid	Sigma-Aldrich Chemie GmbH Munich, Germany
Ethanol		Merck KGaA Darmstadt, Germany
Ethidium bromide	Ethidium Bromide (1% solution)	Sigma-Aldrich Chemie GmbH Munich, Germany
FBS	Fetal Bovine Serum	Invitrogen GmbH Karlsruhe, Germany
GeneRuler™ DNA Ladder, Low Range		MBI Fermentas GmbH St. Leon-Rot, Germany
Glycerol		Sigma-Aldrich Chemie GmbH Munich, Germany
H-8, Dihydrochloride (H8)	PKA inhibitor Chamical formula: $C_{12}H_{15}N_3O_2S \cdot 2HCl$	Calbiochem, Germany
HCl		Merck KGaA Darmstadt, Germany
HEPES Buffer	(4-(2-hydroxyethyl)-1-piperazineethanesulfonic acid)	PromoCell GmbH Heidelberg, Germany
Hoechst 33342 Dye		Sigma-Aldrich Chemie GmbH Munich, Germany
IBMX	3-isobutyl-1-methylxanthine	Sigma-Aldrich Chemie GmbH Munich, Germany
	(Octylphenoxy)polyethoxyethanol,	Sigma-Aldrich Chemie GmbH

IGEPAL® CA-630	Octylphenyl-polyethylene glycol	Munich, Germany
Isopropanol		Merck KGaA Darmstadt, Germany
iQ™ SYBR® GreenSupermix		Bio-Rad Laboratories GmbH Munich, Germany
Leupeptin		Sigma-Aldrich Chemie GmbH Munich, Germany
Light Green SF yellowish		Chroma-Gesellschaft Schmidt GMBH & CO. Münster, Germany
Mayer's haematoxylin		Merck Eurolab AG Dietikon, Switzerland
Methanol		Merck KGaA Darmstadt, Germany
Mowiol 4-88		Roth GMBH Karlsruhe, Germany
MOPS	3-(N-Morpholino)propanesulfonic Acid Sodium Salt	Sigma-Aldrich Chemie GmbH Munich, Germany
NaOH		Merck KGaA Darmstadt, Germany
Nitrocellulose-Membran		Bio-Rad Laboratories GmbH Munich, Germany
Non-Fat Dry Milk		Bio-Rad Laboratories GmbH Munich, Germany
Normal Goat Serum		Dako Glostrup, Denmark
PBS	Dulbecco's PBS (1x) without Ca & Mg (Phosphate buffered saline)	PAA Laboratories GmbH Pasching, Austria
PBS Tablets	Phosphate Buffered Saline Tablets	Sigma-Aldrich Chemie GmbH Munich, Germany
Penicillin / Streptomycin	Penicillin (10000 U/ml) / Streptomycin (10 mg/ml)	PAA Laboratories GmbH Pasching, Austria
Peroxidase Substrate Buffer		Thermo Scientific Rockford, USA
Plasmocin™	Plasmocin Prophylactic	CAYLA

		Toulouse, France
PFA	Paraformaldehyde	Merck KGaA Darmstadt, Germany
PMSF	Phenylmethanesulphonyl Fluoride	Sigma-Aldrich Chemie GmbH Munich, Germany
Ponceau S solution for electrophoresis (0.2 %)		Sevra Electrophoresis GmbH Heidelberg, Germany
Precision Plus Protein Kaleidoscope Standards		Bio-Rad Laboratories GmbH Munich, Germany
Protease Inhibitor Cocktail Tablets		Roche Diagnostics GmbH Mannheim, Germany
PVDF-membrane	Polyvinylidene fluoride membrane	Bio-Rad Laboratories GmbH Munich, Germany
Restore™ Western Blot Stripping Buffer		Bio-Rad Laboratories GmbH Munich, Germany
RIPA	Radioimmunoprecipitation assay Composition: 25 mM Tris-HCl pH 7.6, 150 mM NaCl, 1% NP-40, 1% sodium deoxycholate, 0.1% SDS	Sigma-Aldrich Chemie GmbH Munich, Germany
RO-32-0432	PKC inhibitor Chemical formula: $C_{28}H_{28}N_4O_2 \cdot HCl$	Calbiochem, Germany
Sodium Azide		Sigma-Aldrich Chemie GmbH Munich, Germany
Tri-Sodium Citrate Dihydrate		Merck KGaA Darmstadt, Germany
SDS	Sodium Dodecyl Sulfate	Sigma-Aldrich Chemie GmbH Munich, Germany
Sodium Vanadate		Sigma-Aldrich Chemie GmbH Munich, Germany
TBS	Tris Buffered Saline (x10) 20 mM Tris, 500mM NaCl, PH 7.4	Bio-Rad Laboratories GmbH Munich, Germany
TEMED	N,N,N',N'-Tetramethylethylendiamin	Bio-Rad Laboratories GmbH

		Munich, Germany
Tris	Tris-[hydroxymethyl]amino-methane	MP Biomedicals Illkirch Cedex, France
0.5M Tris-HCl (PH6.8)		Bio-Rad Laboratories GmbH Munich, Germany
1.5M Tris-HCl (PH8.8)		Bio-Rad Laboratories GmbH Munich, Germany
Triton X-100		Sigma-Aldrich Chemie GmbH Munich, Germany
Tween 20	Polyoxyethylene (20) Sorbitan Monolaurate	Sigma-Aldrich Chemie GmbH Munich, Germany
Vitamin C	Ascorbic acid	Sigma-Aldrich Chemie GmbH Munich, Germany
Vitamin D_3	1,25-Hydroxyvitamin D_3 Monohydrate	Sigma-Aldrich Chemie GmbH Munich, Germany
XEM-200	Xylol Substitute	Vogel GmbH Giessen, Germany

2.1.4 Kits

Kit	**Supplier**
cyclic AMP (Direct) Enzyme Immunometric Assay (EIA) Kit	Enzo Life Sciences GmbH Lörrach, Germany
Fix&Perm Kit	An Der Grub Bio Research GmbH Kaumberg, Austria
Immuno Pure Metal Enhanced DAB Substrate Kit	Pierce Rockford, USA
iScript ™ Select cDNA Synthese Kit	Bio-Rad Laboratories GmbH Munich, Germany
LIVE/DEAD® Fixable Dead Cell Stain Kit	Invitrogen GmbH Karlsruhe, Germany
Micro BCA Protein Assay Reagent Kit	Pierce Rockford, USA
Osteoprotegerin (OPG) ELISA Kit	Immundiagnostik AG

	Bensheim, Germany
Osteocalcin (Mouse) ELISA Kit	DRG Instruments GmbH Marburg, Germany
PKC Kinase Activity Assay Kit	Enzo Life Sciences GmbH Lörrach, Germany
RNeasy Mini Kit	Qiagen Hilden, Germany
SuperSignal® West Pico Chemiluminescent Substrate Kits	Pierce Rockford, USA
SuperSignal West Femto Chemiluminescent Substrate Kits	Pierce Rockford, USA

2.1.5 Peptides

Peptide	**Supplier**
Parathyroid Hormone (Human, 1-34)	PeptaNova GmbH Sandhausen, Germany
Parathyroid Hormone 1-34 (Human) [^{125}I-Nle^{8},^{18}, Tyr^{34}], 10 µCi Specific Activity: 81.4 TBq/mmol 2200 Ci/mmol	PerkinElmer Life Sciences, Inc. Boston, USA

2.1.6 Antibodies

Primary Antibodies

Antibody	Supplier	Origin	Concentration/Dilution
ß-Actin (AC-15) Mouse Anti-human Monoclonal Antibody	Santa Cruz Biotechnology CA, USA	Mouse	100 µg/mL WB: 1:2000
Parathyroid Hormone Receptor 1 Mouse Anti-human Monoclonal Antibody [3D1.1]	Santa Cruz Biotechnology CA, USA	Mouse Epitope: Amino acids 155-169	200 µg/mL IF: 1:50 ICC:1:50 IHC:1:20 FC: 5µl for $1x10^6$ cells
Parathyroid Hormone Receptor1 Mouse Anti-human Monoclonal antibody [3D1.1]	Abcam Cambridge, UK	Mouse Epitope: Amino acids 146-169	200 µg/mL IF: 1:50 ICC:1:50 IHC:1:20 FC: 5µl for $1x10^6$ cells
Normal Mouse IgG	Santa Cruz Biotechnology CA, USA	Mouse	200 µg/0.5mL FC: 5µl for $1x10^6$ cells
Alkaline Phosphatase Rabbit Anti-human polyclonal antibody	Quartett GmbH Berlin, Germany	Rabbit	Ready to use
Osteocalcin Rabbit Anti-human polyclonal antibody	Abcam Cambridge, UK	Rabbit	IHC:1:50
Osteopontin Rabbit Anti-human polyclonal antibody	IBL International GmbH Hamburg, Germany	Rabbit	IHC:1:100
Anti-Nuclei, clone 235-1 Monoclonal Antibody	Millipore GmbH Schwalbach/Ts., Germany	Mouse	IHC:1:20
Goat polyclonal Secondary Antibody to Mouse IgG - Fc	Abcam Cambridge, UK	Goat	IHC:1:200

Secondary Antibodies

Antibody	Supplier	Origin	Concentration/Dilution
Goat Anti-Mouse IgG HRP	Santa Cruz Biotechnology CA, USA	Goat	200 µg/0.5mL WB: 1:1000
Goat Anti-mous Dako EnVision®+ System-HRP (DAB)	Dako GmbH Hamburg, Germany	Goat	Ready to use
Goat Anti-rabit Dako EnVision®+ System-HRP (DAB)	Dako GmbH Hamburg, Germany	Goat	Ready to use
Texas Red®-X Goat Anti-mouse IgG (H+L)	Invitrogen GmbH Karlsruhe, Germany	Goat	2 mg/mL IF: 1:500
Alexa Fluor® 647 goat anti-mouse IgG (H+L) highly cross-adsorbed	Invitrogen GmbH Karlsruhe, Germany	Goat	2 mg/mL FC: 1:250

IF: Immunofluorescence ; ICC: Immunocytochemistry ; IHC: Immunohistochemistry ;
WB: Western blotting; FC: Flow cytometry

2.1.7 Oligonucleotides

Gene	Sequence (5'→3')	
β-actin	CATGGATGATGATATCGCCGCG	(for)
	ACATGATCTGGGTCATCTTCTCG	(rev)
ALP	GTGGAAGGAGGCAGAATTGACCA	(for)
	AGGCCCATTGCCATACAGGATGG	(rev)
PTH1R	GGAATCAGACAAGGGATGGACATC	(for)
	TCGGTAGGCATGGCCTTTGTGATT	(rev)
TGF-ß1	GAGCCCTGGACACCAACTAT	(for)
	GACCTTGCTGTACTGCGTGT	(rev)
Ocal	ATGAGAGCCCTCACACTCCTCG	(for)
	GTCAGCCAACTCGTCACAGTCC	(rev)
BMP-4	CCTGGTAACCGAATGCTGATGGTCG	(for)
	AGACTGAAGCCGGTAAAGATCCCGC	(rev)
BMPR-1a	GCTTCATGGCACTGGGATGAAATCA	(for)
	CGACAACATTCTATTGTCCGGCGTA	(rev)

BMPR-2	TGCGGCTGCTTCGCAGAATCAAGAA	(for)
	CCATTCTGAATTGAGGGAGGAGTGG	(rev)
Cyclin D1	AGCTCCTGTGCTGCGAAGTGGAA	(for)
	AGTGTTCAATGAAATCGTGCGGGG	(rev)
BMPR-1b	AGCAAGCCTGCCATAAGTGAGAAGC	(for)
	ACAGGCAACCCAGAGTCATCCTCTT	(rev)
Integrin A6	GAGATGGAGAAGTTGGAGGTGCA	(for)
	CGATCAAGGTCCATGTTTCCAGCA	(rev)
Integrin B4	CTATGAGGCTGATGGCGCCAAC	(for)
	GCAGCTCCACGATGTTGGACGA	(rev)
BMP-2	CTCGGCCTTGCCCGACACTGA	(for)
	TAAGAAGCACGCGGGGACACGT	(rev)

2.1.8 Software

GraphPad PRISM™ 4.0	GraphPad Software, Inc. San Diego, CA, USA
FlowJo 7.2.5	Treestar Ashland, OR, USA
Quantity One software	Bio-Rad Laboratories GmbH, Munich, Germany
KC4 software	BioTek Instruments, Inc. Bad Friedrichshall, Germany

2.2 Methods

2.2.1 Primary cells

PDL Cells

Throught out the whole project, fifth passage periodontal ligament (PDL) cells of six different human donors (12-14 years of age) that showed no clinical signs of periodontitis were studied. The PDL cells were isolated from the middle third of the roots of premolars from teeth that had been extracted for orthodontic reasons, with informed parental consent and following an approved protocol of the ethics committee of the University of Bonn (Reference number 029\08).

After extraction, the teeth were washed with PBS and the middle third of the periodontal ligament was scraped off using a sterile scalpel (Figure 2.1). The apical and gingival parts of the periodontal ligament were discarded to avoid contamination with cell types other than PDL fibroblasts. The scraped pieces were cultured as described in section 2.2.3 Cell Culture. The cells migrating out of the explants were splitted after reaching confluence.

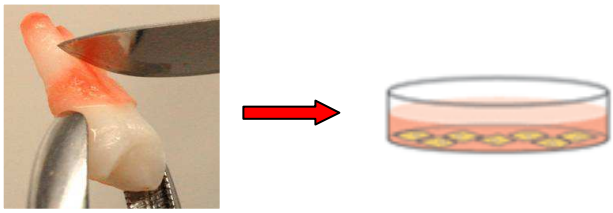

Figure 2.1 Isolation of PDL cells. PDL cells were mechanically isolated from an extracted tooth and cultured in Dulbecco's Modified Eagle Media (DMEM) supplemented with 10% FBS and 1% of an antibiotics mixture of Penicillin / Streptomycin. The cell culture was maintained at 37℃ in an atmosphere of 100% humidity, 95% air, and 5% CO_2.

2.2.2 Cell lines

MG63 Cell line

MG63 cells, a human osteosarcoma cell line, were purchased from European Collections of Cell Cultures (ECACC) (Now: Health Protection Agency). The cells were originally obtained from American Type Culture Collection (ATCC) with catalog number CRL-1427™.

HEK293 Cell line

Human Embryonic Kidney 293 cells, referred to as HEK293 cells were generated by transformation of human embryonic kidney cell cultures. In this study, HEK293 T cell line was used which was a kindly gift from Prof. Dr. Sven Burgdorf (Life & Medical Sciences Institute, Bonn, Germany). HEK293T is an important variant of HEK293 cell line and contains the SV40 Large T-antigen, which allows for substantial replication of transfected plasmids containing the SV40 promoter by the T-antigen.

2.2.3 Cell Culture

Thawing of cells

The cell lines frozen in cryovials were immersed immediately into a 37℃ water bath until they were completely thawed and the contents were transferred to T-75 flasks containing culture medium. The cells were allowed to attach for 24 h prior to a change of the medium.

Cell culture conditions

PDL, MG63 and HEK293 cells were cultured in Dulbecco's Modified Eagle Media (DMEM) supplemented with 10% FBS and 1% of an antibiotics mixture of Penicillin / Streptomycin. The cell culture was maintained at 37℃ in an atmosphere of 100% humidity, 95% air, and 5% CO_2. For different purposes, cells were seeded respectively in 10 cm petri dishes, T-75, 175 cm^2 flasks, as well as 6-well, 12-well, 24-well plates.

Splitting of cells

Cells were trypsinized upon reaching a confluency of about 60-70%. For seeding and passaging, the medium was removed and the cells were washed once with PBS. Then, Trypsin / EDTA (2 ml for 10 cm dishes/T-75 flask, 500 µl for 6-well plates and 200 µl for 24-well plates) was added and incubated at 37℃ for 3-5 min. After slightly rocking, detached cells were resuspended in a three fold excess of growth media and separated to single cell level via pipetting in a sterile 50 ml Falcon tube. The cell suspension was then centrifuged at 500xg for 5 min and the supernatant was discarded carefully without disturbing the cell pellet. The cells were then counted with a hemocytometer (Hemocytometer Neubauer) according to manufacturer's instructions after resupension in 1 ml PBS. Appropriate numbers of resuspended cells were used for seeding new dishes and plates. Cell growth was observed with an inverted microscope, Axiovert 25.

Cell storage

Cells were detached using Trypsin/EDTA solution, the contents was transferred into a 50 ml Falcon tube and centrifuged at 500xg for 5 min to remove the medium. The pellet was resuspended in the cell freezing media and dispensed into cryovials ($1x10^6$cells/ml). The cryovials were allowed to freeze at -20℃ for 2 h and then at -80℃ overnight. The cells were transferred to liqui d nitrogen for long-term storage.

Cell counting

The cells were counted with a Neubauer Hemocytometer. 0.2 ml of the cell suspension was diluted in 0.2 ml of 0.1% Trypan blue in PBS (w/v). Subsequently, 10 µl of well resuspended cell suspension was pipetted into Neubauer counting chamber and counted microscopically. Trypan blue is a dye that stains dead cells, while the live cells remain unstained. The total number of cells in the four marked squares (Figure 2.2) was counted.

A hemocytometer consists of 2 chambers, each of which is divided into 9 squares with a surface area of 1.0 mm^2. A cover glass is supported 0.1 mm over these squares so that the total volume over each square is 0.1 mm^3 (1.0 mm^2 x 0.1 mm) or

10^{-4} cm^3. Since 1 ml is equivalent to 1 cm^3, the cell concentration per ml is the average count per square x dilution factor x 10^4.

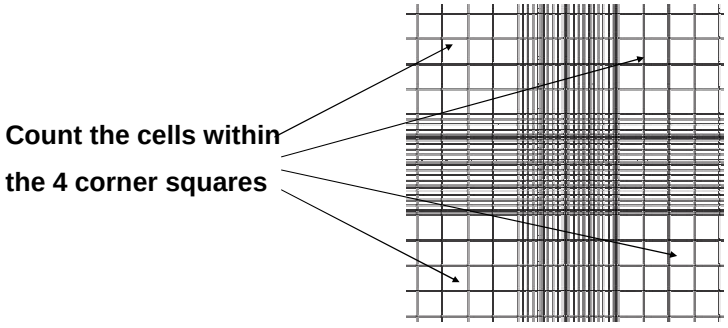

Figure 2.2 Counting cells with Neubauer hemocytometer. Cells stained with trypan blue were loaded onto the hemocytometer and the total number of cells in the four 4 squares (pointed in the figure) was counted. The cell number was calculated according to the following formula. Cells per ml = the average count per square x the dilution factor x 10^4.

2.2.4 Stimulation of PDL cells

For the functional studies, PDL cells of fifth passage from three donors were seeded in 24-well plates and cultured to confluency in DMEM supplemented with 10% FBS and 1% of an antibiotics mixture of Pen/Strep at 37℃ with 5% CO_2. For each donor, at any given concentration of the stimulant, duplicate test series were carried out.

hPTH (1-34)

Confluent PDL cells were treated with 10^{-8} M human PTH (1-34) [hPTH (1-34)] for 1, 24 and 48 h within three incubation cycles of 48 h each. For the remaining time, experimental media was replaced by media without hPTH (1-34) to mimic an intermittent treatment effect. The hPTH (1-34) was diluted in culture medium from a 10^{-4} M stock solution that was prepared in ddH_2O according to the manufacturer' instructions.

Dexamethason

After reaching confluence, the PDL cells were treated with 10^{-6} M dexamethason for 1, 2, 3, 4, 6, 14, 21 d. Dexamethason was prepared by dissolving the powder in 100% ethanol. For control purposes, cells were treated with the same amount of solvent as in the stimulated group.

Vitamin D3

10^{-7} M 1,25-dihydroxyvitamin D3, dissolved in 100% ethanol, was applied to the confluent PDL cells for 2, 4 and 6 d, respectively. Ethanol-treated cultures served as controls.

Inhibition of PKA and PKC

Confluent PDL cells were cultured in the presence of 10^{-12} M hPTH (1–34) for 1 h and 24 h within a 48 h incubation cycle. For the remaining time, experimental media were replaced by tissue culture media without hPTH (1–34). These cycles were carried out three times resulting in a total experimental period of 6 days to mimic the anabolic effects of intermittent PTH. 1 h prior to treatment with intermittent 10^{-12} M hPTH (1–34) or vehicle, either the PKC inhibitor RO-32-0432 (10^{-6} M) or the PKA inhibitor H8 (10^{-5} M) was added to the cultures and remained in the medium for the entire experimental period. Vehicle-treated cultures for each treatment group and cells cultured in the presence of the respective inhibitors but without hPTH (1–34) served as controls. At harvest, osteoprotegerin production was determined as described in section 2.2.16.

2.2.5 RNA isolation

Total RNA was extracted using the RNeasy Mini Kit (Qiagen, Hilden, Germany) following the protocol provided by the manufacturer. The RNA concentration was determined by a NanoDrop ND-1000 spectrophotometer. The total RNA was stored at -80 ℃.

2.2.6 cDNA synthesis

1 ug total RNA was reverse transcribed using the iScript ™ Selected cDNA Synthese kit with oligo(dT)-primers. Buffer and cycling conditions were set according to the manufacturer's instructions:

Reaction set up

Component	Volume per reaction
Nuclease-free water	Variable
5x iScript select reaction mix	4 µl
Oligo(dT)$_{20}$ primer	2 µl
RNA sample (1 µg total RNA)	Variable
iScript reverse transcriptase	1 µl
----------	----------
Total	20 µl

The reaction mix was mixed gently and incubated for 90 min at 42℃, followed by a 5 min incubation step at 85℃ to inactivate reverse transcriptase. The synthesized cDNA was stored at -20℃.

2.2.7 Real Time PCR

Differential gene expression was analyzed by real-time PCR with the iCycler iQ™ using SYBR® Green as fluorophore. Real time PCR is a technique used to monitor the progress of a PCR reaction in real time. At the same time, a relatively small amount of PCR product can be quantified by recording the amount of fluorescence emission at each cycle produced by a reporter molecule, which increases as the reaction proceeds. By plotting the detected fluorescence against the cycle number on a linear scale, the amount of DNA present during the exponential phase of the reaction can be determined. The cycle at which the fluorescence from a sample crosses the threshold is called the cycle threshold, C_t (Figure 2.3). The lower a C_t value, the more copies are present in the specific sample. In general, the threshold is

set by the user and should be in the linear part of the reaction, but not more than half way up the linear part.

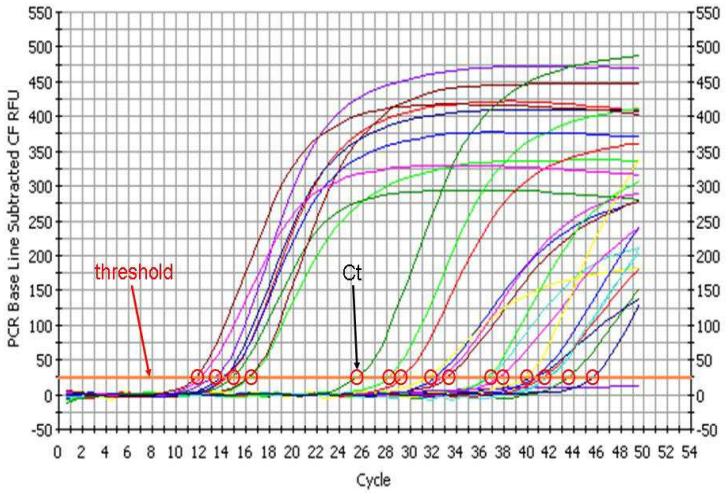

Figure 2.3 Real time PCR Graph. In this Graph, the detected fluorescence is plotted against the cycle number on a linear scale. In real time PCR, the instrument measures the cycle number at which the increase in fluorescence (and therefore cDNA) is exponential. The exponential phase because it provides the most precise and accurate data for quantitation. The Threshold line (orange line) is the level of detection at which a reaction reaches a fluorescent intensity above background. The PCR cycle at which the fluorescence crosses the threshold is termed as C_t (red circles).

SYBR® Green binds to the minor groove of the DNA double helix, but not to single stranded-DNA molecules, which leads to a substantial enhancement in fluorescence based on a change of the absorption characteristics upon DNA-binding. Since it does not distinguish between specific and nonspecific PCR products resulting from contamination, mispriming and primer-dimer artifacts, an important means of quality control is to check that all samples have a similar melting temperature. After real time PCR amplification, the cycler was programmed to do a melt curve analysis depicting the fluorescence change rate over time as a function of temperature. The melting temperature of a DNA double helix depends on its base composition. All PCR products for a particular primer pair should have the same melting temperature, unless there are nonspecific products. A negative control without template was performed to show the lack of intrinsic fluorescence.

The relative gene expression was assessed by the method developed by M.W Pfaffl (Pfaffl, 2001) as shown below (Equation 2.1), with ß-actin serving as the endogenous reference gene.

$$Ratio = \frac{(E_{target})^{\Delta CP_{target}\,(control - sample)}}{(E_{ref})^{\Delta CP_{ref}\,(control - sample)}}$$

Equation 2.1 The mathematical model of relative expression ratio in real-time PCR. The ratio of a target gene is expressed in a sample versus a control in comparison to a reference gene. E_{target} is the real-time PCR efficiency of target gene transcript; E_{ref} is the real-time PCR efficiency of a reference gene transcript; ΔCP_{target} is the CP deviation of control – sample of the target gene transcript; ΔCP_{ref} = CP deviation of control – sample of reference gene transcript. The reference gene should be a stable and secure unregulated transcript, e.g. a house-keeping gene transcript. For the calculation of *Ratio*, the individual real-time PCR efficiencies and the CP deviation (ΔCP) of the investigated transcripts must be known. Real-time PCR efficiencies were calculated, according to the formula: $E = 10^{[-1/slope]}$.

All primers used, unless specified otherwise, were self-designed and evaluated for specificity using a web-based primer design and analysis tool (NCBI/Primer-Blast program, http://www.ncbi.nlm.nih.gov/tools/primer-blast/). The efficiencies of all the primers were determined by dilution series and the optimal annealing temperature was confirmed by performing a gradient PCR. Finally the end-point PCR products were checked on the 2% agarose gel to assure the expected amplicon size and the specificity of the PCR.

The real time PCR was performed using the iQ™ SYBR® Green Supermix (Bio-Rad Laboratories GmbH, Munich, Germany) according to the manufacturer's instructions as follows:

Reaction set up

Component	Volume per reaction
iQ™ SYBR® GreenSupermix	12.5 µl
Primer mix	0.125 µl
cDNA template	1 µl
Sterile water	11.75 µl
---	---
Total	25 µl

2.2.8 Agarose Gel Electrophoresis of DNA

The separation of DNA fragments was performed using submerged horizontal 2% agarose gels. Agarose powder was dissolved in TBE-buffer and boiled in a commercial microwave until a clear, transparent solution was obtained. Ethidium bromide was added to a final concentration of 0.4 µg/ml. The Mini-Sub Cell GT system was assembled following the manufacturer's instructions. Subsequently, the agarose gel was poured into the electrophoresis chamber and allowed to solidify. Before loading samples onto the gel, the gel was covered with the electrophoresis buffer (1xTBE). The DNA moves towards the anode due to the negatively charged phosphate groups. Runs were performed under constant voltage of 60 V to 120 V and migration of nucleic acids was monitored. Gels were documented using the ChemiDoc™ XRS. The size of the DNA fragments was assessed by comparing their size to that of the GeneRuler™ DNA Ladder, Low Range.

TBE-buffer (10x)		**DNA loading buffer (10x)**	
Tris base	890mM	Glycerol	24% (v/v)
Boric acid	890mM	Bromophenol blue	spatula tip
EDTA, pH 8.0	20mM		

Table 2.1 Composition of buffers used for agarose gel electrophoresis.

2.2.9 Immunocytohistochemistry

Tissue staining

For immunohistochemical tissue staining, formalin-fixed and paraffin-embedded tissue sections were used. The tissue sections were deparaffinized in xylene, dipped in decreasing concentrations of alcohol, and then rehydrated in water. Endogenous peroxidase activity was blocked by incubating the slides in a solution of 700 µl H_2O_2 (30%) in 70 ml methanol for 10 min. To unmask the antigen, the sections were immersed in 10 mM citrate buffer (pH 9.0) and heated to 80℃ in an ovan for 30 min. Blocking was done with 4 % BSA/TBS for 30 min at RT. After an overnight incubation with primary anti-PTH1R mouse monoclonal antibody diluted 1:50 in 1% BSA/TBS in

a humidified chamber at 4℃, the slides were washed with TBS buffer for 10 min. Then, the HRP-conjugated secondary antibody (Dako, Hamburg, Germany) was applied to each specimen and incubated for 1 h at RT. After washing 10 min with TBS, freshly prepared DAB substrate was added to the slides until a suitable staining developed. The sections were rinsed with water and counterstained with Mayer's haematoxylin. The sections were rinsed again in water and dehydrated by rinsing the sections in 100% ethanol and XEM-200, respectively twice for 2 min each. The specimens were mounted with DePex and examined under an Axioskope 2 Microscope. Negative controls were included in each experiment to verify antibody specificity, by omitting the primary antibody.

Immunofluorescence staining of cells

PDL, MG63 and HEK293 cells were cultured on glass coverslips (Marienfeld GmbH & Co. KG, Lauda - Kölnigshofen, Germany) placed in 12-well plates and allowed to grow until 60-70% confluence at 37℃ with 5% CO_2. After removal of the culture medium, cells were washed once with PBS and fixed with 500µl acetone for 10 min at -20℃. The acetone was removed and the coverslips were washed with PBS prior to the antigen retrieval step. 500 µl of 10 mM citrate buffer (PH 9.0) was added to each well and the plate was heated for 30 min at 80℃ in an incubator, followed by a washing step with PBS. Blocking was performed by incubating the cells with 1% BSA in PBS for 30 min at RT. Subsequently, the anti-PTH1R mouse monoclonal primary antibody (Abcam, Cambridge, UK) which was diluted 1:50 in 1% BSA, was applied to the specimens at 4℃ over night. Afterwards, the cells were washed for three times with PBS for 5 min each, and subjected to the TexRed-conjugated secondary goat anti-mouse antibody (Invitrogen GmbH, Karlsruhe, Germany) that was diluted 1:500 in 1% BSA for 1 h at RT. After washing with PBS three times for 5 min each, cell nuclei were counter stained with DAPI diluted 1:5000 in ddH_2O from the stock solution (1 mg/ml). Prior to mounting with 15 µl Mowiol, the specimens were washed with PBS and rinsined briefly in ddH_2O. Stained cells were then examined with a Leica TCS SP2 Laser Scanning Spectral Confocal Microscope. Negative controls were included in each experiment to verify antibody specificity, by omitting the primary antibody.

Conventional DAB staining of cells

PDL, MG63 and HEK293 cells were cultured on glass cover slips (Carl Roth GmbH + Co. KG, Karlsruhe, Germany) to 60-70% confluency at 37℃ with 5% CO_2. The cells were then fixed with 4% paraformaldehyde (PFA) in PBS for 10 min at RT after washing with PBS. The endogenous peroxidase and non-specific antibody binding sites were blocked by incubating the specimen in 30% H_2O_2 in methanol for 10 min and 10% normal goat serum 30 min at RT, respectively. After each step, the specimens were washed with TBS for 10 min. Then the cells were exposed for 1 h to the primary anti-PTH1R mouse monoclonal antibody (Abcam, Cambridge, UK) diluted 1:50 in 1% BSA/TBS. After three washes in TBS, each for 5 min, a peroxidase coupled secondary anti-mouse antibody (DAKO EnVision+ System- HRP Labelled Polymer, DAKO, Denmark) was applied for 1 h at RT. Excessive antibody was removed by washing the cells three times with TBS (each time 5 min). The freshly prepared 3,3'-diaminobenzidine substrate (DAB) diluted 1:10 in Peroxidise Substrate Buffer was added and incubated for 10 min at RT. The cells were then counterstained 5 sec in Mayer's haematoxylin solution diluted 1:5 in ddH_2O. After washing thoroughly with water, the specimens were rinsed two times each 2 min respectively in 100% ethanol and XEM-200 (Xylol substitute). The sections were mounted with DePeX and examined under an Axioskope 2 Microscope. Negative controls were included in each experiment to verify antibody specificity, by omitting the primary antibody.

2.2.10 Flow cytometry analysis

The proportion of the PTH1R-positive subpopulations in PDL, MG63 and HEK293 cells were quantified by flow cytometry analysis. For this purpose, cells were seeded in T-75 flasks and allowed to reach confluency. In order to conserve the cell surface receptor proteins, accutase was applied for cell detachment. Accordingly, after removing the culture medium and washing with PBS, cells were exposed to 5 ml of accutase for 10 min at 37℃ and centrifuged at 500x g for 5 min. The cell pellet was resuspended in 1 ml PBS and cell number was determined with a Neubauer Hemocytometer.

Cell surface staining

Approximately 1x10^6 cells were incubated with 5 µl of primary mouse monoclonal antibody raised against PTH1R (Abcam, Cambridge, UK) in 100 µl ice cold PBS with 1% BSA on ice for 30 min. After three washing steps with cell sorting buffer (1% BSA/PBS), cells were incubated on ice for 30 min with Alexa Fluor 647-tagged goat anti-mouse secondary antibody (Invitrogen GmbH, Karlsruhe, Germany) which was diluted 1:250 in 1% BSA/PBS.

Because of the high autofluorescence in the short wave length region, the dead portion of PDL cells was excluded via the LIVE/DEAD® Fixable Dead Cell Stain Kit with near-IR (infra red) dye according to the instructions of the manufacturer. After removing the excessive antibody via centrifugation at 500xg at 4℃, the pellet was washed again with the cell sorting buffer and resuspended in 1 ml ice cold PBS. 1 µl of the freshly reconstituted fluorescent reactive dye was then added to the cell suspension and incubated on ice for 30 min in the dark. The cells were washed once and resuspended in 500 µl ice cold cell sorting buffer for further analysis.

The dead cell discrimination of MG63 and HEK293 cells was achieved by Hoechst 33342 dye. After washing off the excessive antibody, the pellet was resuspended in 500 µl Hoechst 33342 dye which was diluted 1:20000 in cell sorting buffer from the stock solution. The cells were kept in the Hoechst 33342 dye solution on ice in the dark until the scheduled time for analysis. The whole procedure was carried out on ice in order to minimize cell surface receptor internalization.

Intracellular staining

After removal of PBS, about 1x10^6 cells were fixed with reagent A for 15 min and subsequently permeabilized with reagent B for 15 min using the Fix&Perm kit. In each step cells were exposed to the corresponding reagent for15 min followed by a washing step with cell sorting buffer. The same dilution of primary and secondary antibody as stated above was applied for 1 h at RT. Finally, the labeled cells were resuspended in 500 µl cell sorting buffer and kept in the dark until the scheduled time for analysis.

Flow cytometry analysis

The quantitation of the PTH1R-positive proportion of the cells was performed using a LSRII flow cytometer. Before acquiring data**,** the compensation of Alexa Fluor 647 against near-IR and vice versa was adjusted and the specificity of the staining was ensured with a mouse IgG antibody as negative control. The acquired data was analyzed by FlowJo 7.2.5.

2.2.11 Competitive radioactive binding assay

Performing the experiment

In order to assess the binding affinity of PTH1R to hPTH (1-34) and the PTH1R density, homologous competitive radioactive binding experiments were performed using hPTH (1-34) as the cold ligand and its radioactive labeled homologue, human [^{125}I]-[Nle^{8,18}, Tyr^{34}]-PTH (1-34) (PerkinElmer Life Sciences, Inc., Boston, USA), as the hot ligand.

For this assay, PDL, MG63 and HEK293 cells were seeded in 24-well plates and grown to confluence at 37℃ with 5% CO_2. Prior to the assay, the cells were subjected to whole cell binding buffer (DMEM supplemented with 5 % FBS and 0.5 % BSA) for 1 h. After removing the whole cell binding buffer, approximately 40,000cpm [^{125}I]-[Nle^{8,18}, Tyr^{34}]-hPTH (1-34) and 12 concentrations of hPTH (1-34) spanning about six orders of magnitude ($10^{-4.5}$,10^{-5},$10^{-5.5}$,10^{-6},$10^{-6.5}$,10^{-7},$10^{-7.5}$,10^{-8},$10^{-8.5}$,10^{-9},$10^{-9.5}$, and 10^{-10} M), each prepared in a 7-fold concentrated solution in 30 µl binding buffer, were added to 150 µl binding buffer in each well and incubated at RT for 90 min with gentle swirling. The final volume in each well was 210 µl. The unbound ligand was removed by washing the cells three times with 0.5 ml ice-cold PBS. The cells were then lysed by addition of 0.5 ml 1 N NaOH and the lysate was measured for ^{125}I content in a Wallac WIZARD γ-counter.

Analyzing homologous competitive binding data

Nonlinear regression analysis of the data was performed using GraphPad PRISM™ 4.0). This program fits the data to the following equation and determines the inhibitory concentration 50% (IC_{50}):

$$Y = Nonspecific + \frac{(Total - Nonspecific)}{1 + 10^{log[D] - log[IC_{50}]}}$$

Equation 2.2 Y is the total binding measured in the presence of various concentrations of the cold ligand (PTH), and log[D] is the logarithm of the concentration of competitor (PTH). Nonspecific is the binding in the presence of a saturating concentration of D, and Total is the binding in the absence of competitor.

The concentration of unlabeled drug halfway between the upper and lower plateaus is called the IC_{50} (inhibitory concentration 50%) also called the EC_{50} (effective concentration 50%).

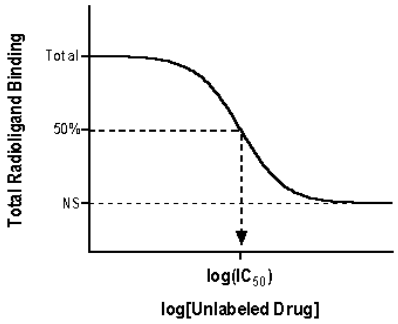

Figure 2.4 Analyzing competitive binding data (Taken from GraphPad Prism). The top of the curve is total binding which is a plateau at a value equal to radioligand binding in the absence of the competing unlabeled drug. The bottom of the curve is a plateau equal to nonspecific binding (NS). The difference between the top and bottom plateaus is the specific binding. The IC_{50} is the concentration of unlabeled drug that blocks half the specific binding.

The K_i, the inhibition constant, can be calculated from the IC_{50} using the equation of Cheng and Prusoff (Cheng and Prusoff, 1973).

$$K_i = \frac{EC_{50}}{1 + \frac{[Ligand]}{Kd}}$$

Equation 2.3 Euqation of Cheng and Prusoff (Cheng and Prusoff, 1973). The K_i is the concentration of the competing ligand that will bind to half the binding sites at equilibrium, in the absence of radioligand. K_d is the equilibrium dissociation constant.

The equation is based on following assumptions:

- Only a small fraction of both the labeled and unlabeled ligands has bound.
- The receptors are homogeneous and all have the same affinity for the ligands.
- There is no cooperativity - binding to one binding site does not alter affinity at another site.
- The experiment has reached equilibrium.
- Binding is reversible and follows the law of mass action.

Because the labeled and unlabeled ligands used in this experiment were homologous and, thus, chemically identical, the assumption was made that both ligands have identical receptor affinities. This simplifies the equation of Cheng and Prusoff further to the following:

$$K_d = K_i = IC_{50} - [Radioligand]$$

Equation 2.4 The simplified form of Cheng and Prusoff equation for homologous competitive binding experiment. K_d is equal to K_i, as the hot and cold ligands are homologous.

The concentration of the radioligand depends on the reaction volume and the amount of radioligand added to the reaction. Consequently, its calculation can be summed up as following:

$$[Radioligand] = \frac{\frac{C(cpm)}{E} \times \frac{1}{D} \times \frac{1}{60} \times \frac{1}{S(TBq/mmol)}}{V(ml)}$$

$$= \frac{\frac{C(cpm)}{87\%} \times \frac{1}{D} \times \frac{1}{60} \times \frac{1}{81.4 \times 10^{12}(Bq/mmol)}}{0.21(ml)}$$

Euqation 2.5 The concentration of hot ligand or radioligand depends on the amount of radioligand, ***C*** (cpm), in the reaction and the volume of reaction, ***V*** (mL), in each well. The reaction volume was 0.21mL. ***E*** is the efficiency of the gamma counter and in this case it was 87% (0.87). ***D*** is the radioactive decay factor (Table 2.2). A Becquerel, Bq, equals one radioactive disintegration per second. As a result, it is further divided by 60. ***S*** is the initial specific activity of the radioligand, which is 81.4 TBq/mmol or 2200Ci/mmol. Bq = $1x10^{-12}$ TBq. The unit of [Radioligand] is M.

Thus, using the equation (2.4) and (2.5), the binding affinity of the radioligand for the receptor (K_d) was determined. K_d is the concentration of ligand which occupies half of the receptors at equilibrium. A low K_d means that the receptor has a high affinity for the ligand. A high K_d indicates a low affinity to the ligand.

To address the question of PTH1R density, the B_{max} was calculated from the following equation:

$$B_{max} = \frac{Top - Bottom}{Fractional\ Occupancy} = \frac{Top - Bottom}{[Radioligand] \Big/ K_d + [Radioligand]}$$

Equation 2.6 To obtain the B_{max}, specific binding (Top – Bottom) is divided by fractional occupancy.

B_{max} is the amount of ligand required to saturate receptors and a measure of the number of receptors at saturation. Based on the above equation, the receptor density can be elucidated as follow:

$$\frac{Receptors}{Cell} = \frac{(Top - Bottom) \times (K_d + [Radioligand])}{[Radioligand]} \times \frac{1}{87\%} \times \frac{1}{D} \times \frac{1}{60} \times \frac{1}{81.4 \times 10^{12} (Bq/mmol)} \times 6.022 \times 10^{23} \times \frac{1}{Cell\ number}$$

Equation 2.7 Using the Avogadro constant, the amount of specifically bound ligand at saturation (B_{max}) can be transformed into the number of receptor molecules. The efficiency of the gamma counter is ***87%***. ***D*** is the radioactive decay factor (Table 2.2). ***$81.4x10^{12}$ (Bq / mmol)*** is the initial specific activity of the radioligand. The cell number was counted on the day of the experiment.

For each cell line, experiments were performed in triplicate.

DAYS	0	2	4	6	8	10	12	14	16	18
0	1.000	.977	.955	.933	.912	.891	.871	.851	.831	.812
20	.794	.776	.758	.741	.724	.707	.691	.675	.660	.645
40	.630	.616	.602	.588	.574	.561	.548	.536	.524	.512
60	.500	.489	.477	.467	.456	.445	.435	.425	.416	.406
80	.397	.388	.379	.370	.362	.354	.345	.338	.330	.322
100	.315	.308	.301	.294	.287	.281	.274	.268	.262	.256
120	.250	.244	.239	.233	.228	.223	.218	.213	.208	.203

Table 2.2 Idione-125 decay chart. The half-life of idione-125 is 60 days (Taken from the product data sheet, PerkinElmer Life Sciences Inc., Boston, USA)

2.2.12 Functional assays for PTH1R activity

cAMP is one of the most important second messengers and modulates various cellular activities in different cell types of numerous species. Receptor-mediated activation of the G protein triggers the activation of adenylate cyclase (AC) which converts ATP to cAMP and subsequently activates protein kinase A (PKA). Protein kinase C (PKC) is a large superfamily of serine- and threonine-specific protein kinases that mediate essential cellular signals involved in activation, proliferation, differentiation and survival. The PKCs participate in cellular events via their activation by second messenger pathways such as diacylglycerol (DAG) and Ca^{2+}.

In order to assess the PHT1R activity, the quantitative determination of intracellular adenosine 3',5'-cyclic monophosphate (cAMP) accumulation and protein kinase C (PKC) activity in the PDL, MG63 and HEK293 cells was performed using a commercially available cAMP enzyme immunometric assay (EIA) kit and a PKC activity assay kit, respectively.

cAMP assay

This assay is based on the competition between cAMP in the sample and a fixed amount of alkaline phosphatese-conjugated cAMP for a limited number of cAMP-specific rabbit polyclonal antibody binding sites. As the concentration of the conjugated cAMP is kept constant while the concentration of cAMP in the sample

varies, the amount of conjugated cAMP that is able to bind to the rabbit polyclonal antibody will be inversely proportional to the concentration of cAMP in the sample. The rabbit polyclonal antibody-cAMP complex binds to the goat anti-rabbit IgG that has been previously attached to the well. The microplate is then washed to remove any excess conjugate and unbound sample. To determine the bound enzyme activity, a substrate solution is added to the well. The final product of this enzymatic reaction has a distinct yellow color and absorbs strongly at 405 nm. The intensity of this color, determined spectrophotometrically, is proportional to the amount of conjugated cAMP bound to the well, which is inversely proportional to the amount of cAMP present in the sample during the incubation.

PDL, MG63 and HEK293 cells were seeded in 24-well plates and allowed to reach confluency. 3-isobutyl-1-methylxanthine (IBMX) is a non-specific inhibitor of phosphodiesterases and promotes the accumulation of cAMP in cells. After removal of the culture medium, cells were pretreated with DMEM supplemented with 1 % BSA, 20 mM Hepes and 1 mM IBMX for 1 h. The stimulation with various concentrations of hPTH (1-34) (10^{-6}, 10^{-7}, 10^{-8}, 10^{-9}, 10^{-10} and 10^{-12} M) continued for 15 min at 37℃. Cells were lysed by treating the ce lls with 0.1 M HCl for 10 min at RT. Insoluble material was removed by centrifugation at 600xg. The supernatant was stored at -20℃ until use.

To normalize for the protein content, the measured cAMP concentration was divided by the total protein concentration in each sample. The samples were tittered back using 0.1 M NaOH for measurement of the total protein concentration via the Pierce BCA (bicinchoninic acid) Protein Assay kit.

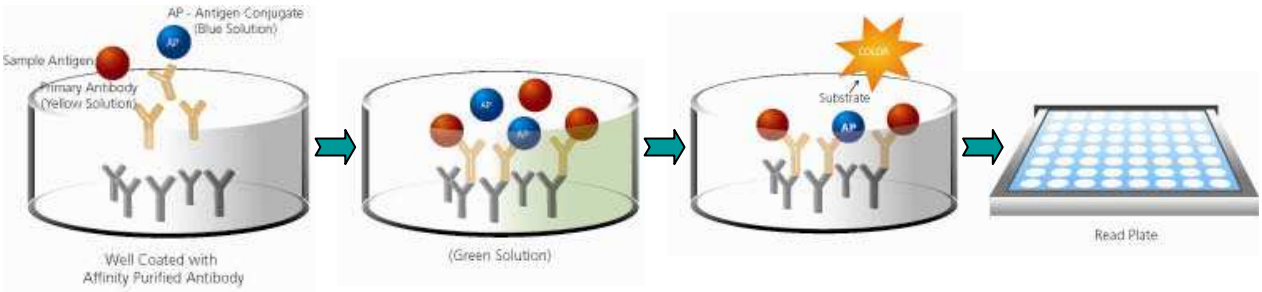

Figure 2.5 Schematic priniciple of cAMP assay (Adapted from cyclic AMP Direct assay kit from Assay Designs, Michigan USA). cAMP in the sample is in red color. Alkaline phosphates conjugated cAMP is in blue color. Primary rabit polycolonal antibody is in yellow color. The mircoplate is coated with goat anti-rabbit IgG. Upon substrate incubation, the reaction generates a yellow color which is read at 405nm.

PKC activity assay

This assay is designed in form of a solid phase enzyme-linked immuno-absorbent assay (ELISA). In this assay, a specific synthetic peptide, which is readily phosphorylated by PKC, is immobilized on the wells of the provided microtiter plate. After adding the samples to the wells, the reaction is initiated by the addition of ATP. The kinase reaction is then terminated by emptying contents in each well. A phosphospecific substrate antibody that binds specifically to the phosphorylated peptide substrate is applied to each well. Subsequently, the primary phosphospecific antibody is detected by a peroxidase conjugated secondary antibody. Upon the addition of tetramethylbenzidine substrate (TMB), a color develops proportional to PKC phosphotransferase activity. The color development is stopped with acid stop solution and the intensity of the color is measured at 450 nm.

The purified active PKC provided by the manufacturer is serially diluted and used as the positive control. Using the graph created by plotting the varying quantities of the purified active PKC against absorbance, the PKC kinase activity in the sample is assessed. The measured PKC kinase activity was normalized to the total protein in each sample. The total protein concentration was determined with the Pierce BCA Protein Assay kit.

For this assay, PDL, MG63 and HEK293 cells were cultured to confluence in 24-well plates. After removal of the culture medium, the cells were subjected to various concentrations of hPTH (1-34) (10^{-6}, 10^{-7}, 10^{-8}, 10^{-9}, 10^{-10} and 10^{-12} M) for 15 min at 37℃ diluted in DMEM. The media was aspirated and the cells were washed with ice cold PBS. Subsequently, the cells were incubated with 130 µl of the lysis buffer 10 minutes on ice [20 mM MOPS, 50 mM β-glycerolphosphate, 50 mM sodium fluoride, 1 mM sodium vanadate, 5 mM EGTA, 2 mM EDTA, 1% NP40, 1 mM dithiothreitol (DTT), 1 mM benzamidine, 1 mM phenylmethanesulphonylfluoride (PMSF) and 10 µg/ml leupeptin and aprotinin]. The cells were scraped by a cell scraper on ice and the lysate was collected in a pre-chilled 1.5 ml microcentrifuge tube. After a centrifugation step at 13,000 rpm for 15 min, the clear supernatant was transferred to a pre-chilled 1.5 ml microcentrifuge. The samples were stored at -70℃ untill the day of assay.

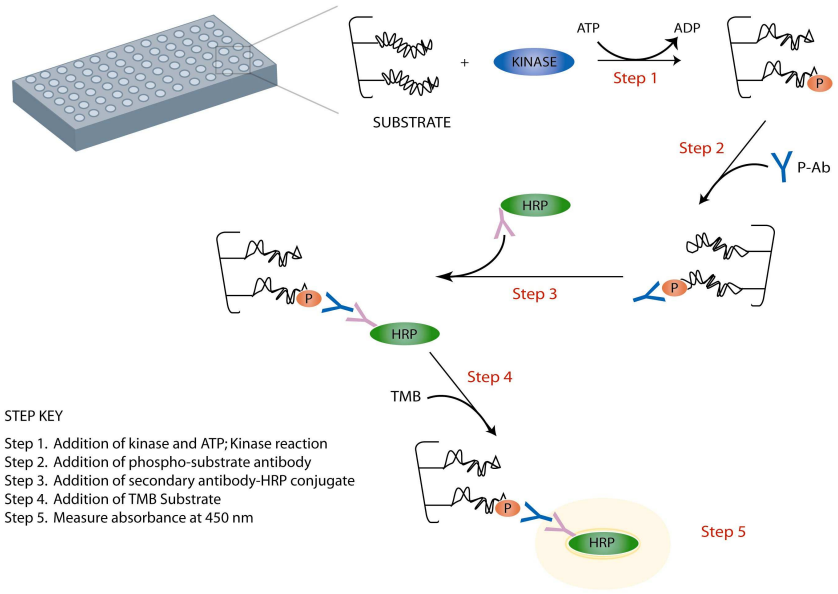

Figure 2.6 The principle chart of the PKC kinase activity assay (Taken from the PKC kinase activity assay kit from Assay Designs, Michigan USA).

2.2.13 Total protein extraction

For western blot analysis, PDL, MG63 and HEK293 cells were cultured in T-75 flasks at 37℃ with 5% CO_2 and allowed to reach confluence. After removal of the culture medium, 5 ml PBS was added to the flasks. The cells were subsequently scraped by a cell scraper and collected into a 15 ml falcon tube. The remaining cells in the culture flask were washed with 5 ml PBS and taken into the same falcon tube, which was centrifuged for 5 min at 1500 rpm. The supernatant was decanted and the cell pellet was washed again with 5 ml PBS. After removal of the PBS, the cell pellet was resuspended in 200 µl RIPA buffer that was freshly mixed with protease-inhibitor-cocktail and allowed to lyse on ice for 15 min. Cellular debris was excluded by centrifuging the cell lysate for 5 min at 12000 rpm at 4℃. The protein extract was stored at -20℃.

2.2.14 Protein quantification

The protein extracted following the protocols described in above sections was quantified using the BCA Protein Assay Reagent kit.

This assay is based on the combination of reduction of Cu^{+2} to Cu^{+1} by protein in an alkaline environment (the biuret reaction) with the highly sensitive and selective colorimetric detection of the resulting cuprous cation (Cu^{+1}) by BCA *(Smith, P.K., et al. 1985).* This reaction generates a purple colored product formed by the chelation of two molecules of BCA with one cuprous ion. The BCA / copper complex is water-soluble and has a strong absorbance at 562 nm that is nearly linear with increasing protein concentrations.

The assay procedure was based on the instructions of the manufacturer. 25 µl of each standard or unknown sample was pipetted into a microplate in duplicate. Subsequently, 200 µl Working Reagent (WR) was added to each well. After mixing thoroughly on a plate shaker for 30 sec, the plate was incubated for 30 min at 37℃. The plate was cooled down to RT and the absorbance nm was measured at 562 with the PowerWave X UV-Vis plate reader.

The WR was prepared by mixing 50 parts of BCA Reagent A with 1 part of BCA Reagent B (50:1, Reagent A:B). A set of standards was made by diluting the bovine serum albumin (BSA) standard included in the assay kit. The protein concentration of the unknown samples was determined from the standard curve plotted for the BSA standards.

2.2.15 Western Blot

The PTH1R in PDL, MG63 and HEK293 cells was quantified at protein level by means of western blot analysis to acquire further information on the cellular localization of the receptors. After separation on sodium dodecylsulfate-polyacrylamide gel electrophoresis (SDS-PAGE), the extracted or fractionized proteins were blotted and detected on a membrane with an antibody raised against PTH1R.

Protein gel electrophoresis (SDS-PAGE)

Sodium dodecylsulfate-polyacrylamide gel electrophoresis (SDS-PAGE) is a technique used to separate proteins based on their molecular weight. In SDS-PAGE, the samples are pre-treated with SDS combined with a reducing agent, such as ß-mercaptoethanol (ß-ME) or dithiothreitol (DTT) by heating at 70℃ or boiling briefly, which leads to the formation of a linear polypeptide chain. SDS is a strong anionic detergent that denatures by disrupting the secondary, tertiary and quaternary structures of the protein. ß-ME or DTT combined with a heating step disrupts all the disulphide bonds in the protein. Due to SDS, the proteins become overall negatively charged and migrate from cathode (-) to anode (+) in accordance to their size.
In SDS-PAGE, to obtain optimal separation of proteins, a stacking gel is cast over the resolving gel. The stacking gel has a larger pore size, a lower pH and a different ionic content than the resolving gel. This allows the proteins to be concentrated into a tight band before entering the resolving gel. Protein separation is achieved in the resolving portion of the gel.
For the separation of the PTH1R proteins, a 10% resolving gel was prepared as follows:

10% resolving gel:

ddH_2O	4 ml
30 % Acrylamide/ bis-acrylamide 37.5:1	3.3 ml
1.5 M Tris-HCl (PH 8.8)	2.5 ml
10% SDS 10%	0.1 ml
10% APS	0.1 ml
TEMED	0.004 ml

The gel was then covered with isopropanol to get a horizontal gel surface and allowed to polymerize (>30 min). After removal of the isopropanol, a 5% stacking gel was cast on top of the resolving gel by combining the following:

5% stacking gel:

ddH_2O	1.4 ml
30 % Acrylamide/ bis-acrylamide 37.5:1	0.33 ml
0.5 M Tris-HCl (PH 6.8)	0.25 ml
10% SDS	0.02 ml
10% APS	0.02 ml
TEMED	0.002 ml

After the stacking gel had polymerized (>30min), the Mini-PROTEAN Tetra cell was assembled according to the instructions of the manufacturer and placed in the cell containing the running buffer. Typically, 20-40 µg of protein was mixed 6:1 with 6X Laemmli buffer (Laemmli, 1970) and heated for 5 min at 95℃. After loading the denatured protein sample and the molecular weight standards, the gel was run at 200 V until the required resolution was obtained.

Protein blotting

The proteins resolved on the gel were transferred onto either a polyvinylidene fluoride (PVDF) membrane or nitrocellulose membrane by a semi-dry blotting method. After SDS-PAGE, the gel was immediately equilibrated in a small container of transfer buffer for approximately 15 min. The nitrocellulose membrane and filter papers were soaked also in transfer buffer for 15-30 min. (The PVDF membrane was first soaked in 100% methanol for 15 sec). The sandwich blot was assembled on the Trans-Blot SD Semi-Dry Transfer Cell in the order shown below. Transfer of proteins was done for 1 h at 15 V.

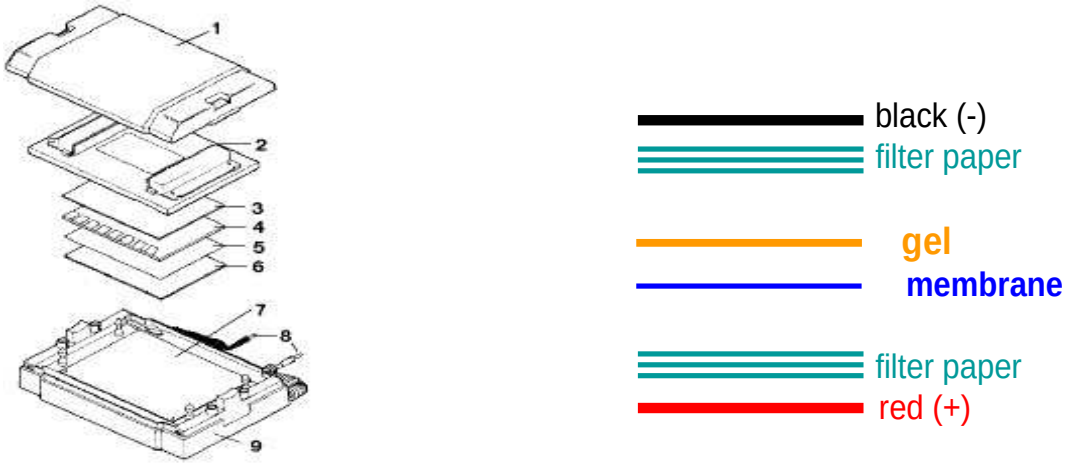

Figure 2.7 Assembly order of the blot for Semi-dry Blotting (Taken from Bio-Rad). **A:** Semi-Dry Transfer Cell. 1. Safety lid, 2. Cathode assembly with latches, 3. Three pieces blot filter paper, 4. Gel, 5. Nitrocellulose/PVDF membrane, 6. Three pieces blot filter paper 7. Spring-loaded anode platform, mounted on four guide posts, 8. Power cables, 9. Base, **B:** Assembly scheme of the Semi-dry Blotting.

Protein detection

Transfer efficiency was checked by staining the membrane with Ponceau S solution. After washing away the Ponceau S staining solution with water, the membrane was blocked in blocking solution on a rocker platform for 1 h at RT. Subsequently, primary PTH1R mouse monoclonal antibodies diluted 1:100 in blocking solution were applied overnight at 4℃. Following three 10-min washes with wash buffer, the blot was incubated for 1 h at RT with the HRP-conjugated secondary goat anti-mouse antibody diluted 1:1000 in blocking solution. After three washing steps of 10 min each with wash buffer and rinsing briefly in TBS, the blot was incubated 5 min in the SuperSignal West Femto Maximum Sensitivity Substrate working solution in the dark. The excess reagent was drained and the blot was covered with clear plastic wrap. Finally, the blot was visualized on a ChemiDoc™ XRS system and analyzed using Quantity One software. The size of the proteins was determined by comparing the protein bands with that of a molecular weight marker.

Stripping for reprobing western blots

In order to detect another protein or proteins of interest, the membrane was stripped using Restore™ Western Blot Stripping Buffer. This was done by incubating the

membrane in the stripping buffer for 15 min at RT with shaking, followed by a washing step with washing buffer.

Used buffers and solutions:

1. Laemmli buffer (6x)

SDS (sodium dodecyl sulfate)	1.2 g
bromophenol blue	6 mg
glycerol	4.7 ml
Tris 0.5 M (pH 6.8)	1.2 ml
ddH_2O	2.1 ml

- Warmed with shaking till the solution was dissolved.
- Added 0.93 g DTT.

After completely dissolved, the buffer was aliquoted and stored at -20ºC.

2. Running buffer: 1x Tris/Glycine/SDS

10x Tris/Glycine/SDS (Bio-Rad) was 1:10 diluted in ddH_2O

3. Wash buffer: 0.1% Tween 20 /TBS

0.1 ml Tween 20 + 99.9 ml TBS (Bio-Rad Laboratories GmbH, Munich, Germany)

4. Transfer buffer: Tris/Glycin/20% Methanol

20 ml Methanol +80 ml Tris/Glycin (Bio-Rad Laboratories GmbH, Munich, Germany)

5. Blocking solution: 5% Milk/0.1% Tween 20 /TBS

2.5g milk + 50 ml 0.1% Tween 20 /TBS

6. SuperSignal West Femto Maximum Sensitivity Substrate working solution

The two substrate components were mixed at a 1:1 ratio.

2.2.16 ELISA

The Enzyme-Linked Immunosorbent Assay (ELISA) was first published by Engvall *et al* (1971) and the first microplate-based ELISA was established by Voller *et al* (1974). Osteoprotegerin levels in the conditioned media were assayed by a commercially available ELISA kit. The principle of this kit is based on a sandwich-type ELISA, in which two highly specific antibodies against OPG are used. The binding antibody is attached to the wells of the microtiterplate, while the detection antibody is labeled with biotin. In a first incubation step the samples and the biotinylated antibody against OPG react simultaneously with the pre-coated antibody on the microtiterplate. Thus, a “sandwich” complex is formed consisting of the binding antibody on the plate, OPG and the biotinylated detection antibody. In a second step, streptavidin-peroxidase is added, which reacts with the detection antibody. After incubation with the substrate, an acidic stopping solution is added, which changes the blue colour to yellow. The intensity of the yellow colour is directly proportional to the concentration of OPG in the sample. A dose-response curve of the absorbance units (at 450 nm) versus concentration is generated. OPG, present in the samples, is determined directly from this calibration curve. The data were assessed as a function of cell number to exclude the possibility that changes in osteoprotegerin production simply result from increased cell numbers due to the culture period and not from an altered production by the individual cell.

2.2.17 Statistical analysis

All statistical tests were performed by GraphPad PRISM™ 4.0. All values were expressed as mean ± standard error of mean (SEM), and compared using Student’s t-test, Dunnett-test, Bonferroni's and Tukey’s test. Statistical significance was accepted at $p < 0.05$.

2.2.18 Methods used in *in vivo* experiments

Induction of osteoblastic differentiation

Fifth passage PDL cells from two donors were cultured in 24-well plates at a seeding density of 10000 cells/well and stimulated with 10^{-6} M dexamethasone for 3 weeks to induce a more differentiated osteoblastic phenotype.

CD-1® nude mice

Twelve male, 4-6 weeks old, CD-1® nude mice with an average body weight of 20g (Charles River Laboratories, Germany), were stabilized at the animal research facility of the University of Bonn of Medicine. Mice were housed one per cage under specific pathogen-free conditions, in a continuously filtered room, maintained between 21-22℃, with 40-60% humidity on 12 h light and dark cycles and given free access to food and water. Animal body weights were recorded before the onset and at the end of the experiment. All experimental protocols were reviewed and approved by the ethics committee of the University of Bonn (reference number 887-50.103709.196).

Surgical implantation of PDL Cells

The PDL cells were resuspended each in fresh growth media, and 3×10^{6} cells were incorporated into gelatin sponges 3–5mm in diameter by capillary action. The implantation procedure was adopted from Pettway et al (Pettway et al., 2008). According to this protocol, animals were anaesthetized with 2 vol% isoflurane and two midlongitudinal skin incisions, approximately 1cm in length, were made on the dorsal surface of each mouse. Blunt dissection was used to form subcutaneous pouches. Two implants per animal were inserted. Post surgically, mice were monitored daily for any signs of infection like shivering, lethargy, and diarrhea. Neither were signs of impaired healing nor adverse side effects of the procedures or drug dosage observed.

Intermittent hPTH (1-34) administration

In order to examine the mineralization capacity of PDL cells and the anabolic potential of intermittent hPTH (1-34) regarding the support of this capacity, mice were

randomly assigned to one of two experimental groups, with one group receiving daily subcutaneous injections of 40 µg/kg body weight recombinant human hPTH (1-34) for a period of 4 weeks starting at day 1 after PDL cell implantation, whereas the other group received sham-injections of an equivalent dose of saline. The dose of hPTH (1-34) used in these studies proved effective in previous experiments (Johnston et al., 2007). On day 28, the animals were anesthetized with isoflurane, blood (by means of cardiac puncture) and mineralized gelatin sponges were collected before euthanasia via cervical dislocation (Figure 2.8).

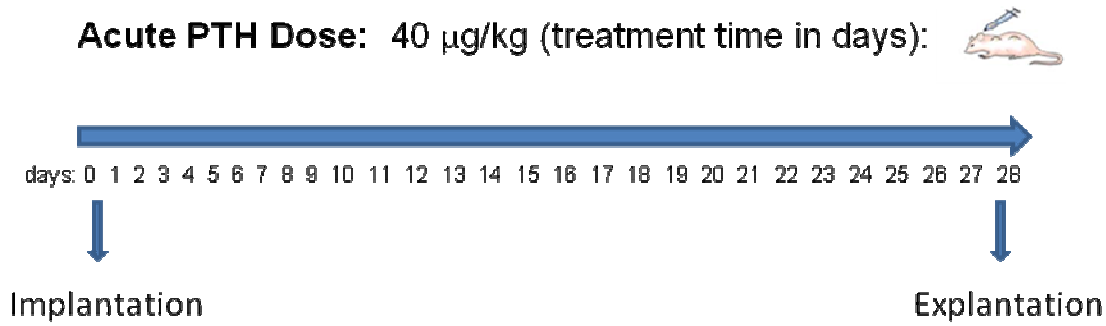

Figure 2.8 Schematic illustration of in vivo injection of PTH (1-34) (adapted from: **(Pettway et al., 2005)**. The experimental design was used to investigate the effect an intermittent anabolic hPTH (1-34) or vehicle (sterile water) treatment on human PDL cells transplanted into immunocompromised mice Subcutaneous injections were administered for 28 days beginning one day after implantation procedures.

Preparation of paraffin tissue sections

The explants were fixed in 4 % phosphate buffered (according to Sörensen) formaldehyde for 24 h at room temperature. Thereafter, they were first hydrated, then dehydrated in an ascending ethanol series and finally embedded in paraffin. As a next step, tissue sections of 5 µm thickness were cut in the sagittal plane, mounted on glass slides and dried at 37 ℃ overnight before further processing. Tissue sections were deparaffinized by passing them through a descending series of ethanol ending with distilled water as described in section 2.2.9 (Tissue staining).

Immunohistochemistry

The immunohistochemical staining of the paraffin embedded tissue sections was performed as described in section 2.2.9 (Tissue staining), with the exception of the used antibodies and the concentration of the antibodies.

The presence of the transplanted PDL cells was confirmed by staining the nuclei of those cells using an antibody specific to human, but not mouse cells (diluted 1:20 in 1% BSA/TBS). In order to avoid the unspecific binding of the secondary antibody, the slides were pre-incubated with a goat polyclonal secondary antibody to mouse IgG - Fc (diluted 1:200 in 1% BSA/TBS) for 1 h at room temperature prior to the incubation with the primary antibody. For a better contrast, the tissue sections were counterstained with light green, instead of Mayer's haematoxylin.

For the staining of alkaline phosphotase, osteocalcin and osteopontin, sections were incubated with a polyclonal primary antibody of rabbit origin in a 1:50 (osteocalcin) or 1:100 (osteopontin) working solution of 1% BSA/TBS either for 1h at room temperature (osteocalcin) or at 4℃ overnight in a humidified chamber (ALP, osteopontin). The anti-ALP antibody was supplied in a ready-to-use working solution by the manufacturer. The slides were rinsed again and incubated for 30 min with a peroxidase labeled polymer conjugated to a goat anti-rabbit immunoglobulin provided as a ready-to-use solution as secondary antibody. The staining of PTH1R was performed as described in section 2.2.9 (Tissue staining). In order to prove the specificity of the immunoreactions, negative controls were carried out by omitting the primary antibody.

Alzarin red staining

The mineralization capacity of transplanted PDL cells was assessed by staining of the calcium deposits with alizarin red solution. To this end, a solution of 2% w/v alizarin red was prepared in ddH_2O and the pH was adjusted to 4.1-4.3 using 0.5% ammonium hydroxide. Sections were deparaffinized and rinsed briefly in ddH_2O. Thereafter, the sections were placed in alizarin red solution and observed microscopically until an orange-red color developed (~5 min). After removing the excess dye, the slides were dehydrated in acetone (20 dips) and then in acetone-xylene (1:1) solution (20 dips). Finally, the slides were cleared in xylene and mounted with DePex. Red-orange color was considered positive for mineral deposition.

Alizarin Red S forms a chelate complex with calcium salts and therefore stains mineralized tissue.

Semiquantitative assessment of the immunoreactivity

Three representative sections per specimen were randomly selected for the assessment of the staining intensity for a particular antigen resulting in a total of 36 specimens per experimental group. Immunoreactivity was determined semiquantitatively by assigning one of the following grades to the specimen: 0: no immunoreactivity; 1: weak immunoreactivity with only single cells presenting faint immunoreactions; 2: moderate immunoreactivity with about 50% of cells showing a visible immunoreaction; 3: strong immunoreactivity in most of the cells. Reproducibility of the readouts was ensured by analyzing 36 selected specimens in duplicate. An intraobserver error was demonstrated to happen in less than 4% of the cases and the deviation did not exceed one grade.

Serum analysis of osteocalcin

To demonstrate a systemic effect of the intermittent hPTH (1-34) administration on bone turnover, serum was isolated from blood via centrifugation at 1500 rpm for 30 min at 4℃ and stored in single use aliquots at -80℃ for future analysis. The quantification of serum levels of osteocalcin was performed using a commercially available ELISA assay (mouse) following the manufacturer's instructions. The assay principle is the same as described in the previous section (2.2.16 ELISA), with the exception of used antibodies.

Statistical analysis

For any given experiment, each data point represents the mean ± SEM of 36 independent specimens. Statistical significance of the data was analyzed using the Mann-Whitney-U Test. P-values <0.05 were considered to be significant.

3 RESULTS

3.1 Primary characterization of PDL cells in vitro

Morphological characterization

At higher seeding densities, cultured PDL cells exhibited a fibroblast-like morphology with a spindle-like shape, which is typical of fibroblasts (Figure 3.1). When seeded at lower densities, the appearance of cell clusters was observed. The rate of cell growth varied among the donors. The doubling time of PDL primer cell lines generally ranged from 3 to 5 days. These characteristics remained constant up to passage six. Figure 3.1, **A** and **B** represent the confluent and preconfluent stage of PDL cells, respectively.

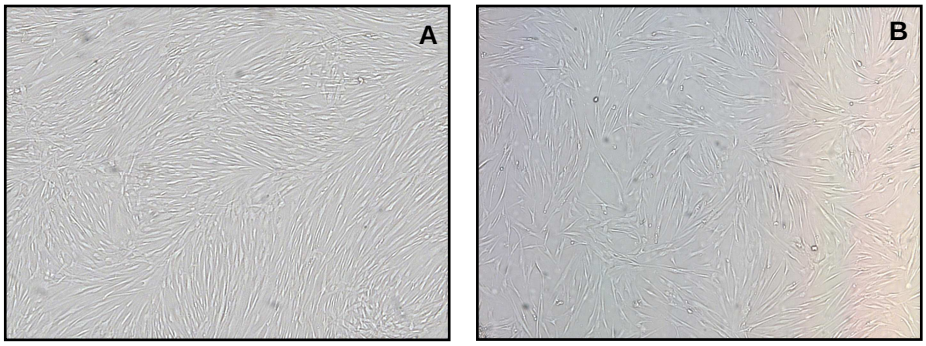

Figure 3.1 Confluent and preconfluent PDL cells. PDL cells were mechanically isolated from an extracted tooth. In culture, PDL cells exhibited a spindle-shaped fibroblast-like morphology. **A:** PDL cells at confluent stage. **B:** PDL cells at preconfluent stage. Magnification: X100

Molecular characterization

The confluent and preconfluent PDL cells of the six donors were characterized for the mRNA expression level of marker genes involved in osteogenesis such as ALP, osteocalcin, PTH1R, bone morphogenetic protein (BMP)-2 and -4, bone morphogenetic protein receptor (BMPR)-1a, -1b and -2, integrin A6, integrin B4, transforming growth factor-β1 (TGF-β1) and cyclin D1. The confluent cells were cultured to ~100% confluence, while preconfluent cells to ~70% confluence. In data analysis, the mRNA expression level of these markers in confluent cells was compared to that in preconfluent cells. As shown in Figure 3.2, the confluent PDL

cells revealed a relatively higher gene expression level of these markers than preconfluent cells, with the highest being the expression level of osteocalcin (~26-fold). Regarding PTH1R gene expression, the confluent cells showed an almost 15-fold higher mRNA level than the preconfluent cells. The lowest difference was observed in cyclin D1 gene expression level, with almost 4-fold in confluent cells.
As a result of these divergences which are caused by the state of confluency, we used the PDL cells at confluent stage in all forth coming experiments.

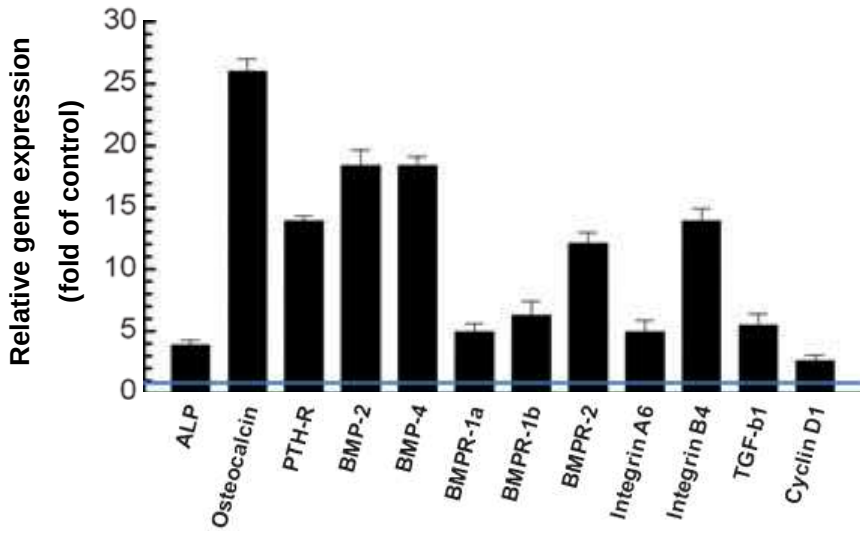

Figure 3.2 Characterization of confluent vs. preconfluent periodontal ligament (PDL) cell cultures. Fifth-passage human PDL cells from six donors were cultured to either 70% confluence (preconfluent cells) or 100% confluence and were then characterized for the mRNA expression level of marker genes involved in osteogenesis such as [alkaline phosphatase (ALP), osteocalcin, parathyroid hormone receptor (PTH-R), bone morphogenetic protein (BMP)-2 and -4, bone morphogenetic protein receptor (BMPR)-1a, -1b and -2, integrin A6, integrin B4, transforming growth factor-β1 (TGF-β1) and cyclin D1 by the use of a microarray. For comparison, the expression level of the investigated genes in preconfluent cells was set to 1 and served as a reference for the expression at the confluent state. Each value represents the mean + SEM for 6 independent cultures

3.2 Autofluorescence characteristics of PDL cells

One prominent characteristic of PDL cells is the autofluorescence, which was first observed, as the fixed cells were stained using FITC-conjugated antibody and examined with a Zeiss Axioskop 2 fluorescence microscope. The unstained cells emitted a significantly high green fluorescence, which was at the same level as that

of the stained cells (Figure 3.3, **A**, **B** and **C)**. However, no detectable red autofluorescence was observed using TRITC filter sets (Figure 3.3, **D**).

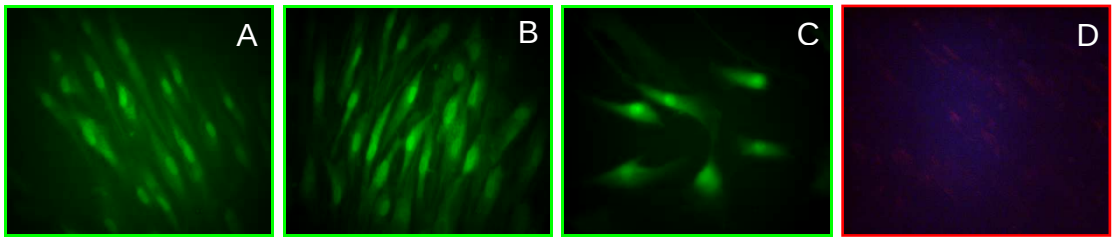

Figure 3.3 Green autofluorescence of fixed PDL cells. After fixing with 4% paraformaldehyde for 10 min, PDL cells were stained for PTH1R using a FITC coupled secondary antibody and examined with a fluorescence microscopy using FITC and TRITC filter sets. The images were acquired using the same adjustments. Magnification: X200. **A:** unstained PDL cells. **B:** only secondary antibody treated PDL cells. **C:** PTH1R antibody and respective secondary FITC coupled antibody treated PDL cells. **D:** unstained PDL cells examined using TRITC filter sets.

As shown in Figure 3.4, the autofluorescence was mainly localized in the perinuclear area, while in other parts of the cytoplasm and in the nucleus, it was hardly detectable. Moreover, the intensity of the autofluorescence differed among the cells examined, ranging from an extremely high level to almost no detectable autofluorescence in some cells.

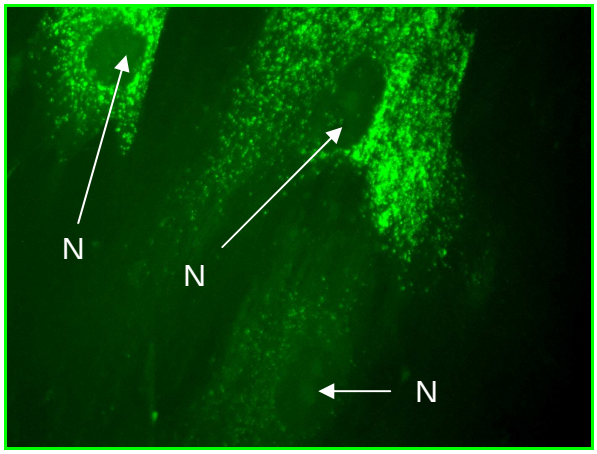

Figure 3.4 Localization of the green autofluorescence in PDL cells. The 4% paraformaldehyde fixed cells were examined with a fluorescence microscope. Magnification: X630. In this image, three cells can be seen, of which two exhibit high autofluorescence around the nucleus, while the last one has almost no detectable autofluorescence. The nuclei of the cells are indicated with **N**.

In order to clarify the effect of fixation agents on autofluorescence, the PDL cell suspension in PBS and coverslip-cultured unfixed PDL cells were examined directly

using FITC filter sets. In both experimental setups, a high level of green autofluorescence was detected (Figure 3.5, **A** and B). This observation confirmed that the green fluorescence stems from PDL cells, and is not caused by the fixation agent.

Figure 3.5 Green autofluorescence of unfixed PDL cells and PDL cell suspension. A: Unfixed PDL cells. PDL cells cultured on coverslip were washed once with PBS and mounted on a microscope slide. **B:** PDL cell suspension. After trypsinizing, PDL cells were washed once with PBS and centrifuged down to pellet. The pellet was then resuspended in PBS and one drop of the suspension pipetted onto a microscope slide. The so prepared sections were then examined with a Zeiss Axioskop 2 fluorescence microscope using FITC filter sets. Magnification: X200.

The autofluorescence characteristics of PDL cells were further investigated with a LSR II flow cytometry using different filter sets. For comparison, other cells lines such as HaCaT, MG63, HEK293 cells and oral keratinocytes were included. The flow cytometry data revealed that PDL cells exhibit very low autofluorescence in the long wavelength region (from red to far infrared) such as Alexa Fluor 645, being the lowest among the five investigated cell lines (Figure 3.6, **A**), and high auto fluorescence in short wavelength region such as FITC, being the highest among the cell lines investigated (Figure 3.6, **B**). Thus, based on the low autofluorescence characteristic of PDL cells in red fluorescence region and antibody availability, Texas Red and Alexa Fluor 647-conjugated antibodies were chosen for immunofluorescence staining and flow cytometry analysis of PDL cells, respectively.

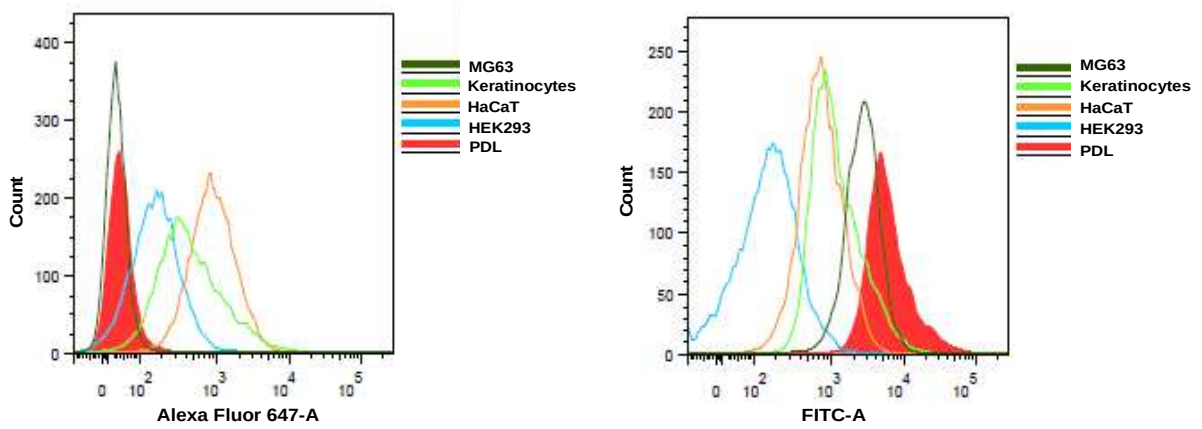

A B

Figure 3.6 Comparison of the autofluorescence of PDL, MG63, HaCa T, HEK293 cells and keratinocytes in Alexa Fluor 647 and FITC filter sets. After detachment, the cells were washed once with PBS and centrifuged. The cell pellet was then resuspended in sorting buffer (1% BSA in PBS) and screened using different filter sets with a LSR II flow cytometry. The data analysed with FlowJo 7.2.5 software. As indicated above, the five cell types were represented with different colors. **A:** Autofluorescence intensity in Alexa Fuor 647 filter sets. **B:** Autofluorescence intensity in FITC filter sets.

To elicit further information on the autofluorescence, PDL cells were permeabilized after a fixation step and viewed under a Zeiss Axioskop 2 fluorescence microscope. The permeabilization step decreased dramatically the autofluorescence of the cells, as shown below (Figure 3.7, **A** and **B**). This result was further confirmed by the flow cytometry analysis, wherein the autofluorescence intensity of fixed but not permeabilized PDL cells was compared to that of fixed and subsequently permeabilized PDL cells (Figure 3.7, **C**). Thus, in the immunofluorescence staining of the PTH1R, the problem of autofluorescence was circumvented by permeabilizing the PDL cells after a fixation step.

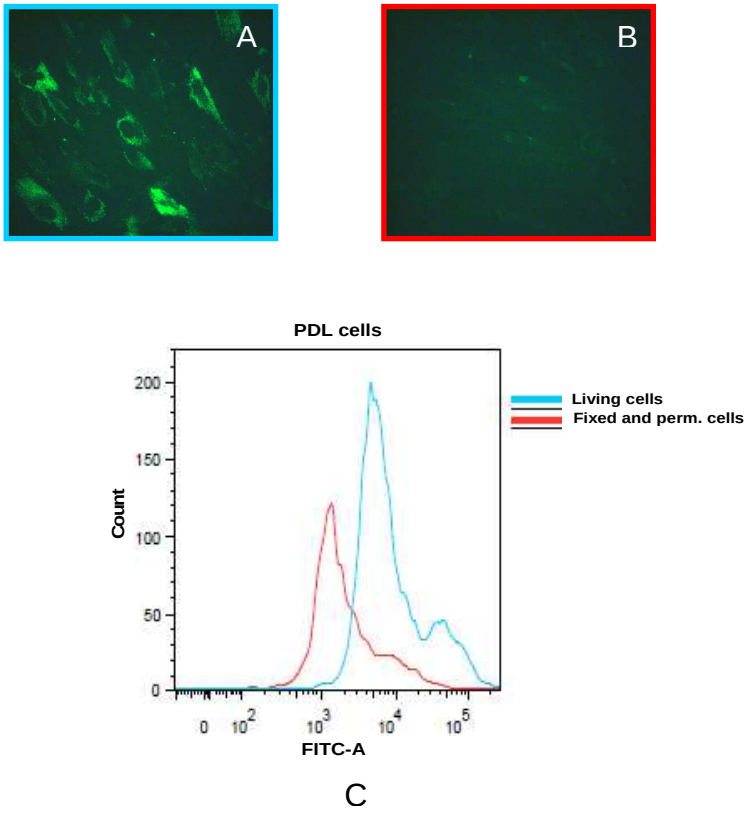

Figure 3.7 Comparison of autofluorescence in fixed and fixed subsequently permeabilized PDL cells. A: Fluorescence image of fixed PDL cells **B:** Fluorescence image of fixed and subsequently permeabilized PDL cells. **C:** Comparison of autofluorescence intensity of PDL cells after fixation and permeabilization. For fixation, cells were treated with 4 % paraformaldehyde for 10 min. For permeabilization, cells were treated for 5 min with 1% triton X-100 after a 15 min fixation. The sections were examined with a fluorescence microscope and LSR II flowcytometry. Magnification: X400.

3.3 Analysis of relative gene expression level of PTH1R

The relative expression levels of mRNA encoding the PTH1R was measured in PDL, MG63 and HEK293 cells, using real time PCR method.

The results showed a distinct expression of PTH1R gene in the three cell lines. However, the gene expression level of the PTH1R varied among these cell lines. While the highest mRNA expression was found in HEK293 cells, with ~14-fold higher gene expression of PTH1R compared to PDL cells, MG63 cells expressed app. 2-fold lower PTH1R mRNA level than PDL cells (Figure 3.8, **A**). The PCR products run on the agarose gel showed a distinct band of the correct size (250 bp) (Figure 3.8, **B**).

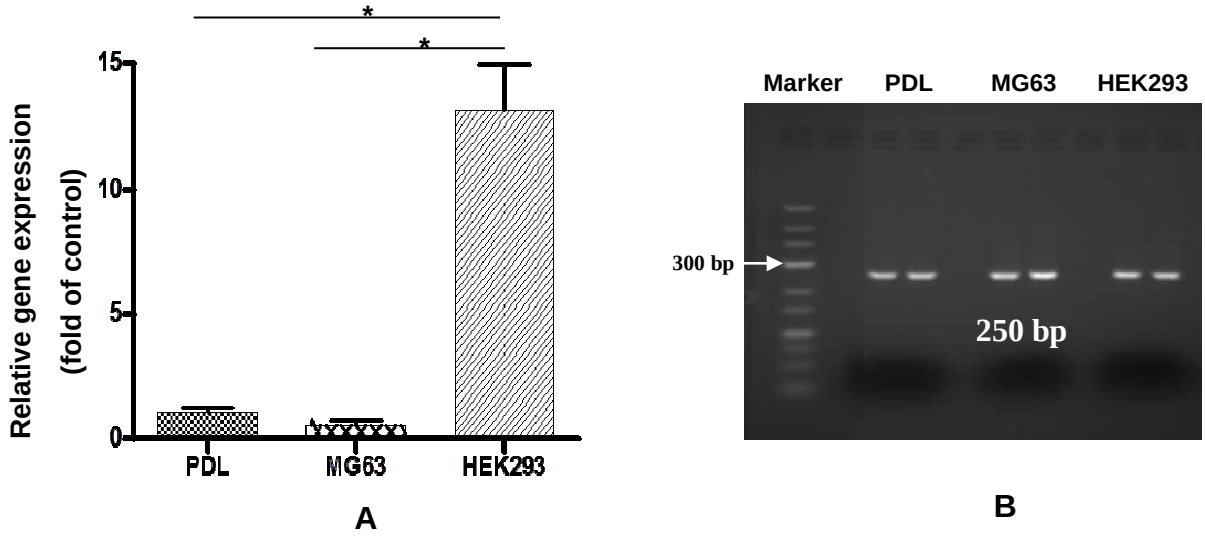

Figure 3.8 Comparison of gene expression level of PTH1R in PDL, MG63 and HEK293 cells. Real time PCR was performed from total RNA of PDL, MG63 and HEK293 cells. Expression of mRNA for PTH1R was normalized using expression of β-actin as a reference (relative expression). The values were then compared to that of PDL cells. **A:** Relative gene expression level analysis using real time PCR method. All values were expressed as mean ± SEM, and compared using one-way ANOVA. Statistical significance was accepted at $p < 0.05$ (*****: $p < 0.05$). **B:** The PCR products were run on a 2% agarose gel and the size of the PCR products was assessed using GeneRuler™ DNA Ladder, Low Range. As expected, the amplicon size was 250 bp.

3.4 Detection and cellular localization of PTH1R

Detection

To detect the PTH1R in PDL tissues, paraffin-embedded tissue sections prepared from extracted teeth were stained with antibody against PTH1R.

As Illustrated in Figure 3.9, a distinct positive immunoreaction for PTH1R was observed in the PDL tissue. The overall staining pattern indicated that the PTH1R was distributed equally throughout the whole PDL tissue. Meanwhile, no difference was observed in the distribution of the PTH1R on the side of alveolar bone and tooth root (Figure 3.9, **A**). At cellular level, the immunostaining for PTH1R was observed mainly in PDL fibroblasts and endothelial cells, whereas the epithelial cell rests of Malassez (ERM) remained unstained (Figure 3.9, **B, C and D**). As expected, cementoblasts and odontoblasts showed also a positive immunostaining for PTH1R

(Figure 3.9, **E and F**). The unstained negative control sections ensured the specificity of the used primary antibody (Figure 3.9, **a and b**). This PDL tissue as shown in Figure 3.9 was isolated mechanically and cultured for the establishment of the PDL cell culture, as described in the materials and methods section.

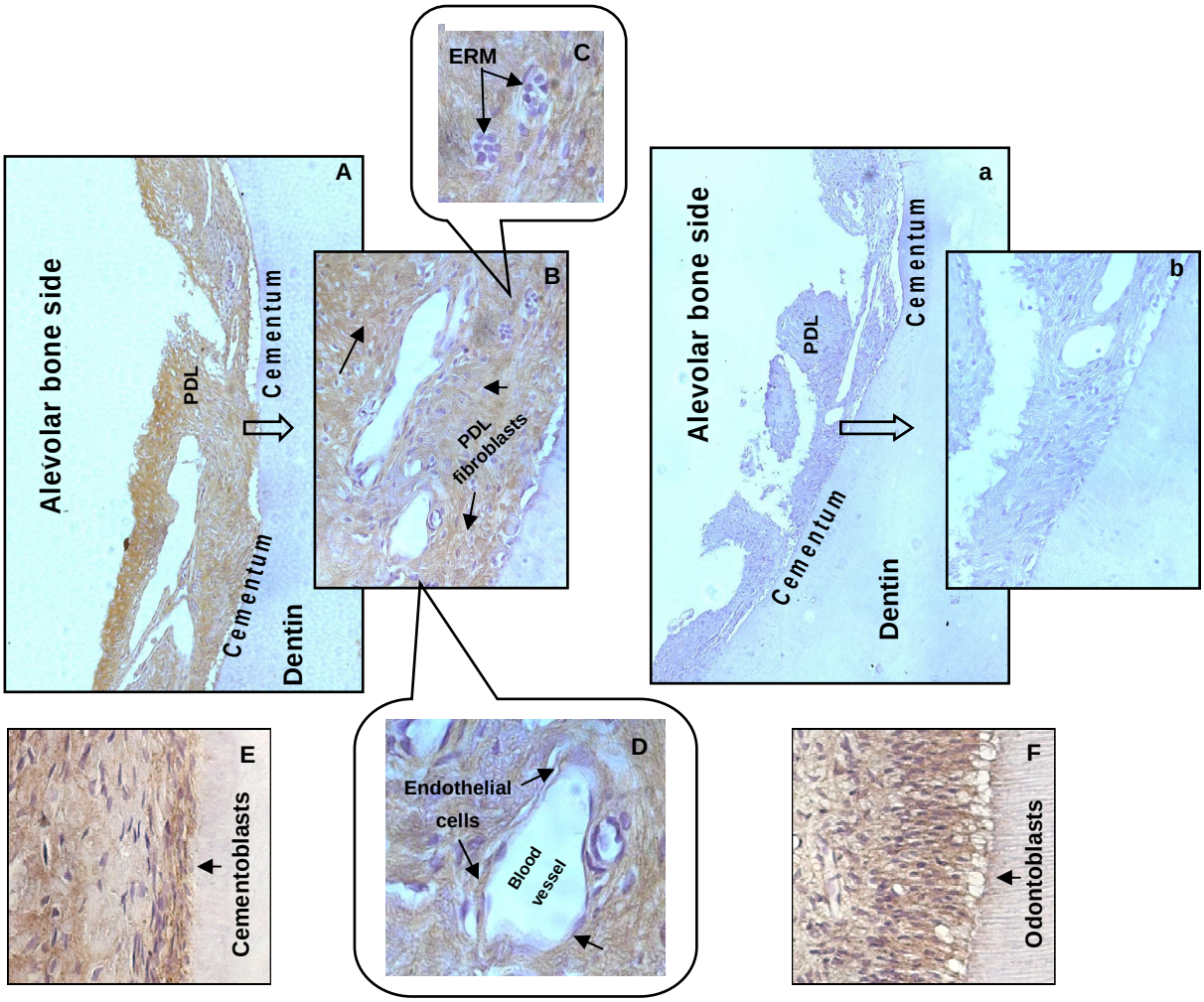

Figure 3.9 Immunohistochemical detection of PTH1R in PDL tissue section of human. A: DAB stained PDL tissue section. Magnification: X100. **B:** X400 magnification of the with arrow indicated area in figure A. Black arrows indicate the PDL fibroblasts. **C:** Black arrows: the epithelial cell rests of Malassez (ERM). Magnification: X400. **D:** Black arrows: endothelial cells. Magnification: X400. **E:** Black arrows: cementoblasts. Magnification: X200. **F:** Black arrows: odontoblasts. Magnification: X200. **a:** Negative control section in which the PTH1R antibody was omitted. Magnification: X100. **b:** X400 magnification of the with arrow indicated area in figure **a**. Magnification x400. The images were acquired with a light microscope. The figure is representative of sections from two separate specimens.

The detection of PTH1R was further extended to *in vitro* by staining the cultured PDL cells using antibody-based methods.

As demonstrated in microscopic images **A** and **B** in Figure 3.10, the PTH1R in cultured PDL cells was visualized with DAB (brown) and Texas Red fluorochrome (red), respectively. Sections stained without the primary antibody served as negative control (Figure 3.10, **a** and **b**).

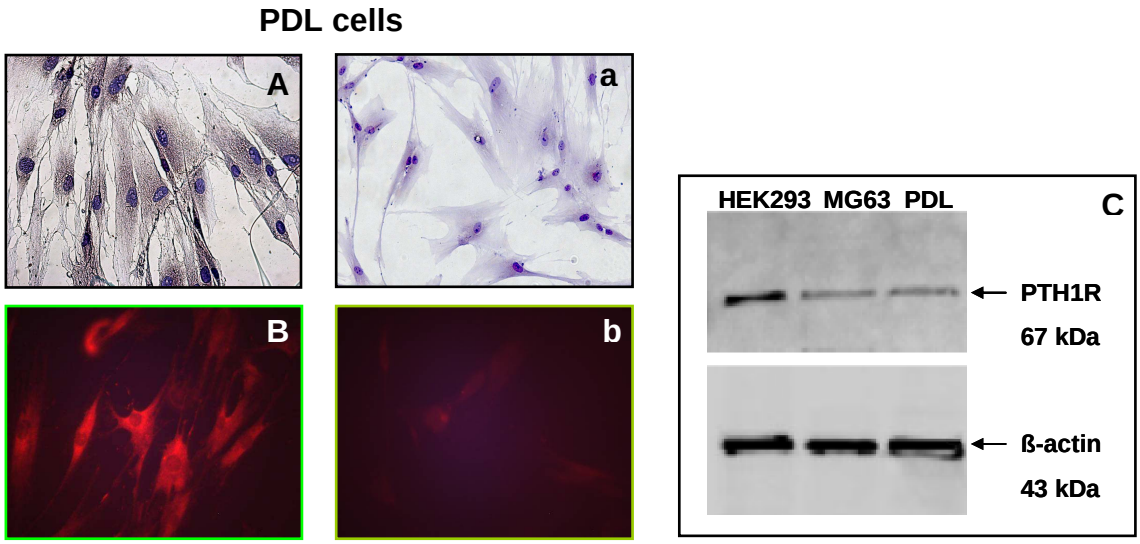

Figure 3.10 Immunohistochemical detection of PTH1R in cultured PDL cells and semi-quantification of PTH1R in PDL, MG63 and HEK293 cells using western blot method. A: PDL cells stained with DAB (brown color). **a:** The negative control section in which the PTH1R antibody was omitted. **B:** Immunofluorescence staining of the PTH1R in PDL cells. For detection, a goat anti - mouse secondary antibody conjugated with Texas Red was used. **b:** The negative control section without the primary antibody. Magnification: X400. The figure is representative of two separate experiments. **C:** Semi-quantification of PTH1R in PDL, MG63 and HEK293 cells using western blot method. Cell lysates of PDL, MG63 and HEK293 cells were resolved by SDS-PAGE and the protein was detected with anti-PTH1R and anti-ß-actin antibody, respectively. In each lane, the same amount of protein was loaded and the protein levels were normalized by β-actin levels.

As next, we investigated the PTH1R protein level in PDL, MG63 and HEK293 cells using westernblot method. As shown in Figure 3.10, **C**, the band detected in HEK293 cells was much more intensive than those of in MG63 and PDL cells, while the intensities of the bands in these latter cell lines were at the same level. These results confirmed the presence of PTH1R at protein level in the three cell lines investigated and showed that HEK293 cells contain much more PTH1R proteins than PDL and MG63 cells, while the amount of this receptor protein was at the same level in the latter cell lines. This finding is in accordance with the result of the mRNA expression level of PTH1R in the three cell lines.

Localization

After having established the immunohistochemical staining of PTH1R, we have addressed the question of the PTH1R localization in PDL, MG63 and HEK293 cells. As expected, a distinct immunostaining of the PTH1R was observed on the plasma membrane of all the three cell lines investigated (Figure 3.11, **A**, **B**, **C** and **D**). However, the strongest immunoreactivity was seen in the cytoplasm of the three cell lines. On the other hand, a weak nuclear staining for PTH1R was seen in MG63 and PDL cells, whereas the nuclei of HEK293 cells were almost devoid of staining. The specificity of the staining was ensured by the negative controls without the primary antibody was omitted (Figure 3.11, **a**, **b**, **c** and **d**).

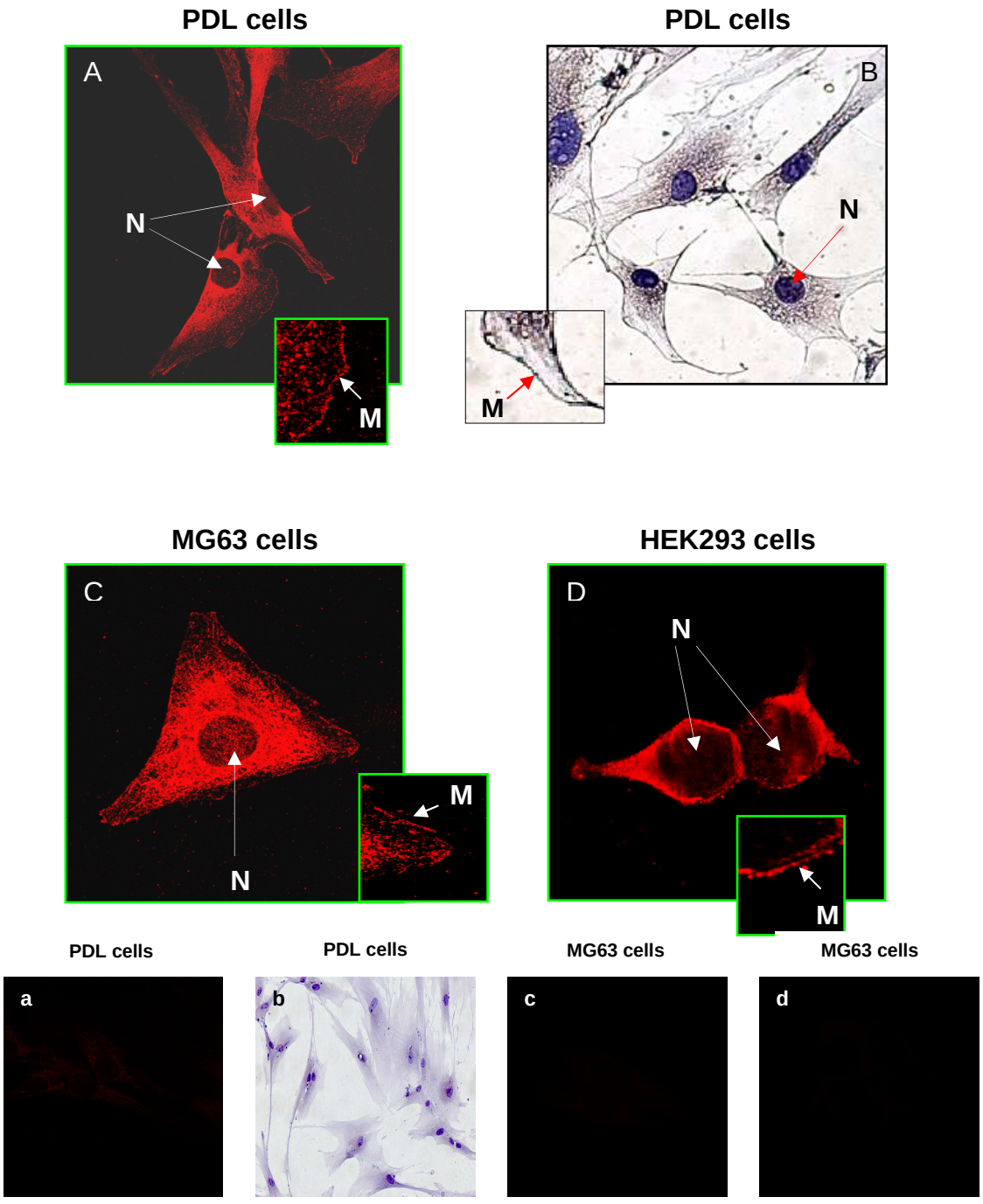

Figure 3.11 Subcellular localization of PTH1R in PDL, MG63 and HEK293 cells. A: PDL cells were stained for PTH1R with Texas Red (red) and examined with a confocal laser scanning microscopy. Magnification: x400. **B:** PDL cells were stained for PTH1R with DAB (brown) and examined with a light microscope. Magnification: x400. **C and D:** MG63 and HEK293 cells were stained for PTH1R with Texas Red (red) and examined with a Leica TCS SP2 confocal laser scanning microscopy. Magnification: X630. The nucleus and plasma membrane were indicated with white arrows. **N:** nucleus; **M:** plasma membrane. Images: **a, b, c and d** are the corresponding negative controls of **A**, **B**, **C** and **D,** respectively.

Internalization of PTH1R

Agonist activation of G protein-coupled receptor (GPCR) results in the redistribution of the receptor protein away from the cell surface into internal cellular compartments through a process of endocytosis known as internalization. To demonstrate the internalization of the PTH1R from the plasma membrane upon ligand binding, PDL, MG63 and HEK293 cells were challenged with 10^{-7} M hPTH (1-34) for 30 min and stained for PTH1R.

As shown with white arrows in Figure 3.12, the hPTH (1-34) treatment for the indicated period of time reduced dramatically the Texas Red fluorescence signal on the plasma membrane of PDL and MG63 cells. However, since HEK293 cells have a relative small cytoplasm and large nucleus, the difference in the fluorescence signal intensity on the plasma membrane could not be distinguished.

The internalization process further confirmed the presence of functional PTH1R in PDL and MG63 cells. Regarding HEK293 cells, this process needs to be visualised by other approaches.

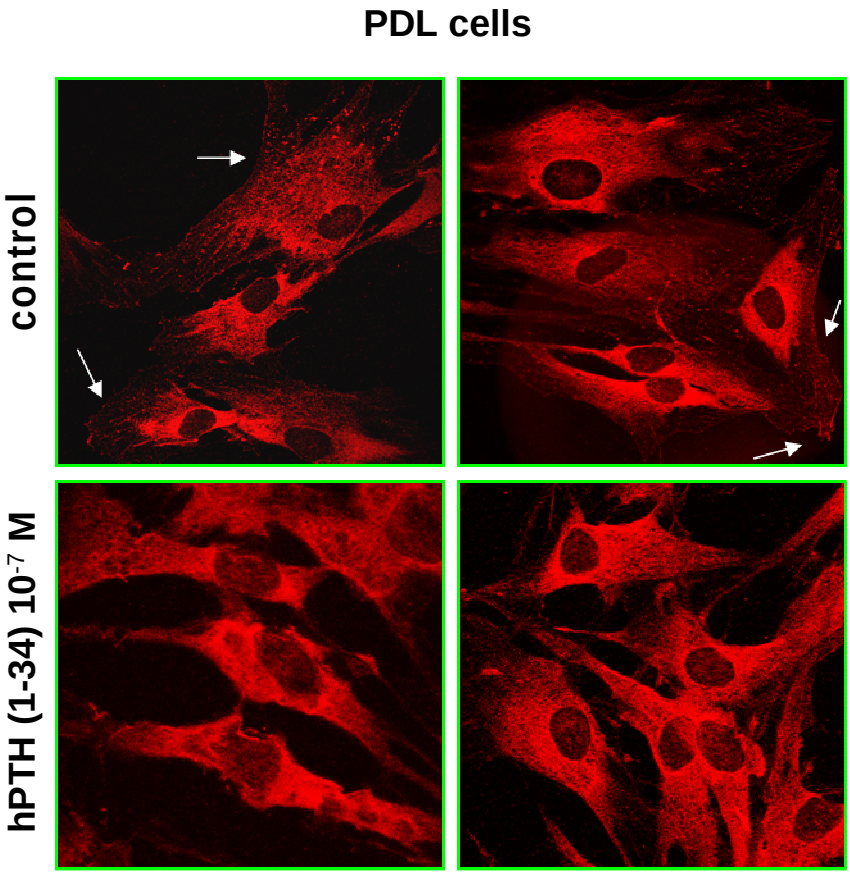
PDL cells
control
hPTH (1-34) 10-7 M

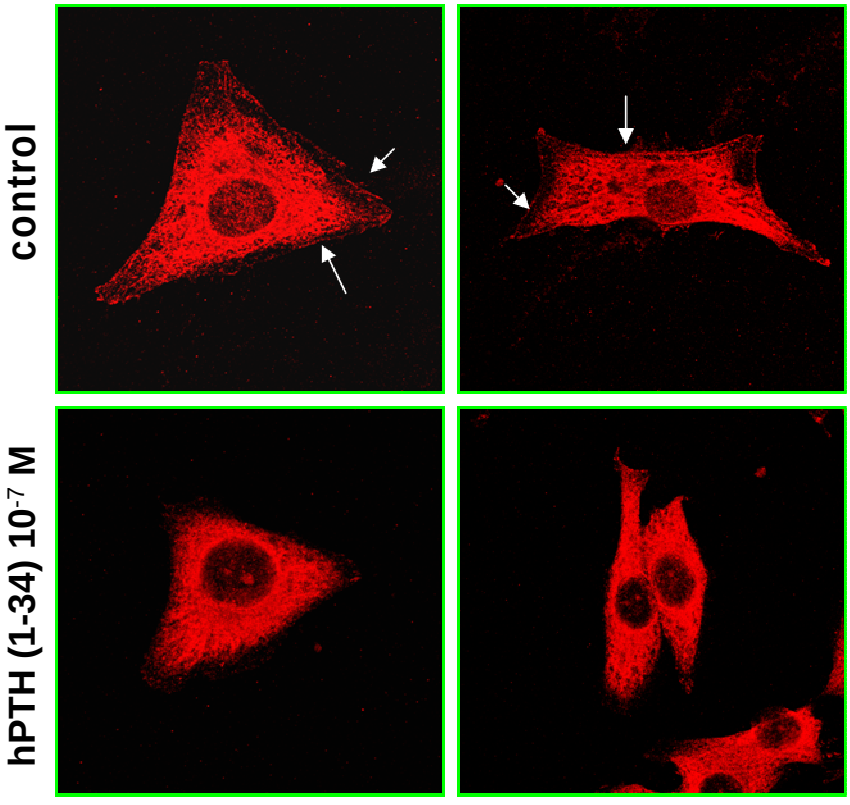
MG63 cells
control
hPTH (1-34) 10-7 M

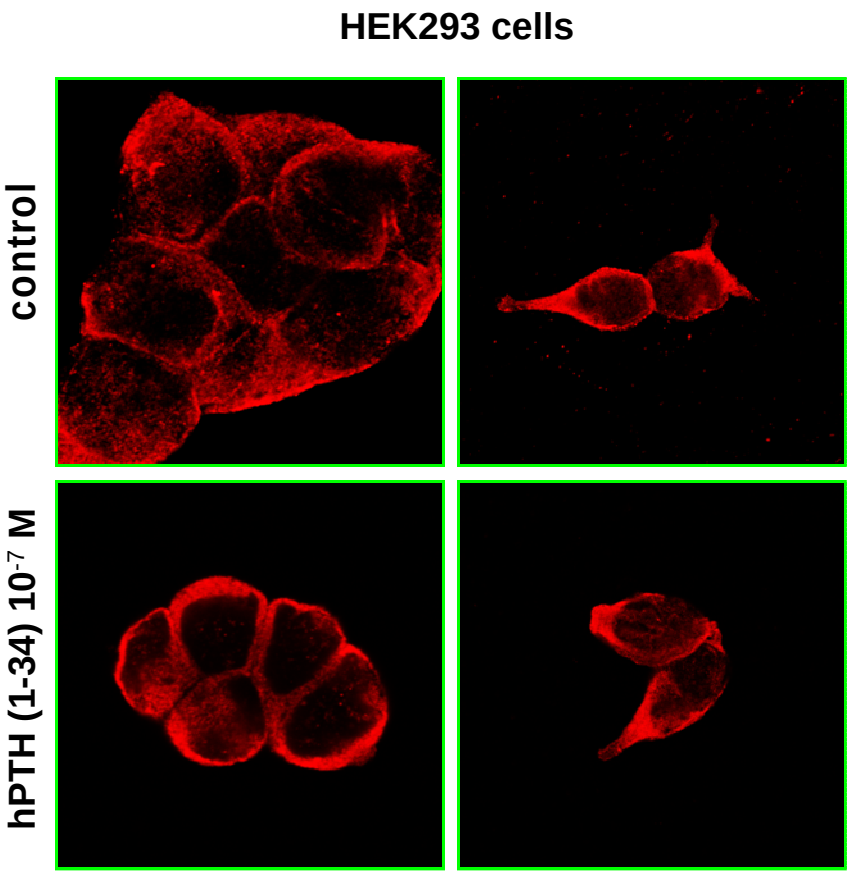

Figure 3.12 Internalization of PTH1R in PDL, MG63 and HEK293 cells. PDL, MG63 and HEK293 cells were stimulated with 10^{-7} M hPTH (1-34) for 30 min and subsequently stained for PTH1R with Texas Red (red). In control groups, PDL, MG63 and HEK293 cells were treated with vehicle for 30 min and subsequently stained for PTH1R with Texas Red. The specimens were examined with a Leica TCS SP2 confocal laser scanning microscopy. Magnification: X630. The detected PTH1R on the plasma membrane were indicated with white arrows. The figures are representative of two separate experiments.

3.5 Flow cytometry analysis of the PTH1R-positive subpopulation in PDL, MG63 and HEK293 cells

Albeit morphological homogeneity, PDL cells are considered to contain a variety of subpopulations with different functional characteristics. On the other hand, previous studies showed that MG63 cell line is representative of early undifferentiated osteoblast-like cells. Although HEK293 cells were originally derived from embryonic kidney, the exact cellular origin of these cells is still unclear, as embryonic kidney cultures may contain small numbers of almost all cell types of the body. These facts

lead to the question of whether these cell lines possess distinct subpopulations, which present PTH1R. To address this question, we analysed PDL, MG63 and HEK293 cells using a flow cytometery. To this end, we have established a protocol for the cell sorting analysis and optimized the antibody concentration.

First, the living cells were sorted, as the antibody cannot penetrate the intact membrane effectively and can only bind the epitope in the extracellular part of the PTH1R on the plasma membrane. In each experiment, data from at least 10,000 cells was acquired and analyzed with FlowJo 7.6.1 software. Dead cells were excluded using a commercially available dead cell staining kit. In the course of data processing, cell clumps and debris were distinguished from the main population by gating the cells on the scatter plots with forward scatter (FSC) vs. side scatter (SSC). The forward scatter represents the size, and side scatter the granularity of cells (Figure 3.13, **A**). Subsequently, the gated cell population was further analyzed on the dot plot with the X-axis representing the fluorescence intensity of the fluorescent reactive dye used for dead cell discrimination and Y-axis representing the Alexa Fluor 647 dye. Mouse IgG1 monoclonal antibody served as isotype control (Figure 3.13, **B, D and F**). The upper right quadrant (Q2) of each plot indicates the dead cells that are positive for PTH1R. The Q3 represents the PTH1R-positive cells, which are intact (Figure 3.13, **C, E and G**).

After gating out dead cells, no PTH1R-positive subpopulation was detected in PDL cells, while almost all of the HEK293 cells were positive for PTH1R. In contrast, approximately 40% of MG63 cells were positive for PTH1R, indicating the presence of a subpopulation which contains PTH1R (Figure 3.14).

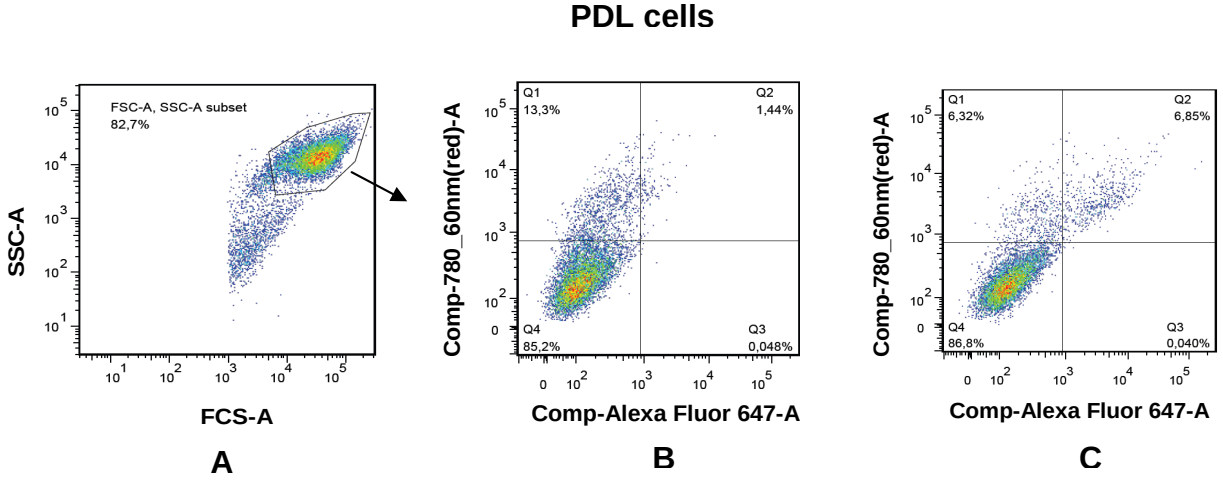

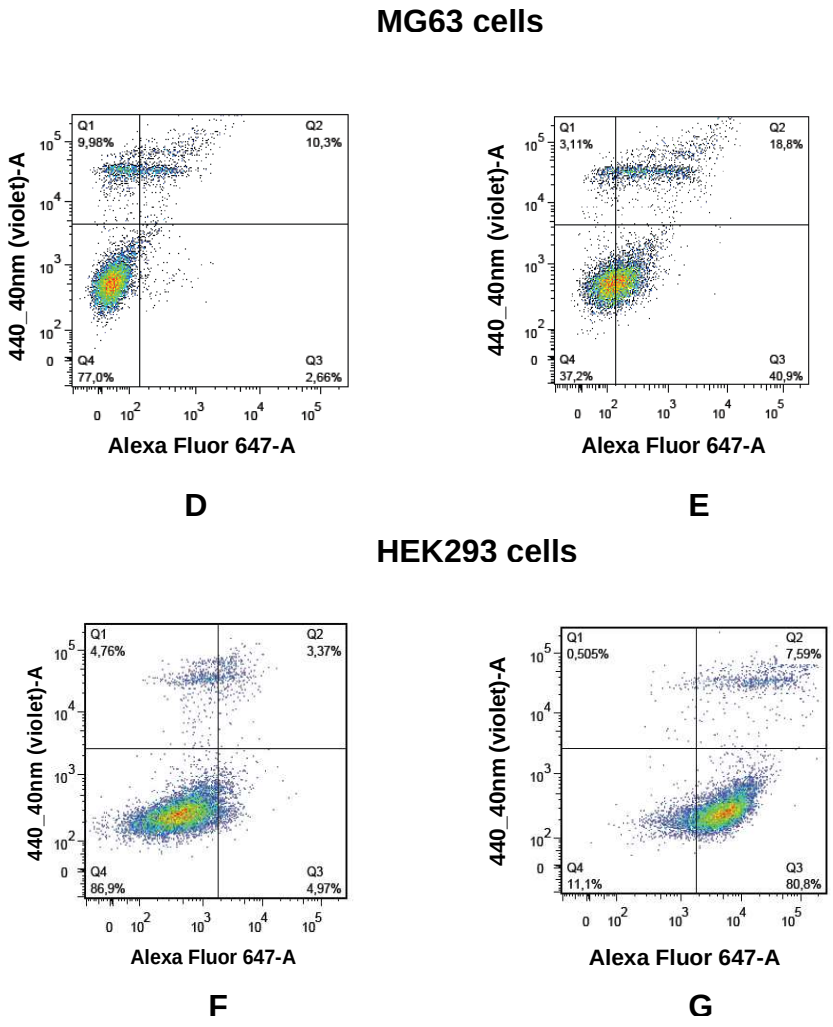

Figure 3.13 Flow cytometry analysis of PTH1R-positive subpopulation in intact PDL, MG63 and HEK293 cells. A: A representative scatter plot. Cell clumps and debris were discriminated by gating the main population of PDL cells (circled). X-axis represents side scatter (SSC-A) and Y-axis represents forward scatter (FSC-A). **B, D and F:** Representatives of flow cytometry analysis of isotype control (mouse monoclonal antibody) treated cells. **C, E and G:** Representatives of flow cytometry analysis of PTH1R-positive subpopulation in cells. Dots in lower right quadrant (Q3) represent the intact PTH1R-positive cells.

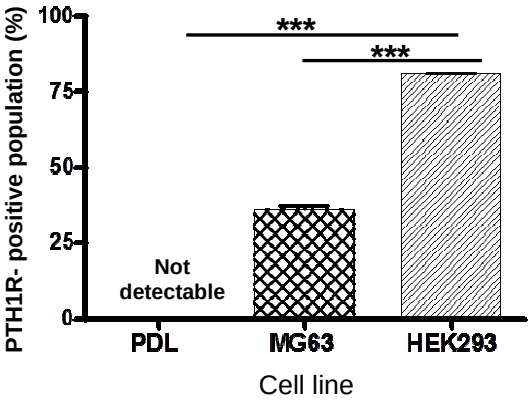

Figure 3.14 Quantification of PTH1R-positive subpopulations in PDL, MG63 and HEK293 cells. Y-axis: Portion of intact cells positive for PTH1R (%). Data were acquired from one of two separate experiments, both yielding comparable results. Each value represents the mean + SEM for 6 independent cultures. ***** :** P<0.001 (Dunnett-test).

We next permeabilized the cells and stained intracellular PTH1R. To this end, prior to the staining, the cells were fixed and subsequently permeabilized with a commercial kit. After gating the main population of cells, the SSC was plotted against Alexa Fluor 647 on the Y-axis. Mouse IgG1 monoclonal antibody served as isotype control. In this case, all three cell lines showed ~100% positive population for PTH1R (blue circled region) (Figure 3.15).

Taken together, in terms of surface PTH1R, we could observe a distinct PTH1R-positive subpopulation in MG63 cells, but not in HEK293 cells. Regarding PDL cells, because of the used PTH1R antibody's inaccessibility to the surface antigen in living PDL cells, we could not detect any PTH1R-positive subpopulation. However, after permeabilization, all of the three cell lines were almost 100% positive for PTH1R.

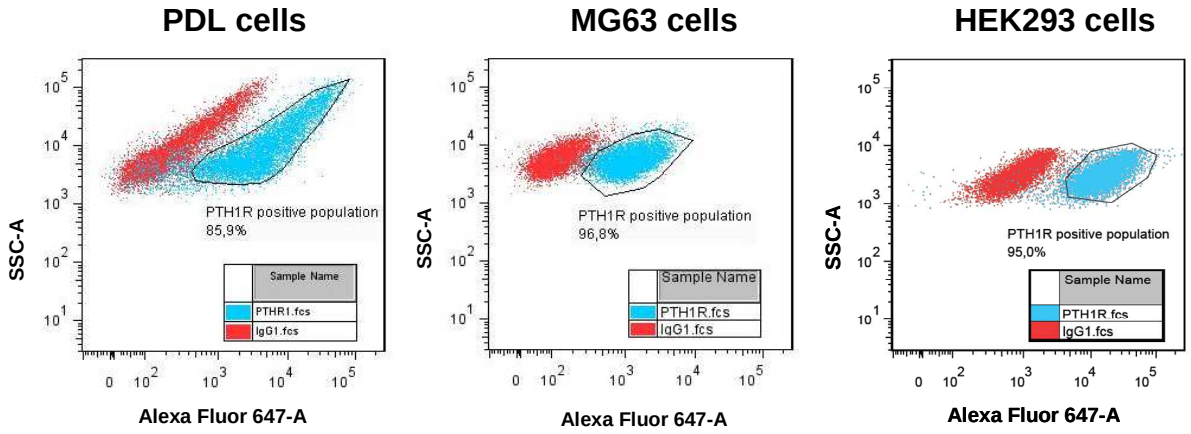

Figure 3.15 Flow cytometry analysis of PTH1R-positive subpopulation in fixed and permeabilized PDL, MG63 and HEK293 cells. Cell clumps and debris were discriminated by gating the main population of cells. X-axis represents side scatter (SSC-A) and Y-axis represents Alexa Fluor 647 dye. The population in red represents the isotype control (mouse monoclonal antibody) treated cells, as negative control. The population in blue represent the PTH1R-positive cells.

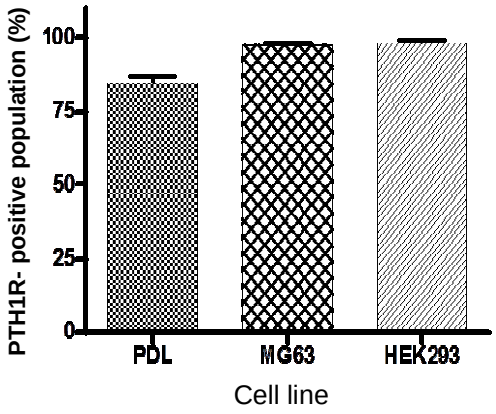

Figure 3.16 Quantification of PTH1R-positive subpopulations in fixed and permeabilized PDL, MG63 and HEK293 cells. Y-axis: Portion of cells positive for PTH1R (%). Data were acquired from one of two separate experiments, both yielding comparable results. Each value represents the mean + SEM for 6 independent cultures.

3.6 Binding characteristics of PTH1R and its density

The binding affinity and density of PTH1R have been intensively studied in osteoblast-like cells as well as in PTH1-transfected HEK293 cells, however not yet in PDL cells. To fill the gap, we assessed the binding characteristics of the PTH1R in

PDL, MG63 and HEK293 cells using a homologous competitive binding assay. In this assay, a constant concentration of radioactive labelled ligand, h[^{125}I]-[Nle^{8,18}, Tyr^{34}]-PTH (1-34) competed with a series of concentrations of its unlabelled homologous, hPTH (1-34) for the binding sites. The acquired data was analyzed with the nonlinear curve-fitting program of GraphPad PRISM™ 4.0 and IC_{50} (inhibitory concentration 50%) was determined. Binding affinity (K_d) and receptor density (B_{max}) were calculated by the equation of Cheng and Prusoff using IC_{50} values and the concentration of radioligand, as stated in materials and methods.

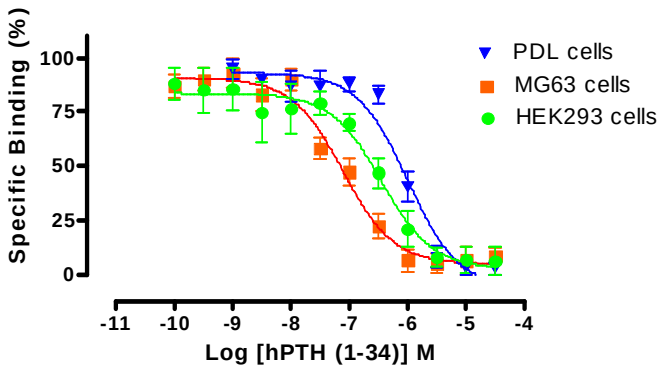

Cell line	Receptor density Receptors/ cell million	Kd (nM)
PDL	3.03 ± 0.57	1030 ± 10
MG63	0.365 ± 0.1	80.1 ± 20.2
HEK293	2.27 ± 1.4	670 ± 417

Figure 3.17 Binding characteristics of PTH1R in PDL, MG63 and HEK293 cells. In the graphic, the competitive binding curves of hPTH (1-34) against [^{125}I]-[Nle^{8,18}, Tyr^{34}]-PTH 1-34 (h) in PDL (▼), MG63 (■) and HEK293 cells (●) are shown. Y-axis: specific binding (%). X-axis: concentrations of hPTH (1-34), respectively: $10^{-4.5}$,10^{-5},$10^{-5.5}$,10^{-6},$10^{-6.5}$,10^{-7},$10^{-7.5}$,10^{-8},$10^{-8.5}$,10^{-9},$10^{-9.5}$,10^{-10} M. In the table, the estimated K_d and B_{max} values for PTH1Rs in PDL (blue), MG63 (red) and HEK293 cells (green) are shown. Data represent the average (± SD) of two independent experiments**,** each performed in triplicate.

Among the three cell lines, the binding affinity of hPTH (1-34) to PTH1R in PDL cells was the lowest (K_d=1030±10 nM), while the PTH1R density in this cell line was the highest (3.03±0.57 million receptors/cell). The highest binding affinity was estimated in MG63 cells (K_d=80.1±20.2 nM), with the lowest receptor density (0.365±0.1 million receptors/cell. The binding affinity of hPTH (1-34) and the receptor density in HEK293 cells were K_d=670±417 nM and 2.27±1.4 million receptors/cell respectively, and these two values reside between those of PDL and MG63 cells.

3.7 Regulation of PTH1R gene expression in PDL cells

It is well established that the expression of PTH1R mRNA in osteoblasts is regulated by extracellular factors, such as dexamethason (Ureña et al., 1994a; Yaghoobian and Drüeke, 1998; Haramoto et al., 2007), 1,25-dihydroxyvitamin D_3 (Xie et al., 1996; Sneddon et al., 1998) and PTH (Jongen et al., 1996). Accordingly, we investigated the effects of these factors on the expression level of PTH1R mRNA in PDL cells. For this aim, PDL cells of three donors were stimulated with 10^{-6} M dexamethason, 10^{-7} M $1,25(OH)_2$ D_3 and 10^{-8} M hPTH (1-34) and the gene expression level was assessed using real time PCR method.

Dexamethason

As illustrated in Figure 3.18, **A**, stimulation with 10^{-6} M dexamethason led to a significant increase in PTH1R mRNA level over a period of 21 days, resulting in a 148-fold higher level compared to the untreated group on day 1. In the corresponding control groups, the PTH1R mRNA level also increased in a time-dependent manner.
The effect of dexamethason on PTH1R gene expression increased with the time in the first four days, with the highest increase in PTH1R mRNA level on the 4th day (~12-fold of the corresponding control group), as shown in graphic **B** (Figure 3.18). Thereafter, the effect of dexamethason declined gradually, resulting in the decrease of the PTH1R gene expression. Correspondingly, the relative increase in the PTH1R mRNA level on the 14th and 21st day dropped to ~3-fold of that of the control groups. (Figure 3.18, **B**).

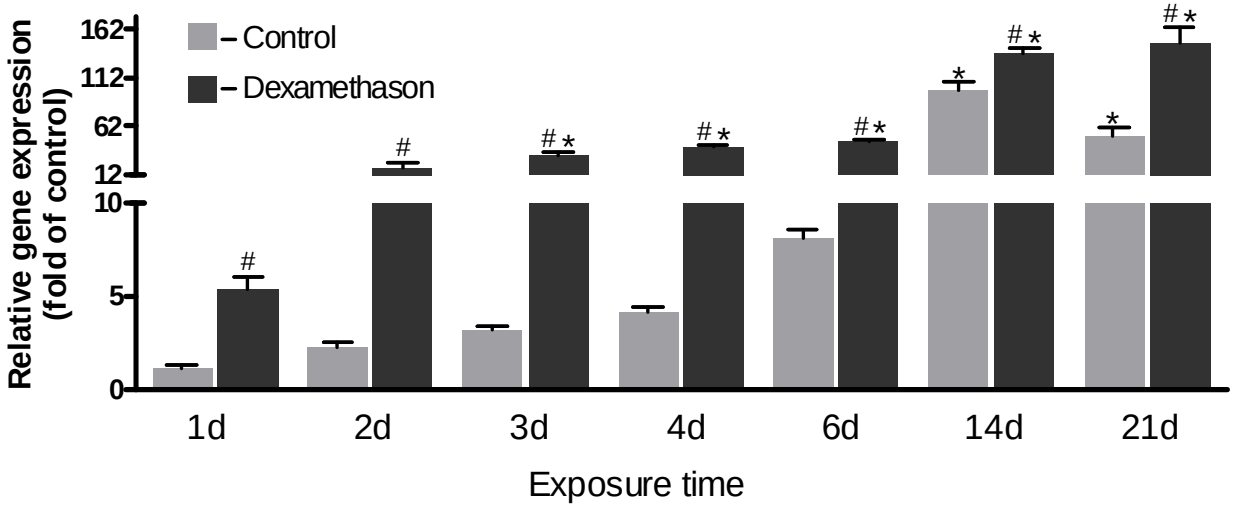

A

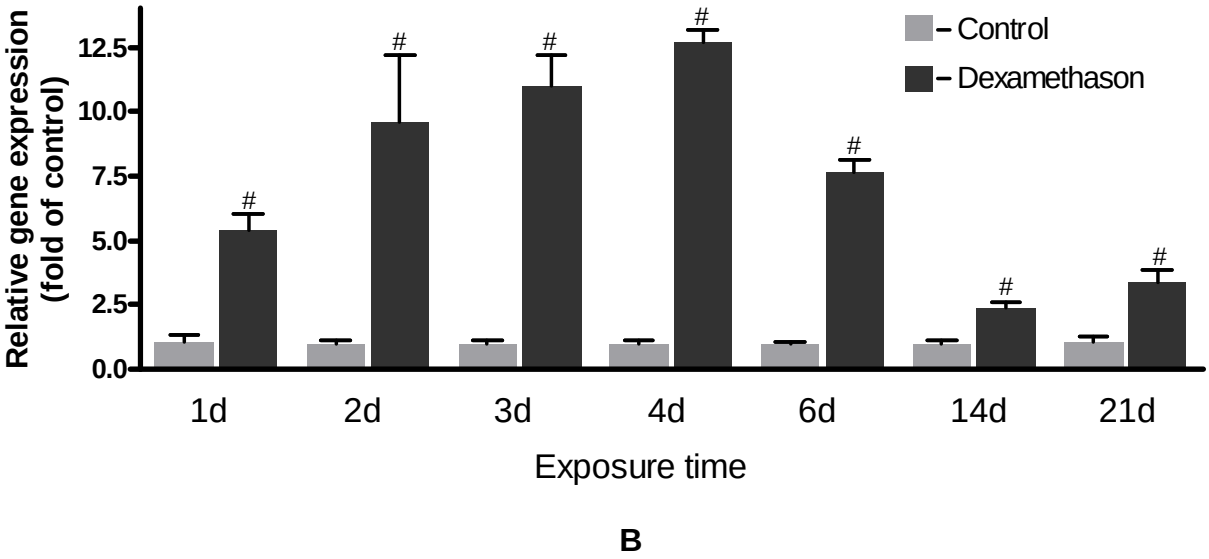

Figure 3.18 Effect of 10^{-6} M dexamethason on mRNA level of PTH1R in PDL cells. The effect of dexamethason (10^{-6} M) on PDL cells of three donors was studied using real time PCR. Data were acquired from one of two separate experiments, both yielding comparable results. Each value represents the mean ±SEM for 6 independent cultures. **A:** Comparison of all the experimental groups and vehicle-treated controls to the vehicle-treated control of the 1st day. The vehicle-treated control on the 1st day was taken as reference for normalization. **# :** P<0.05 (t-test), experimental group vs. vehicle-treated control (at the same time point); ***** : vehicle-treated controls on the fist day vs. all other vehicle-treated controls and experimental groups (Dunnett-test). **B:** Comparison of experimental groups to corresponding vehicle-treated control (at the same time point). Each experimental group was normalized to the corresponding control group (at the same time point). **# :** P<0.05 (t-test), experimental group vs. corresponding vehicle-treated control.

1,25-dihydroxyvitamin D_3

Over the 6 days of stimulation with 10^{-7}M 1,25-dihydroxyvitamin D_3, the PTH1R mRNA level was increased in a time-dependent manner, with the highest level on 6th day (~10-fold of the control group of the 1st day, as shown in graphic **A** (Figure 3.19). In the control groups, the mRNA level of PTH1R also increased with the time.

An apparent effect of 1,25-dihydroxyvitamin D_3 was seen on the 6th day of stimulation, with an increase of ~14-fold over the corresponding control group, as illustrated in graphic **B** (Figure 3.19).

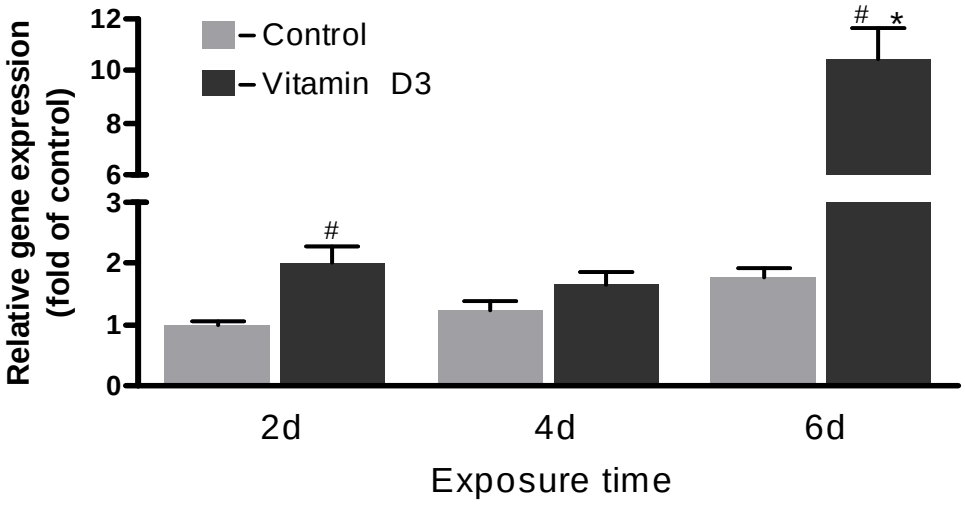

A

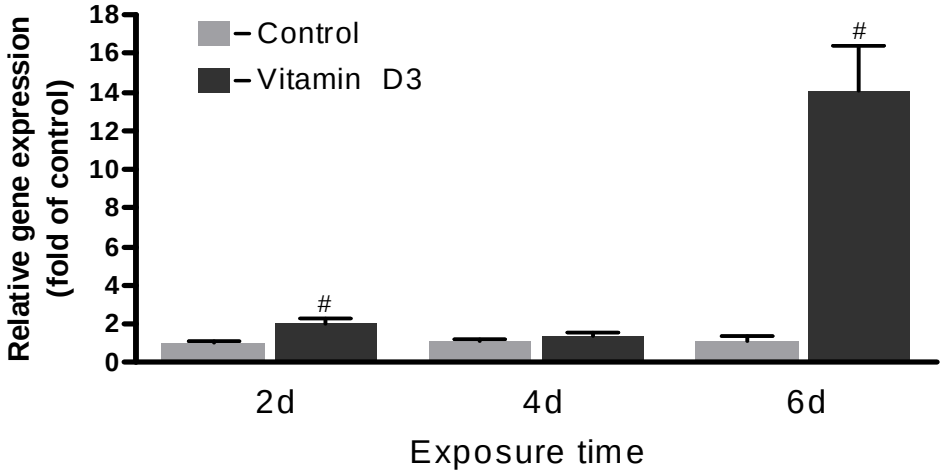

B

Figure 3.19 Effect of 10^{-7} M 1,25-dihydroxyvitamin D3 on the gene expression level of PTH1R in PDL cells. The effect of 1,25-dihydroxyvitamin D_3 (10^{-7} M) on PDL cells of three donors was studied using real time PCR. Data were acquired from one of two separate experiments, both yielding comparable results. Each value represents the mean ±SEM for 6 independent cultures. **A:** Comparison of all the experimental groups and vehicle-treated controls to the vehicle-treated control on the 1st day. The vehicle-treated control on the 1st day was taken as reference for normalization. **# :** P<0.05 (t-test), experimental group vs. vehicle-treated control (at the same time point); ***** : vehicle-treated controls on the first day vs. all other vehicle-treated controls and experimental groups (Dunnett-test). **B:** Comparison of experimental groups to corresponding vehicle-treated control (at the same time point). Each experimental group was normalized to the corresponding control group (at the same time point). **# :** P<0.05 (t-test), experimental group vs. vehicle-treated control (at the same time point).

hPTH (1-34)

PDL cells were exposed to 10^{-8} M hPTH (1-34) continuously as well as intermittently for 1 h and 24 h within 3 incubation cycles of 48 h each. In the first cycle, PTH1R mRNA expression was increased ~1.7-fold by 1h intermittent treatment and ~2.5-fold by continuous treatment (48h), but decreased ~2-fold by 24 h intermittent treatment, compared to the control group (Figure 3.20, **A**). In the second cycle, the mRNA level of PTH1R was further elevated to ~3-fold by the 1 h hPTH (1-34) application (Figure 3.20, **B**). The 24 h/cycle intermittent treatment further decreased PTH1R mRNA expression to ~20% of the control (Figure 3.20, **C**). However, when hPTH (1-34) was continuously applied for 96 h, the PTH1R mRNA level was significantly down-regulated to ~0.5-fold of the control group, which was a ~5-fold drop compared to the same treatment in the first cycle (Figure 3.20, **D**). In the third cycle of treatment, the PTH1R mRNA level fell back almost to control levels, regardless of intermittent or continuous application of hPTH (1-34) (Figure 3.20, **A**).

Taken together, a distinct effect of the hPTH (1-34) on PTH1R gene regulation was observed in the first two cycles of treatment. While the 1 h intermittent exposure up-regulated PTH1R gene expression, 24 h intermittent administration inhibited it. The continuous administration of this peptide elevated the gene expression of PTH1R in the first cycle, but took an opposite effect in the second cycle and decreased the gene expression of PTH1R.

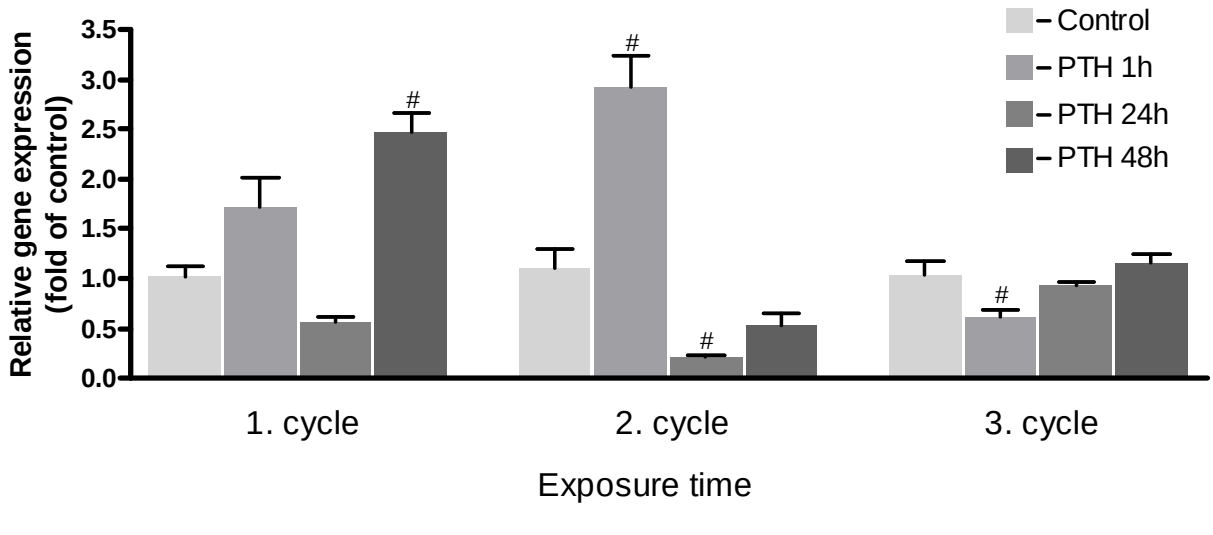

A

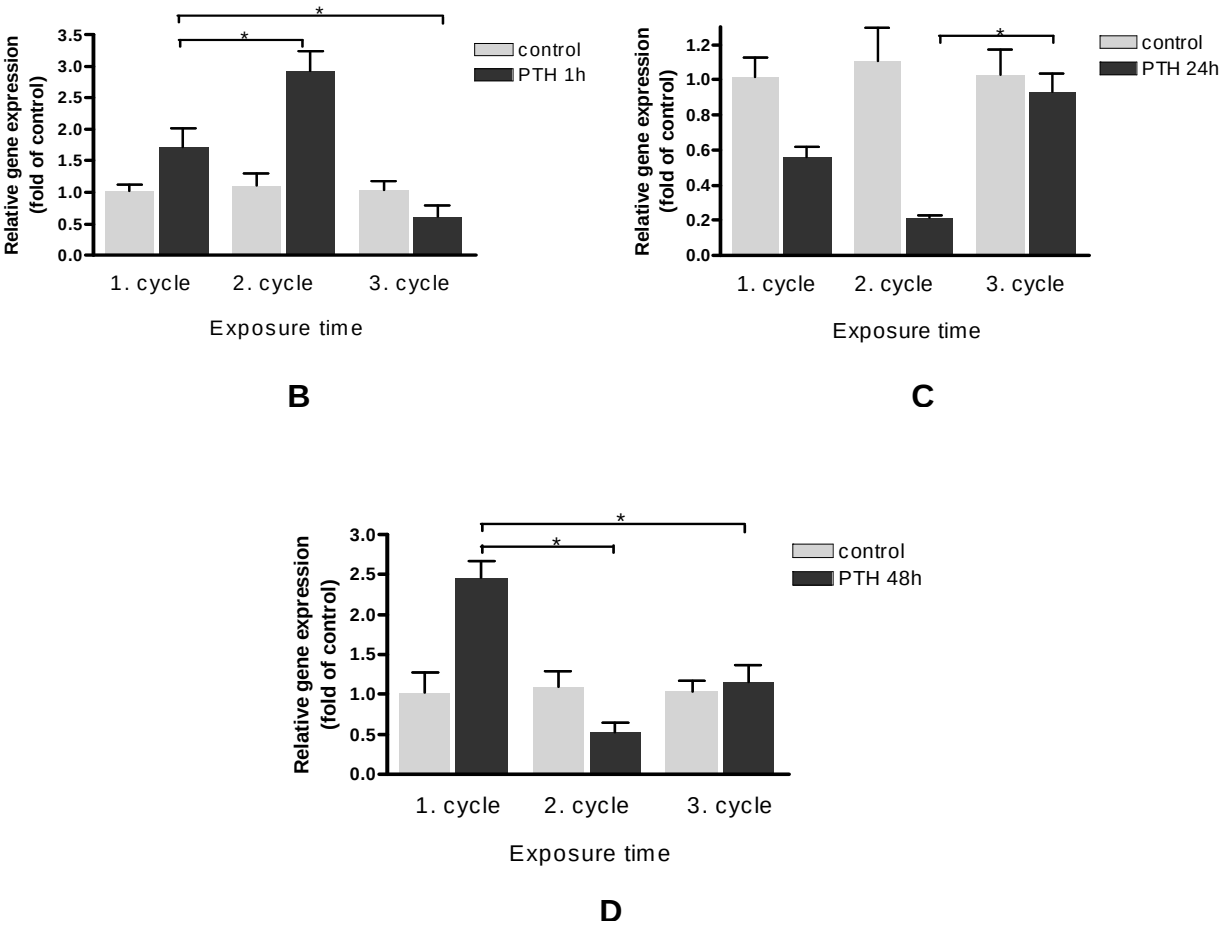

Figure 3.20 Effect of 10^{-8} M hPTH (1-34) on the gene expression level of PTH1R in PDL cells. The effect of intermittent (exposed respectively for 1 h and 24 h) and continuous application of hPTH (1-34) (10^{-8} M) on PDL cells of three donors was studied using Real time PCR. Data were acquired from one of two separate experiments, both yielding comparable results. Each value represents the mean ±SEM for 6 independent cultures. **A:** Graphic of all three incubation cycles. The vehicle-treated control in each cycle was taken as reference for normalization. **# :** P<0.05 (Dunnett-test), vehicle-treated control vs. each experimental group (in each cycle). **B:** Graphic of 1 h intermittent hPTH (1-34) (10^{-8} M) treatment in 3 incubation cycles. **C:** Graphic of 24 h/cycle intermittent hPTH (1-34) (10^{-8} M) treatment in 3 incubation cycles. **D:** Graphic of continuous hPTH (1-34) (10^{-8} M) treatment in 3 incubation cycles**.** In Graphic **B, C and D, * :** P<0.05 (Tukey's test).

3.8 Signal transduction of PTH1R

Upon ligand binding, PTH1R activates mainly two signalingpathways: cAMP/PKC and PLC/PKA (Mannstadt et al., 1999), which, in turn, regulate the downstream physiological response of cells. To elucidate the signal transduction of PTH1R, we exposed PDL cells of three donors, MG63 and HEK293 cells to 10^{-6}, 10^{-7}, 10^{-8}, 10^{-9},

10^{-10} and 10^{-12} M hPTH (1-34) for 15 min and measured for cAMP accumulation level and PKC activity.

cAMP accumulation

The cAMP production of PDL cells in response to hPTH (1-34) after 15 min was not accumulative, but rather concentration-dependent (Figure 3.21, **A**). The highest effect of hPTH (1-34) on PDL cells was seen at 10^{-12} M with a more than 120% increase, followed by a ~90% increase at 10^{-8} M. cAMP accumulation was also observed at 10^{-7} M treatment with a 60% increase. The PDL cells showed no apparent change in cAMP level, when exposed to 10^{-10}, 10^{-9} and10^{-6} M hPTH (1-34).
In HEK293 cells, low concentrations of hPTH (1-34) (10^{-12} and 10^{-10} M) did not induce apparent changes in the cAMP accumulation (Figure 3.21, **C**). The first response of cAMP to hPTH (1-34) stimulation was observed at 10^{-9} M, with a ~70% increase in the cAMP level compared to the control group. After a slight decrease at 10^{-8} M, the cAMP accumulation was increased to the highest level at 10^{-7} M of hPTH (1-34), with a ~230% increase in cAMP level in contrast to the control. The second highest response of cAMP to hPTH (1-34) was detected at concentration of 10^{-6} M, with a ~120% increase in cAMP level (compared to control)
Like HEK293 cells, the MG63 cells triggered no apparent response in terms of cAMP accumulation until stimulated with 10^{-9} M hPTH (1-34) (Figure 3.21, **B**). After a slight increase at 10^{-9} M, cAMP production dropped by ~35 % from the baseline level, when treated with 10^{-8} M hPTH (1-34). The highest cAMP accumulation was induced by10^{-6} M hPTH (1-34) with 40% increase from the baseline level.
The baseline cAMP production was not at the same level in the three cell lines studied. (PDL cells: 18.26 pmol/mg total protein, MG63 cells: 15.56 pmol/mg total protein and HEK293: 10.62 pmol/mg total protein) (Figure 3.21, **D**). No change in cAMP level was observed in all three cell lines, when exposed to 10^{-10} and 10^{-9} M hPTH (1-34). Another similarity was seen at the 10^{-7} M of hPTH (1-34), with a significant increase in the cAMP production in all the three cell lines. When subjected to 10^{-12} and 10^{-8} M hPTH (1-34), PDL cells demonstrated a significantly higher increase in the cAMP accumulation compared to MG63 and HEK293 cells.

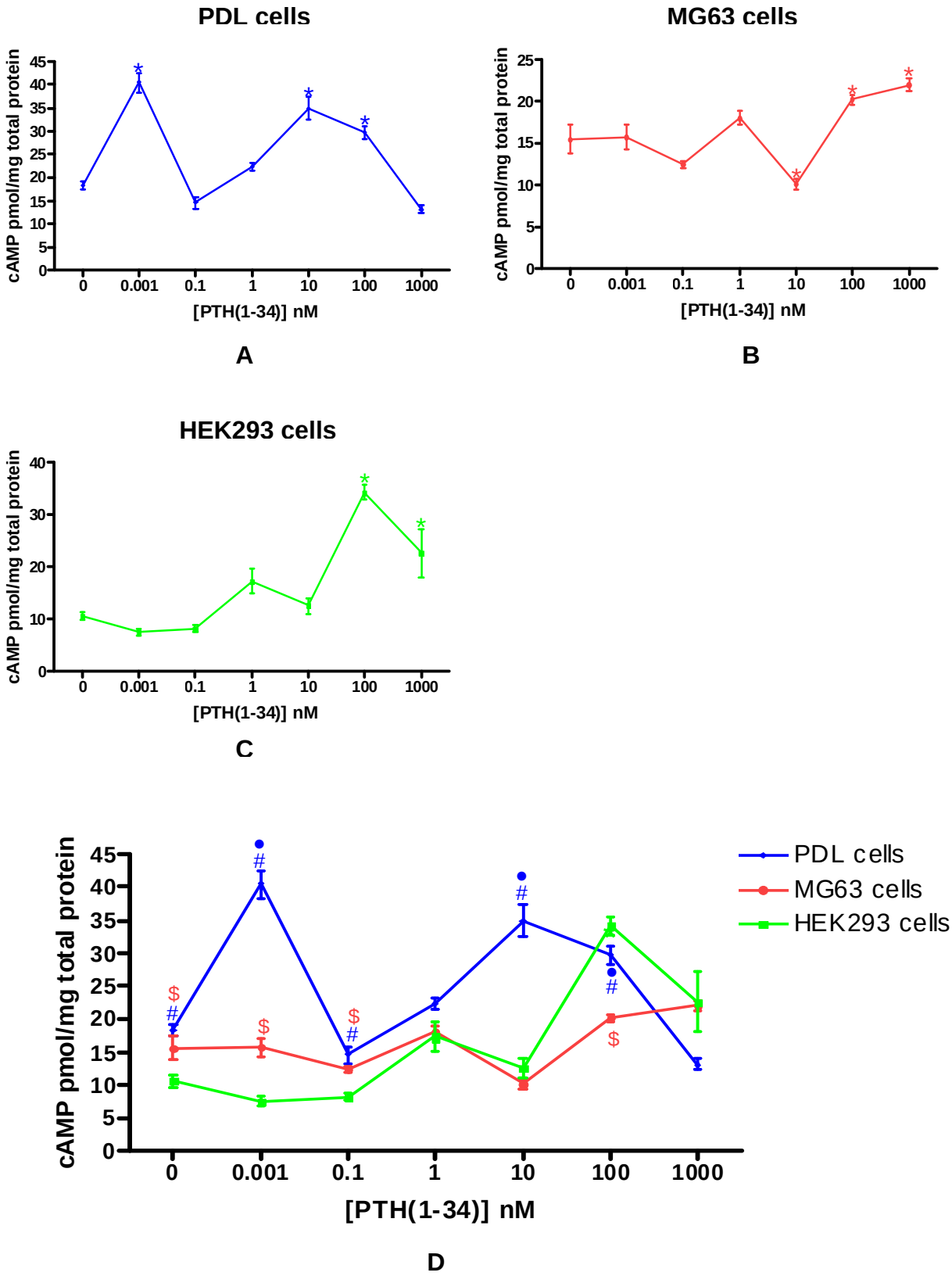

Figure 3.21 Effect of hPTH (1-34) on cAMP accumulation in PDL, MG63 and HEK293 cells. The effect of hPTH (1-34) on cAMP production was analysed after 15 min of stimulation using a commercial cAMP assay kit. Each value represents the mean ± SEM for 6 independent experiments. **A:** cAMP accumulation upon hPTH (1-

34) stimulation in PDL cells. **B:** cAMP accumulation upon hPTH (1-34) stimulation in MG63 cells. **C:** cAMP accumulation upon hPTH (1-34) stimulation in HEK293 cells. In Graphic**, A, B and C, * :** P<0.05 (Dunnett-test), vehicle-treated control vs. each experimental group. **D:** Comparison of cAMP accumulation in the three cell lines studied in response to hPTH (1-34) stimulation. **# :** P<0.05 PDL cells vs. HEK293 cells, **● :** P<0.05 PDL cells vs. MG63 cells, $ **:** P<0.05 MG63 cells vs. HEK293 cells (Tukey's test).

PKC activity

The activity of PKC was assessed by quantifying the active PKC protein, which was produced in PDL, MG63 and HEK293 cells upon the stimulation with hPTH (1-34) for 15 min.

In PDL cells, the production of active PKC protein was again dependent on the concentration of hPTH (1-34) (Figure 3.22, **A**). At first, the level of the active PKC protein dropped slightly at 10^{-12} M and then increased to the highest level at 10^{-10} M (~23% increase). The 10^{-9} M stimulation had almost the same effect as the 10^{-10} M stimulation. The lowest active PKC amount was seen at 10^{-8} M with ~66% decrease, followed by ~36% decrease at 10^{-7} M (compared to control group). Stimulation with 10^{-6} M hPTH (1-34) caused almost no change in the baseline level of active PKC protein.

The response of MG63 to the stimulation was different from the other two cell lines (Figure 3.22, **B**). The effect of hPTH (1-34) was first seen at 10^{-9} M with ~43% decrease, which was then slightly up-regulated at 10^{-8} M (~20%). At concentrations 10^{-7} M and 10^{-8} M, hPTH (1-34) demonstrated the same effect as observed with 10^{-9} M treatment.

In HEK293 cells, the amount of active PKC protein declined gradually from the baseline level to the lowest level, until 10^{-9} M treatment (~30% decrease from the baseline level) and was then subsequently up-regulated to the highest level with ~24%, at 10^{-6} M (Figure 3.22, **C**).

In average, the baseline amount of the active PKC protein in PDL cells was 5~7-fold higher than that in MG63 and HEK293 cells, while the last two cell lines produced almost the same baseline level of the active PKC protein.

When the plots were combined into one graph, the response of the active PKC protein production to hPTH (1-34) stimulation in each cell line revealed an almost opposite direction of cAMP accumulation (Figure 3.22, **D, E and F**). At a given point of hPTH (1-34) stimulation, if the cAMP accumulation was up or down-regulated, the

active PKC protein level was down or up-regulated and the magnitude of the response was almost at the same level.

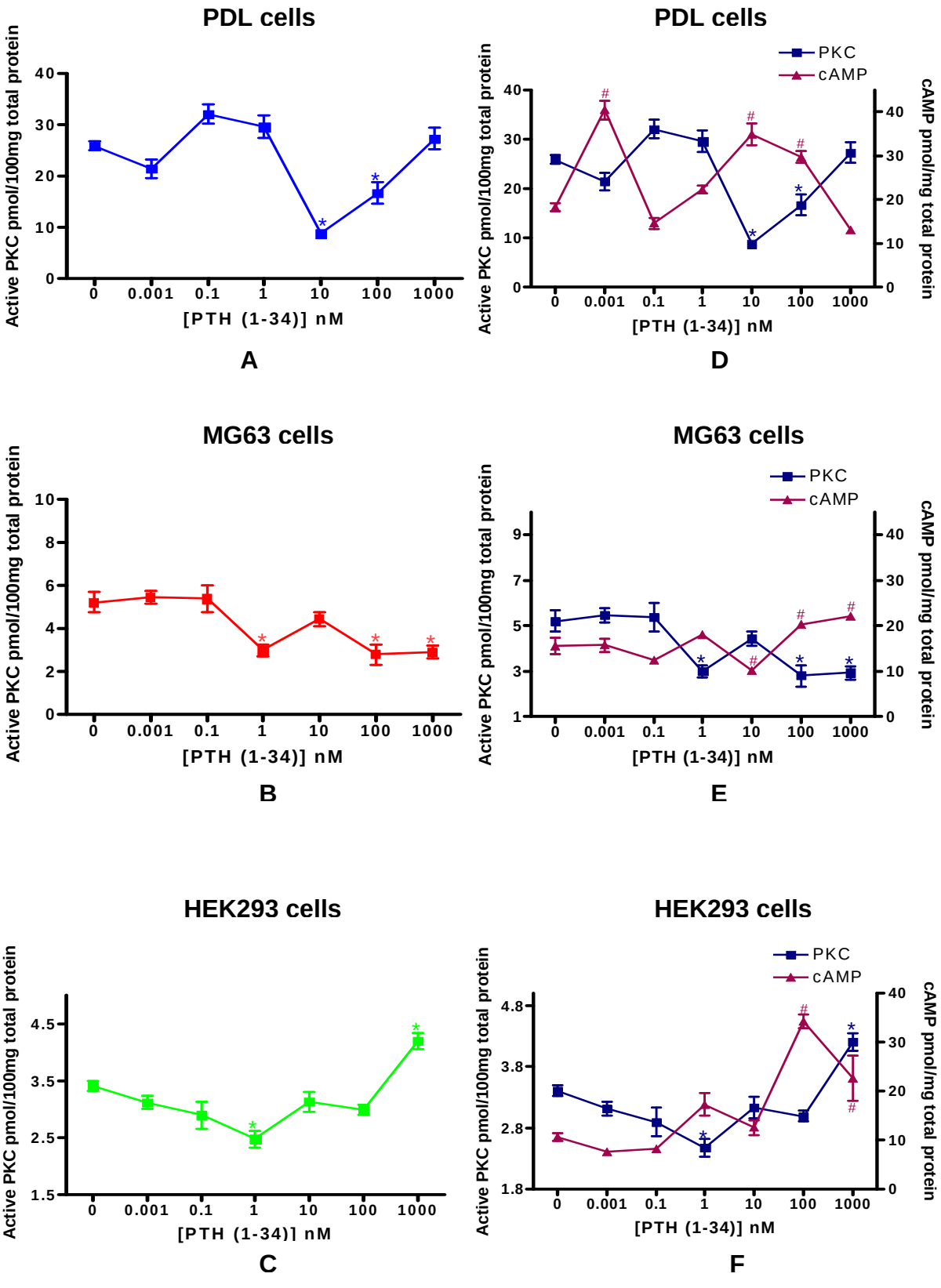

Figure 3.22 Effect of hPTH (1-34) on PKC activity in PDL, MG63 and HEK293 cells. The effect of hPTH (1-34) on PKC activity after was assessed using a commercial PKC activity assay kit. Each value represents the mean ±SEM for 6 independent experiments. **A:** Active PKC amount upon hPTH (1-34) stimulation in PDL cells. **B:** Active PKC amount upon hPTH (1-34) stimulation in MG63 cells. **C:** Active PKC amount upon hPTH (1-34) stimulation in HEK293 cells. In Graphic**, A, B and C, * :** P<0.05 (Dunnett-test), vehicle-treated control vs. each experimental group. **D:** cAMP accumulation vs. active PKC protein level in PDL cells in response to hPTH (1-34) stimulation. **E:** cAMP accumulation vs. active PKC protein level in MG63 cells in response to hPTH (1-34) stimulation. **F:** cAMP accumulation vs. active PKC protein level in HEK293 cells in response to hPTH (1-34) stimulation. In Graphic**, D, E and F, * :** P<0.05 (Dunnett-test), vehicle-treated control vs. each experimental group in PKC activity assay. **# :** P<0.05 (Dunnett-test), vehicle-treated control vs. each experimental group in cAMP accumulation assay.

3.9 Effect of 10^{-12} M hPTH (1-34) on osteoprotegerin

The observation that a concentration as low as 10^{-12} M hPTH (1-34) triggers the cAMP/PKA pathway in PDL cells was further confirmed by other lines of data, wherein the effect of 10^{-12} M hPTH (1-34) on osteoprotegerin production of these cells was investigated.

In confluent PDL cells, intermittent 10^{-12} M hPTH (1–34) administration for both 1 h/cycle and 24 h/cycle significantly reduced osteoprotegerin at protein level (Figure 3.23). This regulation scheme was sustained, when the PKC pathway was blocked with RO-32-0432. However, the blocking of PKA pathway with H8 did not induce any notable change in the basal protein level of this cytokine.

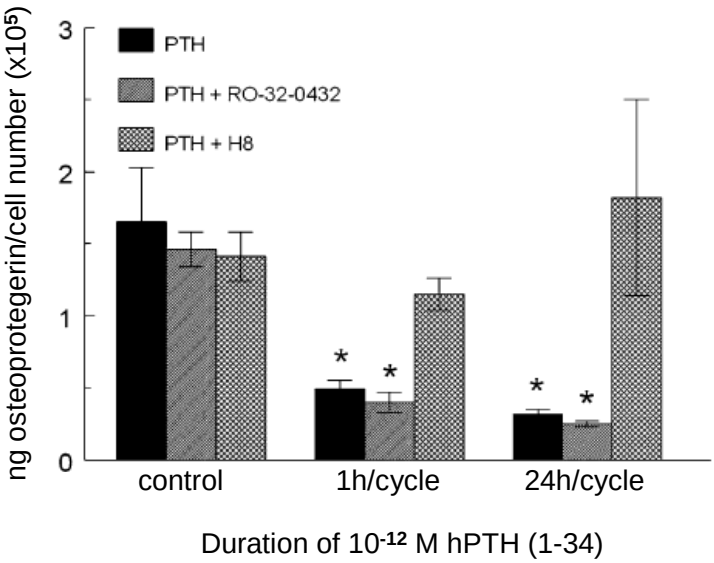

Figure 3.23 Regulation of the osteoprotegerin production by intermittent 10^{-12} M hPTH (1–34) in confluent PDL cells. The cells were treated intermittently with 10^{-12} M hPTH (1–34) for 1 or 24 h during three cycles of 48 h each. Vehicle treated cultures served as controls. The osteoprotegerin content in the conditioned medium was assayed by ELISA and expressed as a function of the cell number. From all data obtained, the osteoprotegerin level at the onset of hPTH (1-34) administration (T0) was subtracted serving as a baseline correction. Data were acquired from one of two separate experiments, both yielding comparable results. Each value represents the mean ± SEM for six independent cultures. ***** : P<0.05, experimental group vs. vehicle control at a particular maturation state.

3.10 Effect of intermittent hPTH (1-34) on human periodontal ligament cells transplanted into immunocompromised mice.

In this section, we analyzed the effect of an intermittent hPTH (1-34) administration on human periodontal ligament cells *in vivo*. To this end, gelatin sponges containing explanted and dexamethasone pre-differentiated human PDL cells were transplanted into immunocompromised mice and grown for 4 weeks with daily injections of hPTH (1-34). Markers of osteoblastic differentiation including alkaline phosphatase, osteopontin, and osteocalcin as well as well PTH1R were immunohistochemically determined. Meanwhile, the degree of mineralization was analyzed by staining tissue specimens with alizarin red.

Effect of intermittent PTH (1-34) on osteocalcin blood serum level

Daily subcutaneous injections of 40µg/kg hPTH (1-34) raised the blood serum level of osteocalcin by approximately factor 3 (41.61±13.02ng/ml) compared to the control animals which only received sham-injections (13.90±2.81ng/ml). These differences proved statistically significant (Figure 3.24).

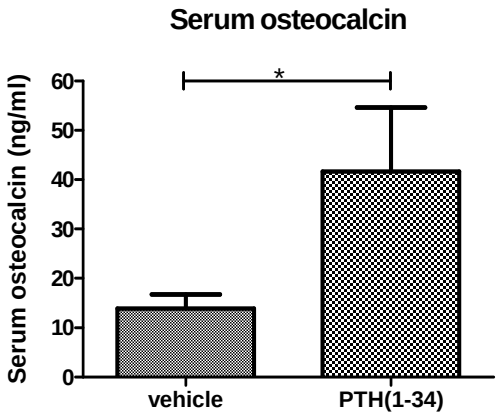

Figure 3.24 hPTH (1-34)-induced increase of osteocalcin serum levels as a hint towards enhanced bone turnover. Prior to sacrifice of the animals at the end of the experimental period, blood was collected by cardiac puncture and the osteocalcin level was determined in the serum by ELISA. The bar graph shows the mean ± SEM for 6 mice per experimental group. ***:** P<0.05, experimental group vs. vehicle control.

Identification of human PDL cells in mouse tissue

Proof of the human origin of the cells under investigation was provided by an immunohistochemical staining specific to human but not mouse cell nuclei. In all specimens, a positive immunoreaction demonstrated the presence of human transplanted PDL cells in the gelatin sponges after growing 4 weeks in the mouse (Figure.3.25, **A**). Mouse tissue, which served as a negative control, remained unstained (Figure.3.25, **a**).

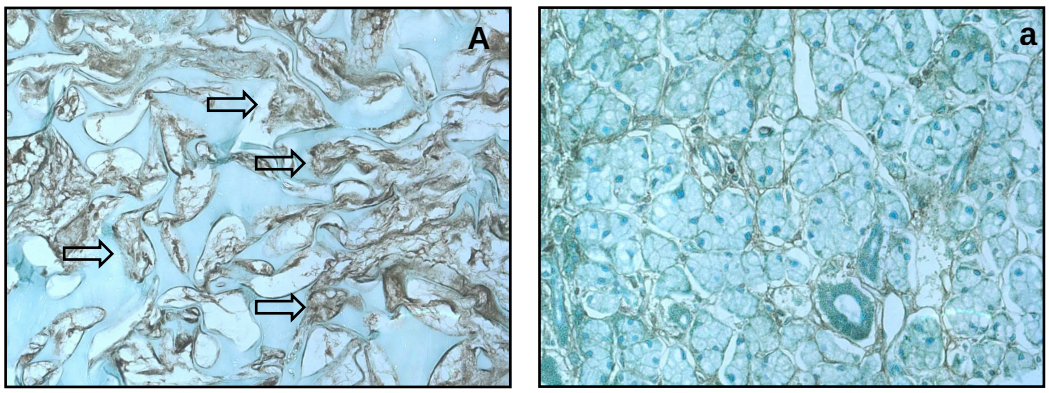

Figure 3.25 Proof of human cells in the specimens explanted from the mice. Following sacrifice, specimens were processed for immunohistochemical detection of human cell nuclei to identify human PDL cells. **A:** The nuclei of the transplanted PDL cells were immunohistochemically stained using an antibody specific to human, but not mouse cells. Open arrows indicated the stained PDL cells in the gelatin sponges. **a:** Mouse tissue, which served as a negative control, remained unstained. Magnification: x400.

Histology

Histology of the recovered specimens revealed the collagenous structure of the scaffolds, which mostly appeared as a fibrous network containing porous spaces ranging from 5 to 10 µm. In those spaces, a gradual distribution of the PDL cells including extracellular matrix throughout the gelatin sponges with the outer areas being more populated by PDL cells than the inner regions became evident (Figure 3.26).

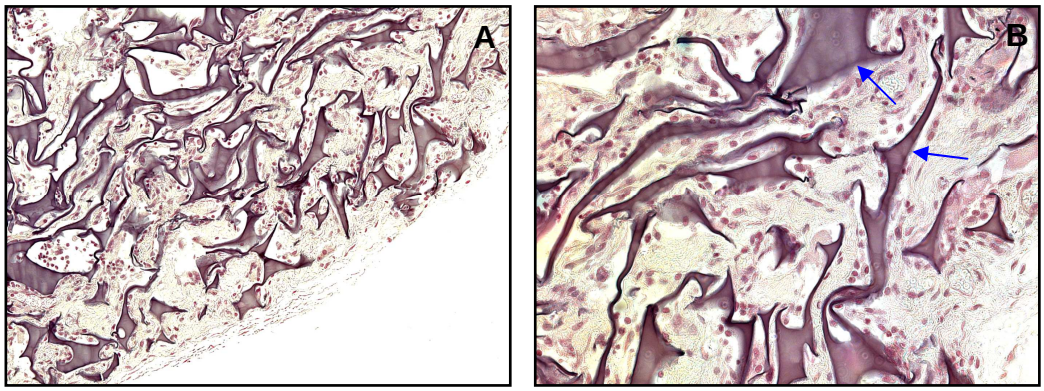

Figure 3.26 Histology of the recovered specimens. Following sacrifice, specimens were stained with haematoxylin-eosin (HE). Blue arrows indicate the gelatin sponges. The cytoplasm of transplanted PDL cells was stained red **A:** Magnification: x200. **B:** Magnification: x400.

ALP, osteopontin, osteocalcin and PTH1R immunohistochemistry

In the control specimens, alkaline phosphatase, osteopontin, and osteocalcin immunoreactivity was detected in the cytoplasm of the PDL cells and in the extracellular matrix, respectively, with the intracellular staining being stronger than the extracellular. PTH1R exhibited the same staining pattern as found in PDL tissues, as described previously. Correlating with the cell distribution pattern, the staining was found to be more intense in the outer areas as compared to the inner zones of the specimens. Intermittent hPTH (1-34) administration in the post surgical period resulted in a visible increase of both the number of immunoreactive cells and the staining intensity for all four antigens under investigation as compared to the sham-injected controls (Figure 3.27, **A-D** and **a-d**). This visual impression was further substantiated by semiquantitative assessment using a rating system ranging from 0 to 3 and proved statistically significant for all parameters tested (Figure 3.28).

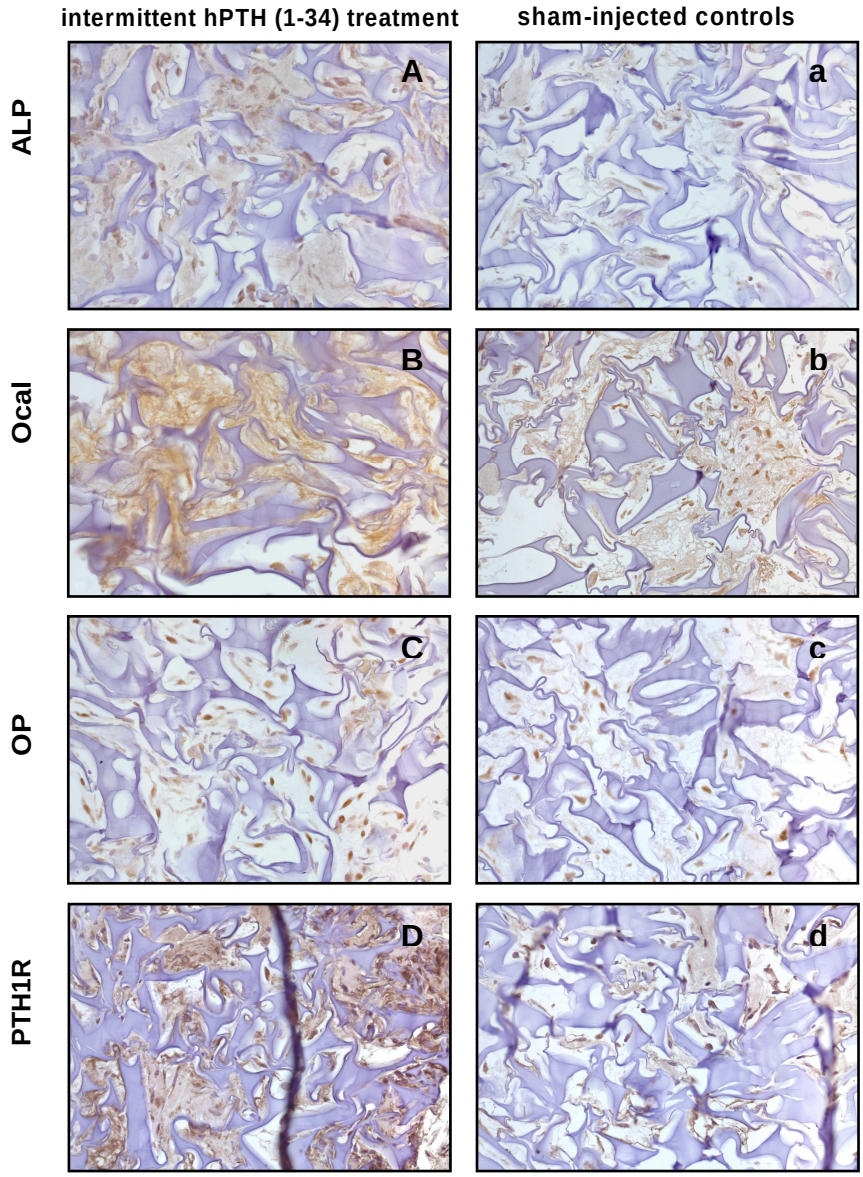

Figure 3.27 Immunohistochemical detection (DAB) of alkaline phosphatase (ALP), osteocalcin (Ocal), osteopontin (OP) and PTH1R in the explants retrieved from the immunodeficient mice after 28 days. The respective panels on the left represent specimens of the animals treated with hPTH (1-34) intermittently (**A-D**), whereas those on the right are representative of the sham-injected group (**a-d**). Magnification: x400.

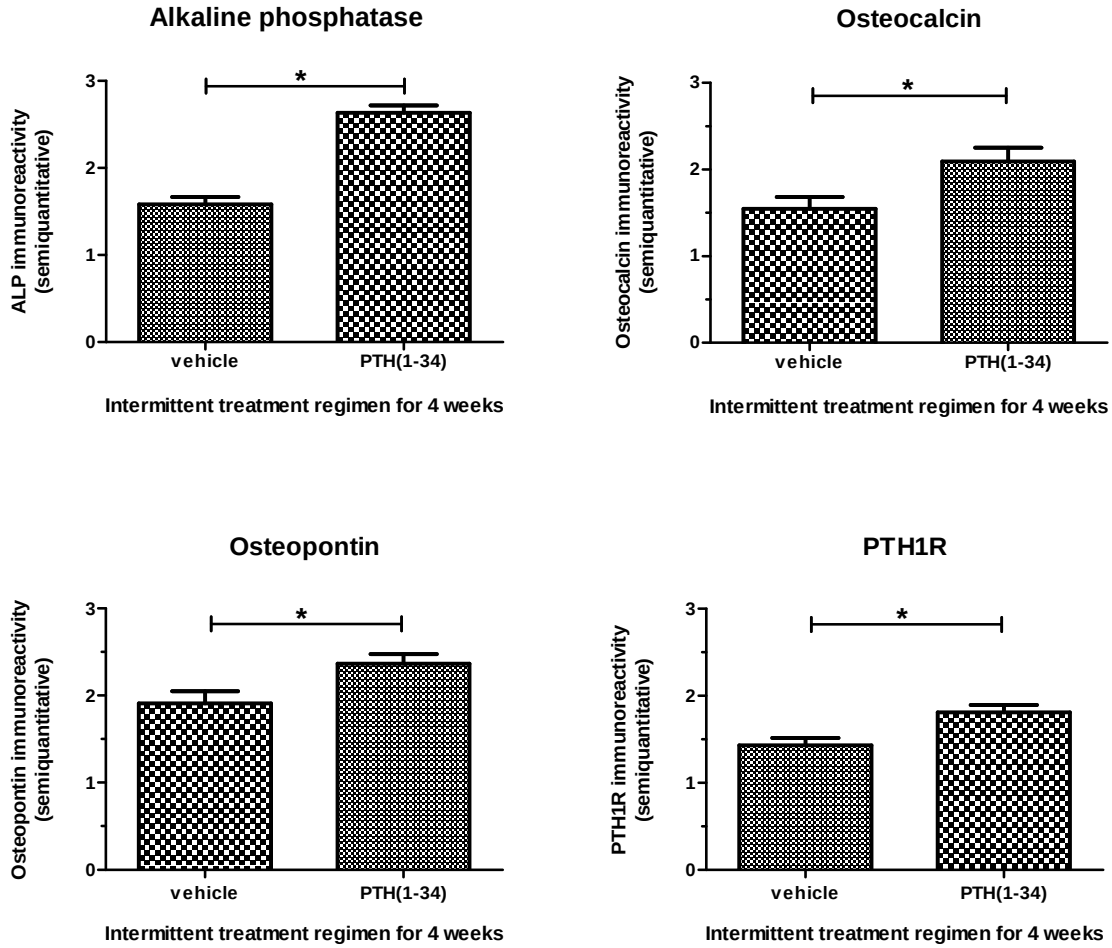

Figure 3.28 Semiquantative immunohistochemical analysis of alkaline phosphatase (ALP), osteocalcin (Ocal), osteopontin (OP) and PTH1R protein expression in the transplanted human PDL cells. Fourth passage PDL cells from two donors were stimulated with dexamethasone for three weeks prior to implantation into 6 CD-1® nude mice using gelatin sponges as a carrier. Post implantation, 40µg hPTH (1-34)/kg body weight were administered subcutaneously once daily for a period of 4 weeks. Sham injections of saline served as vehicle controls. Following sacrifice, specimens were processed for immunohistochemical staining and semiquantitative assessment of immunoreactivity. The bar graph shows the mean $\pm$ SEM for 36 specimens per experimental group. *****: $P<0.05$, experimental group vs. vehicle control.

Biomineralization

Alizarin red staining as a marker of biomineralization followed a similar staining pattern as described for the osteoblastic marker proteins with ossicles from hPTH (1-34) treated animals exhibiting a significantly higher degree of mineralization than ossicles from vehicle-treated animals (Figure 3.29).

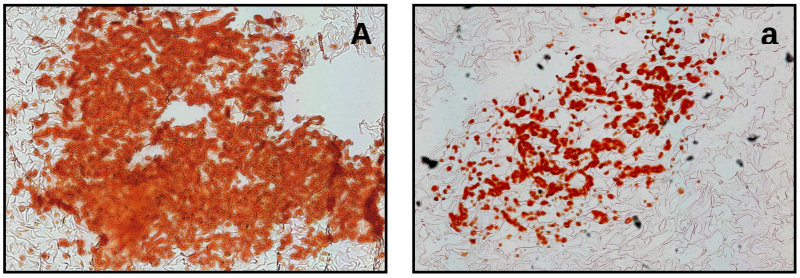

Figure 3.29 Alizarin red staining of calcium deposits in the explants retrieved from immunodeficient mice after 28 days. Alizarin red staining indicates areas of mineralization. **A**: PTH-treated mice. **a**: sham-injected mice. Magnification: x100.

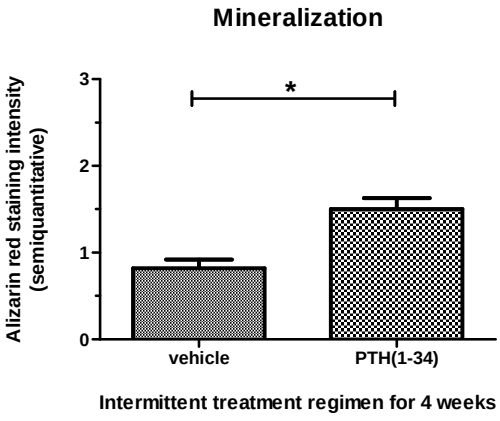

Figure 3.30 Semiquantative immunohistochemical analysis of mineralization of the transplanted human PDL cells. Fourth passage PDL cells from two donors were stimulated with dexamethasone for three weeks prior to implantation into 6 CD-1® nude mice using gelatin sponges as a carrier. Post implantation, 40µg hPTH (1-34)/kg body weight were administered subcutaneously once daily for a period of 4 weeks. Sham injections of saline served as vehicle controls. Following sacrifice, specimens were processed for Alizarin red staining and semiquantitative assessment of staining intensity. The bar graph shows the mean $\pm$ SEM for 36 specimens per experimental group. ***:** P<0.05, experimental group vs. vehicle control.

4 DISCUSSION

In addition to the classic catabolic effects, it is now widely accepted that PTH exerts anabolic effects on bone, when administered intermittently. As a result of the regenerative characteristic, PTH (1-34) (Teriparatide) has been approved for the treatment of osteoporosis (Hodsman et al., 2003).

Periodontitis is one of the most common diseases, which causes the resorption of alveolar bone and can result in the loss of teeth, if treated not adequately. Over the past several years, numerous *in vivo* and *vitro* studies have been conducted to reveal the anabolic effect of PTH on PDL tissue and alveolar bone (Nohutcu et al., 1995; Ouyang et al., 2000; Barros et al., 2003; Lossdörfer et al., 2005, 2006b). The result of these findings suggests that PTH has anabolic effects on oral bone.

The dual actions of PTH are mediated primarily through the PTH1R, which is a class II G protein-coupled receptor. Upon ligand binding, PTH1R can activate diverse signaling pathways, including cAMP/PKA and PLC/PKC pathways (Vilardaga et al., 2011). In light of this, understanding the physiology of the PTH1R is crucial to promote the regenerative effect of PTH. PTH1R has been exclusively studied in kidney and bone cells. However, the knowledge on PTH1R characteristics and physiology in PDL cells is still in its infancy.

The objective of this study was to characterize the PTH1R in PDL cells, in terms of its cellular localization, binding affinity, density, signal transduction and gene regulation by diverse stimulants such as dexamethasone, vitamin D_3 and hPTH (1-34), as well as to compare these characteristics with those of MG63 and HEK293 cells as representatives of bone and kidney cells, respectively.

4.1 Cell culture establishment and cell characterization

A crucial aspect of *in vitro* study is the establishment of a healthy cell culture model, which promises the reproducibility of experimental data. This becomes even more important with the use of primary cell line cultures. Moreover, albeit the similarity in morphology, PDL cells are considered to possess multiple characteristics, including fibroblastic and osteoblastic properties (Yamashita et al., 1987). The shift between

the multiple characteristics could be dependent on the condition and state of the PDL cell culture. Therefore, in the whole project, healthy, fifth passage PDL cells from different donors were used for each experimental setup. Additionally, it has been demonstrated that the confluent degree of PDL cells is correlated with the expression of differentiation markers and responsiveness to hPTH (1-34) stimulation (Lossdörfer et al., 2006a, 2006b). Along the line, it is likely that the expression of PTH1 is also dependent on the state of confluence. To address this question, PDL cells at confluent and preconfluent stages were characterized for marker genes involved in osteogenesis, and a comparative gene expression profile of these markers, confluent vs. preconlfuent, was established using real time PCR method. Accordingly, to assure the consistent expression of PTH1R, we used confluent PDL cells for each experimental setup in this study.

PTH1R are abundantly expressed in the bone and kidney (Langub et al., 2001). MG63 cells are commonly used as osteoblastic models, and HEK293 cells originated from human embryonic kidney (Graham et al., 1977). Thus, these two cell lines were included in this study to compare the characteristics of PTH1R in these cell lines to those of PTH1R in PDL cells.

4.2 Autofluorescence of PDL cells

The high autofluorescence of PDL cells was a major obstacle in the successful immunofluorescence staining of PTH1R in these cells. The FITC-conjugated secondary antibody was the choice of method at the beginning of our immunofluorescence staining based experiments. However, we observed a very intensive green fluorescence also in the unstained PDL cells. There are generally two possible sources of this unspecific fluorescence; external factors and autofluorescence. The external factors include fixation agents such as paraformaldehyde and to some degree also the used culture medium. As next, we changed the culture medium and stained directly the cells without fixation, which did not alter the intensity of the unspecific green fluorescence.

Autofluorescence, termed also as “natural fluorescence”, is the fluorescence found in natural substances. Cells in most organisms exhibit some intrinsic level of

autofluorescence, which is most commonly caused by metabolites and structural components such as NADH, riboflavins, and flavin coenzymes (Mosiman et al., 1997). Autofluorescence spectra are generally broad and encompass most of the visible spectral range, overlapping the emission spectra of commonly used fluorescent dyes (Billinton and Knight, 2001) (Figure 4.1).

Autofluorescent source	Organism/tissue	Emission wavelength/nm	Excitation wavelength/nm
Flavins	CHO cells	520	380, 460
	Rat hepatocytes	525	468
	Bovine and rat neural cells	540–560	488
	Goldfish inner ear	540	450
	Periplaneta americana	"Yellow–green"	UV
NAD(P)H	Rat cardiomyocytes	~509	~395
	S. cerevisiae, rat hepatocytes	440–470	366
	CHO cells	440–450	360
Lipofuscins	Rhesus monkey, rat, human medulla	"green"	460–490
	Rat heart	550	450–490
	Muscle, myocardium, hepatocytes	~540–560	360
	Human brain	481–673	435
	Rat liver	430	345
	Rat retina	>510	390–490
AGEs	Chinese hamster and human lenses	434	365
	In vitro	440–450	370
	Human cornea	385	320
	Diabetic human skin	440	365
Collagen and elastin	Human aorta and coronary artery	>515	476
	Human skin	470–520	442
Protoporphyrin IX	Human psoriatic skin	635	442
Lignin	*Phyllostachys pubescens*	UV	470–510
	Pinus radiata	488	~530
Chlorophyll	Green algae thylakoid	488	685 (740)

Figure 4.1 Common biochemical sources of autofluorescence in a wide variety of cell types and organisms, with their respective emission and excitation maxima (Taken from: Billinton and Knight, 2001).

The immunofluorescence images and flow cytometry analysis revealed that PDL cells exhibits a high green autofluorescence, which overlaps with the emission range of FITC. However, the autofluorescence decreases dramatically in the long wavelength region (from Alexa Fluor 647 to far infra red). In order to cast further insight, the autofluorescence characteristics of PDL cells were compared to those of MG63, HEK293, HaCaT cells and keratinocytes using FITC and Alexa Fluor 647 sets. Interestingly, among these cell lines, PDL cells and MG63 showed similar properties in terms of autofluorescence intensity (Figure 3.6). This could mean that the two cell lines have similar metabolic activities, since the metabolites are the common cause of autofluorescence. Another interesting observation is that the intensity of autofluorescence of the five cell lines in the emission wavelengthes for FITC appears to reflect the capacity of these cell lines to synthesize extracellular matrix proteins and collagens. High amount of NAD(P)H and flavin molecules

indicate an intensive cellular metabolism, which in turn is a sign of an intensive synthesis of extracellular matrix proteins and collagens. Along the same line, the intensity of autofluorescence in the emission wavelengths for FITC would reflect the intensity of matrix proteins and collagens synthesis. Indeed, PDL cells and MG63 cells are characterized by their intensive synthesis of extracellular matrix proteins and collagens, which are needed to form hard tissues. On the other hand, keratinocytes, and HaCat cells are of epithelial origin and associated with soft tissues. This would indicate that these cell lines are less specialized in synthesis of extracellular matrix proteins and collagens. Although HEK293 cells are considered to be of epithelial origin, they might be less mature than keratinocytes and HaCaT cells, because they were generated at a less mature stadium by transformation of human embryonic kidney cells.

The intensity of autofluorescence was decreased significantly by permeabilization of the cells (Figure 3.7). One possible explanation could be that the agents which cause the autofluorescence are either quenched by permeabilizing reagents or washed out through the permeabilized cell membrane.

4.3 Detection and comparison of the mRNA expression level of PTH1R in PDL, MG63 and HEK 293 cells.

The real time PCR products run on the agarose gel confirmed the presence of PTH1R at transcriptional level in PDL, MG63 and HEK293 cells. It is well known that MG63 cells express PTH1R (Carpio et al., 2001; de Gortázar et al., 2006; Tenta et al., 2006; Avnet et al., 2008). However, to the best of our knowledge, this is the first evidence that native (non-transfected) HEK293 cells express PTH1R. In most studies related to PTH1R, the used HEK293 cells were transfected with PTH1R gene (Iida-Klein et al., 1997; Ferrari et al., 1999; Chauvin et al., 2002; Gesty-Palmer et al., 2006; Qiu et al., 2010; Feinstein et al., 2011). In terms of PTH1R mRNA expression level, the three cell lines differed significantly, with HEK293 cells expressing the highest level of PTH1R mRNA. This divergence in the gene expression level appears to be cell type specific. These results were further supported by the western blot anylsis of PTH1R, wherein this receptor protein was detected and semi-quantidfied in

PDL, MG63 and HEK293 cells, respectively. The semi-quantitavie analysis indicated that PTH1R in these cell lines follows at translational level the same regulation scheme as observed at trascriptional level, which was evidenced by the quantification of mRNA level of PTH1R.

4.4 Detection of PTH1R proteins in PDL tissue as well as in PDL, MG63 and HEK293 cells

The results of immunhistochemical staining of tissue sections not only confirmed the presence of PTH1R protein but also revealed an equal distribution of this receptor throughout the whole PDL tissue, with no prevalence to alveolar bone side or tooth root. At cellular level, PTH1R was found mainly in PDL fibroblasts as well as in endothelial cells, whereas no immunostaining was observed in epithelial cell rests of Malassez (ERM). ERM are discrete clusters of residual epithelial cells that arise from fragmentation of the Hertwig's root sheath and persist in the periodontal ligament throughout life (Gonçalves et al., 2008). These cells form a network around the root and can be identified easily as small clumps of epithelial cells within the periodontal ligament, close to the surface of radicular cementum. Several studies have reported the expression of different types of proteins by the ERM, such as cytokeratins and neuropeptides, as well as extracellular matrix and cell-surface proteins including a variety of growth factors, cytokines and extracellular matrix-degrading proteinases (Rincon et al., 2006). To date, however, there is no available evidence that support the presence of PTH1R in these cells, although the expression of parathyroid hormone related protein (PTHrP) is postulated (Beck et al., 1995). The presence of PTH1R in endothelial cells was already reported by several researchers (Isales et al., 2000; Rashid et al., 2007). Along with PDL fibroblasts and endothelial cells, cementoblasts and odontoblasts showed also positive immunostaining for PTH1R (Figure 3.9, **E** and **F**). These results are consistent with the already published data of other investigators (Tenorio and Hughes, 1996; Kato et al., 2005b, 2005a).

As next, we confirmed the persistence of the expression of PTH1R in cultured PDL cells by staining the cells for PTH1R. In this step, we established and optimized a suitable immunohistochemical staining protocol for PTH1R in PDL cells, as the

antigen accessibility of the antibody could vary depending on the cell type. In both of the tissue staining and cell staining for PTH1R, we could achieve better results using an antigen retrieval method. There have been several methods developed to circumvent the problem of antigen masking which is generally caused by aldehyde fixation. After having systematically tested and optimized these methods, we used 10 mM citrate buffer (PH 9) for the antigen retrieval of PTH1R. To this end, the tissue sections as well as the cells were incubated in this buffer at 80℃ in an incubater for 30 min. Additionly, the distinct bands of correct size detected by western blot method supported furhter the presecne of PTH1R protein in PDL, MG63 and HEK293 cells.

4.5 Localization of PTH1R

GPCRS are cell surface receptors located within the lipid bilayer of the cell with an extracellular N-terminal domain, a seven transmembrane domain and an intracellular C-terminal domain. The biosynthesis of GPCRs begins at the endoplasmatic reticulum (ER) where they are subsequently folded and assembled (Figure 4.2). Properly folded receptors are then recruited and packaged into ER-derived coat protein complex II (COPII) -coated vesicles (Dong et al., 2007). These transport vesicles carry the cargo receptors further to the ER-golgi intermediate complex, the Golgi apparatus and the trans-golgi network, where the receptors undergo post-translation modifications (e.g. glycosylation). Once receptors have achieved their mature status, they leave the ER and are transported through the secretory pathway to their destination on the plasma membrane (Duvernay et al., 2005). On other hand, the misfolded receptors are transported back into the cytosol and degraded by the ER associated pathway (Tsai et al., 2002).

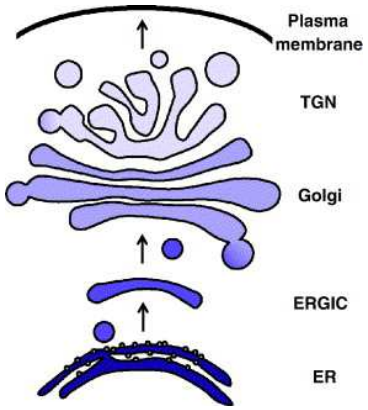

Figure 4.2 Schematic overview of GPCR physiology (Taken from: Duvernay et al., 2005). GPCRs are synthesized, folded and assembled in ER (endoplasmic reticulum); post-translational modified in ERGIC (ER–Golgi intermediate complex), TGN (*trans*-Golgi network) and finally transported through the secretory pathway to their destination at the plasma membrane.

Thus, prior to activation, GPCRs are distributed not only on the plasma membrane, but also can be found in the ER, golgi apparatus and packaged in transport vesicles depending on their mature status. In addition, the nuclear localization of several members of class I and III GPCRs has been also reported (Lu et al., 1998; Bhattacharya et al., 1999; Lee et al., 2004; Jong et al., 2005).

In all the three cell lines studied, PTH1R showed the classic scheme of GPCR localization, with distribution on the plasma membrane and in the cytoplasm (Figure 3.11). However, unlike HEK293 cells, MG63 and PDL cells showed additionally a weak nuclear staining, implying the nuclear localization of these receptors (Figure 3.11, C). Indeed, both nuclear and cytoplasmic localization of PTH1R were previously reported in cultured osteoblast-like cells (ROS 17/2.8, UMR-106, MC3T3-E1, and SaOS-2) (Watson et al., 2000). In the cytoplasm, the staining was mainly observed around the nucleus, indicating the presence of premature PTH1R in the ER and golgi apparatus. Additionally, there were also intensively stained dots observed in the cytoplasm, which might represent the mature receptors heading to their destination on the cell membrane via the secretory pathway. These findings are consistent with the GPCR physiology in inactive state.

Like other GPCRs, the activation of PTH1R leads to phosphorylation of its cytoplasmic tail by GRKs, which then facilitate association with ß-arrestin proteins, resulting in internalization and desensitization of the receptor (Malecz et al., 1998; Tawfeek et al., 2002). ß-Arrestin-PTH1R interactions lead to internalization (endocytosis) of the receptor, which are then either destined for degradation,

resulting in receptor down-regulation (Tian et al., 1994; Ureña et al., 1994b; Massry and Smogorzewski, 1998), or recycled back to the cell surface, leading to receptor resensitization (Chauvin et al., 2002).

In order to confirm the internalization of PTH1R upon ligand binding, the three cell lines were treated with 100nM hPTH (1-34) for 30 min and subsequently stained for PTH1R. This concentration and time period of stimulation was successfully applied by Qiu et al to observe the internalization of a tagged hPTH (1-34) along with PTH1R in osteoblasts (Qiu et al., 2010).

As illustrated in Figure 3.12, the vivid line of membrane staining observed in unstimulated PDL and MG63 cells was not present in hPTH (1-34) stimulated cells, demonstrating the internalization of the receptors upon ligand binding. However, as HEK293 cells have relative large nuclei and small space between plasma membrane and cytoplasm, the internalization of the receptors could not be successfully visualized.

4.6 Identification of PTH1R-positive subpopulation

To address the question of whether a PTH1R-positive subpopulation exists in PDL, MG63 and HEK293 cells, these cells were stained for PTH1R and analysed using flow cytometry method.

At first, the living cells were analysed, since PTH1R resides on the plasma membrane and the PTH1R antibody binds an epitope in the extracellular part of the receptor. Furthermore, the receptors residing on the cell membrane are functional active, at least in terms of responsiveness to ligands. After gating out dead cells, MG 63 cells revealed a PTH1R-positive subpopulation of 40%, while HEK293 cells were almost 100% positive. In PDL cells, however, no PTH1R-positive subpopulation could be detected.

The heterogeneity of MG63 cells for PTH1R appears to be a matter of maturation state. Indeed, MG63 cells have been shown to exhibit both mature and immature osteoblastic features (Pautke et al., 2004), indicating the differentiation potential of this osteosarcoma cell line. On the other hand, PTH1R is widely recognized as an

osteoblast-differentiation marker. These facts along with our result are suggestive of the presence of a PTH1R-positive subpopulation in MG63 cells.

In the data interpretation of HEK293 cells, we considered the shift of the whole cell population rather than recording the absolute percentage of the positive cells. In this case, the HEK293 cells reached an almost 100% positivity, which would be app.80%, if the absolute percentage of the positive cells would be taken into account. Indeed, depending on where to set the threshold between the positive and negative cells, there could be recorded false negative cells in the real negative cell population and vice versa.

Despite numerous optimization steps including: titration of antibody concentration, cell-detachment with different reagents such as accutase, EDTA and trypsin and using PTH1R antibodies from other sources, we failed to detect any PTH1R-positive population in PDL cells. On the other side, the presence of PTH1R on the plasma membrane was visualized using immuno-staining method (Figure 3.11, **A**). One possible explanation for this paradox is that the used primary antibodies cannot bind successfully to the corresponding epitope on PTH1R in PDL cells, because of the limited access of the antibody to its antigen.

When permeabilized, all of the three cell lines showed almost 100% PTH1R-positive population. In fact, the permeabilized plasma membrane allows the antibody molecules to bind to intracellular antigens. Thus, having access to cell inside, the PTH1R antibody obviously can bind to receptors both on the plasma membrane and in the cytoplasm of MG63 and HEK293 cells. In case of PDL cells, the antibody can bind to the intracellular receptors. It might be also possible that the fixing and permeabilizing processes could have made the antigen accessible for the antibody, resulting in the successful staining of the plasma membrane receptors. Indeed, the optimal results of immunofluorescence staining of PTH1R were also achieved only after treating the cells with optimized fixing, permeabilizing and antigen retrieval methods.

4.7 Binding affinity and receptor density of PTH1R

The binding affinity and density of PTH1R in PDL, MG63 and HEK293 cells were studied using a competitive radioactive binding assay. There are generally two types of this assay. One is performed with isolated cell membranes, while the other is performed with intact cells. In the present study, we have employed an intact cell binding assay. In the assays with intact cells, the plasma membrane receptors can be studied in their native environment without disturbing the membrane. PH gradients or other ions across the membrane remain intact during the binding assay. Additionally, interactions between the receptors and their associated effector systems as well as the cytoskeleton or other associated components also will be assured. However, in this assay, it is much more difficult to control the assay conditions to identify factors that modulate receptor binding. Another disadvantage of this assay is that certain radioligands may also be transported into the cell leading to an apparent nonspecific binding. On the other hand, this trapped radioligand can appear as specific binding without association, if the agent used to define nonspecific binding also inhibits the uptake of radioligand.

The binding characteristics of PTH1R were quite different in the three lines, with the lowest affinity in PDL cells (K_d=1030±10 nM) and the highest in MG63 cells (K_d=80.1±20.2 nM). Both PDL (3.03±0.57 million receptors/cell) and HEK293 cells (2.27±1.4 million receptors/cell) revealed a relative high density of PTH1R, while MG63 cells showed the lowest receptor density (0.365±0.1). The calculated K_d value and the number of receptors in MG63 cells were similar to those in rat osteosarcoma cells, ROS 17/2.8 cells and in another rat osteosarcoma cell line, UMR-108 (Demay et al., 1985; Rao and Murray, 1985), while these results differed greatly from other reports on the binding characteristics of PTH1R (Pliam et al., 1982; Yamamoto et al., 1988; Enomoto et al., 1989). These discrepancies might be due to changes in PTH1R depending on the cell type and different experimental conditions as well as to different ligands used in the respective binding assays. Virtually all the reports on the binding characteristics of PTH1R resulted from the HEK293 cells transfected with either native or mutant PTH1R. Thus, the results of these studies on binding characteristics of this receptor vary depending on the experimental purpose and design. In this study, we present the first results of binding studies on PTH1R in PDL cells, which showed low binding affinity, yet a relative high value for receptor density.

These data are suggestive of a cell type specific binding characteristic of PTH1R. On the other hand, as mentioned above, most of the studies on the binding characteristics of PTH1R were performed in cells transfected with either native PTH1R or mutant PTH1R. Additionally, the experimental conditions under which the binding assays were performed could have great impact on the results.

4.8 Regulation of PTH1R mRNA level in PDL cells

It is widely known that PTH1R is tightly regulated in osteoblast-like cells and opossum kidney (OK) cells by extracellular cell factors such as dexamethasone (Rodan et al., 1984; Ureña et al., 1994a), 1,25-dihydroxyvitamin D_3 (Titus et al., 1991) and PTH (Ureña et al., 1996; Jongen et al., 1996). In light of this, we have studied the effect of these factors on PTH1R mRNA expression using real time PCR method.

We used the concentration of 10^{-6} M dexamethasone, according to a previous study in which the effect of dexamethasone on PTH1R mRNA has been examined in ROS 17/2.8 (Ureña et al., 1994a). However, we prolonged the time course of the treatment to 21 days, in order to find out the time point at which this glucocorticoid exerts its highest effect on PTH1R mRNA expression.

The effect of dexamethasone on PTH1R mRNA level in PDL cells was accumulative in the first four days, and exhibited its highest effect on the 4^{th} day. Beginning on the 6^{th} day, it gradually lost its effect (Figure 3.18). These findings are consistent with the results of the studies in osteoblast-like cells, in which dexamethasone increased PTH1R mRNA level (Ureña et al., 1994a; Haramoto et al., 2007).

We adopted the concentration of 10^{-6} M 1,25-dihydroxyvitamin D_3 from a previous study in which the regulation of PTH1R mRNA level by 1,25-dihydroxyvitamin D_3 has been examined in ROS 17/2.8 cells. Similarly, the exposure time was prolonged to 6 days. No apparent effect of 1,25-dihydroxyvitamin D_3 was observed in the first four days. However, on the 6^{th} day, it dramatically increased PTH1 mRNA level, with almost 14 fold increase (compared to control) (Figure 3.19). 1,25-dihydroxyvitamin D_3 has been reported to decrease mRNA level and receptor number of PTH1R in ROS 17/2.8 cells (Xie et al., 1996). This discrepancy could be cell type dependent.

Furthermore, ROS 17/2.8 cells were exposed to 1,25-dihydroxyvitamin D_3 in that study for 3 days, which we prolonged to 6 days in our study.

The pleiotropic actions of PTH are mediated primarily through the binding and activation of PTH1R, which in turn is regulated by PTH (Kawane et al., 2001). It has been reported that PTH either down-regulates or up-regulates PTH1R expression, depending on the cell type (Langub et al., 2001). Since PTH exerts dual effects depending on the administration mode, it is also plausible that this discrepancy in the regulation of PTH1R mRNA could be a result of different ways of its application. With this in mind, we have studied the effect of both intermittent and continuous PTH administration on PTH1R mRNA level in PDL cells.

As expected, different ways of PTH administration exerted different effects on PTH1 mRNA level. In the first two cycles, 1 h intermittent exposure increased the level of PTH1R mRNA, while 24 h intermittent treatment decreased it. The continuous treatment increased after the first cycle PTH1 mRNA expression, but decreased it after the second cycle. After the third cycle, none of the three ways of treatments showed an apparent effect. Thus, it is likely that different actions of PTH regulate the PTH1R expression specifically. The relationship between the dual effects of PTH and regulation of its receptor remains to be further elucidated.

4.9 Signal transduction of PTH1R

The actions of PTH1R are thought to be mediated mainly by activating Gs and Gq, which in turn regulate the activity of cAMP/PKA and PLC/PKC signaling cascades, respectively (Vilardaga et al., 2011). In light of this, we have investigated these two signaling pathways in PDL, MG63 and HEK293 cells, by challenging the cells with a series of hPTH (1-34) concentrations such as 10^{-6}, 10^{-7}, 10^{-8}, 10^{-9}, 10^{-10} and10^{-12} M. To this end, we quantified the cAMP accumulation and the active PKC protein using commercial kits.

In terms of cAMP accumulation and active PKC amount, the three cell lines showed discrete patterns in response to the hPTH (1-34) stimulation. Interestingly, the response in PDL cells was not accumulative with increasing concentrations of hPTH (1-34), rather it was more of a concentration-dependent response, as evidenced by

10^{-12} M and 10^{-8} M hPTH (1-34) inducing the highest cAMP accumulation and by 10^{-10} M and 10^{-6} M hPTH (1-34) showing no effect on the basal level of cAMP. In contrast, the response in HEK293 cells followed more or less an additive curve up to the stimulation with 10^{-6} M hPTH (1-34). The same scheme of regulation by this peptide was also found in MG63 cells, although the amplitude of the increase in cAMP accumulation was much smaller than in HEK293 cells. However, the exception was observed at 10^{-8} M hPTH (1-34) with even lower amount of cAMP than at the basal level. We considered this value as a deviation caused by experimental conditions, since the degradation of cAMP molecule was avoided by inhibition of phosphodiesterase using 3-isobutyl-1-methylxanthine (IBMX). The classic view on the response of cAMP to hPTH (1-34) assumes the additive accumulation of the cAMP with growing concentrations, as evidenced with MG63 and HEK293 cells. However, to our knowledge, we present the first evidence of a none-additive accumulation of cAMP molecule in response to PTH stimulation, with different concentrations of the hormone inducing similar magnitude of cAMP response. Indeed, our other lines of data (Lossdörfer et al., 2005) proved the effect of 10^{-12} M hPTH (1-34) on the signaling pathways in PDL cells. In that study, confluent PDL cells were challenged intermittently with 10^{-12} M hPTH (1–34) for both 1 h/cycle and 24 h/cycle. This treatment regime significantly reduced osteoprotegerin at protein level (Figure 3.23). Interestingly, blocking of the PKC pathway did not alter this regulation scheme, whereas blocking of the cAMP/PKA pathway hampered greatly the effect of 10^{-12} M hPTH (1–34) on the level of this cytokine.

One possible explanation for the apparent discrepancy might be ascribed to the heterogeneity of PDL cells which contain PTH1R with different binding characteristics leading to different responsiveness to PTH. As addressed previously, PDL cells are considered to possess multiple characteristics, including fibroblastic and osteoblastic properties (Yamashita et al., 1987). On the other hand, PTH1R seems to have different binding characteristics depending on the cell type, as observed in our study as well as in reports by others (Jonsson et al., 2001; Smock et al., 2001; Gentili et al., 2003; Alokail and Peddie, 2008).

In all the three cell lines, the response of the active PKC to hPTH (1–34) showed an exact opposite scheme of regulation compared to the response of cAMP. This became evident, when the response curves of cAMP and PKC were plotted on the same graph. Interestingly, at a given concentration of hPTH (1-34), if the cAMP level

was up-regulated, then the active PKC amount level was down-regulated, and vice versa, indicating a synchronical regulation of the two pathways after stimulation with hPTH (1-34). Indeed, the important role of the cross talk between cAMP/PKA and PKC pathways in the regulation of collagenase production and DNA synthesis by PTH in osteoblasts was pointed out by Civitelli *et al.* and Sugimoto *et al.* (Sugimoto et al., 1994), whereas studies in other cell systems showed that the interaction between the two signalling cascades does not follow the same pattern in all cell types. Depending on the agonist and cell line, synergistic or antagonistic actions might be found (Sugimoto et al., 1994). Several studies have shown that the cross-talk between these pathways leads to further modulation of hormonal responses and cellular integration of signals (Cole, 1997). Furthermore, the activation of PKC was thought to induce tissue- and cell-specific changes in adenylyl cyclase activity by altering the phosphorylation state of the components of the receptor-G protein-effector complex (Cole, 1997). However, the nature of the interactions between PTH responsive dual signal transduction systems in PDL cells remains to be elucidated.
Taken together, these findings suggest that the concentration of hPTH (1-34) plays a pivotal role in the regulation of downstream signal transduction of PTH1R, at least in our used cell culture model. With respect to the applied concentrations of hPTH (1-34), the cAMP/PKA and PLC/PKC signal cascades are regulated in PDL cells in a different way compared to that in MG63 and HEK293 cells, indicating a cell type specificity of the regulation scheme of the signal transduction pathways. Alternatively, the heterogeneity of the primary PDL cell lines may be of importance.

4.10 Effect of intermittent hPTH (1-34) on human periodontal ligament cells transplanted into immunodeficient mice.

The last part of this project was to study the regenerative capacity of human PDL cells and the anabolic effect of intermittent hPTH (1-34) administration *in vivo*. For this aim, we implied a cell-based tissue engineering model, which was first utilized by Pettway *et al* (Pettway et al., 2005). In this model, the researchers implanted gelatin sponges containing dexamthasone pre-treated bone marrow stromal cells into immunodeficient mice, which were then given daily subcutaneous injections of hPTH

(1-34). The gelatin sponge serves as a structural scaffold for the transplanted cells and provides a temporary extracellular matrix to allow for cell attachment (Lutolf and Hubbell, 2005; Ma, 2008). The pre-treatment of PDL cells with dexamethasone was based on the results of studies that point to the necessity of this supplement for PDL cells to facilitate mineralization of the extracellular matrix (Mukai et al., 1993). In another study, PDL cells were reported to be unable to form mineral-like nodules without prior aplication of osteodifferentiation medium, while the dexamethasone supplementation resulted in positive von Kossa staining (Flores et al., 2008). According to Sheehan *et al*. (2010), the anabolic effect of intermittent PTH on bone varies with the species studied as well as with the duration and mode of administration. Studies conducted in murine models suggest that the anabolic effect of intermittent PTH on bone is variable depending on the dose and duration/mode of administration as well as the species studied (Sheehan et al., 2010). Based on the results of previous studies by Johnston *et al*. (Johnston et al., 2007), we decided for daily subcutaneous injections of 40µg/kg body weight hPTH (1-34) for a period of 4 weeks starting at day 1 after PDL cell implantation.

Albeit the high potential of PDL cells for the regeneration of PDL tissue, there have been few *in vivo* studies providing proofs on the regenerative capacity of these cells. Akitzuki *et al.* demonstrated a successful regeneration of periodontal tissue utilizing a PDL cell sheet in a dehiscence model *in vivo* in beagle dogs (Akizuki et al., 2005). In our study, we present the first *in vivo* evidence for an anabolic effect of intermittent hPTH (1-34) on human PDL cells in terms of osteoblastic/cementoblastic differentiation and biomineralization. To this end, key proteins in osteoblastic/cementoblastic differentiation such as alkaline phosphatase, osteopontin, osteocalcin and PTH1 were investigated using immunohistochemical methods. Additionally, as a measure for biomineralization, calicium deposits in tissue section were stained with alizarin red. In order to evaluate the skeletal response to subcutaneously injected hPTH (1-34), the serum level of osteocalcin was quantified. Osteocalcin is widely accepted as a marker for bone turnover and was shown to be influenced by PTH treatment under different conditions and in different mouse gene types (Sheehan et al., 2010).

The results of the immunohistochemical analysis proved that the implanted human PDL cells not only survived, but also were able to develop a bone/cementum like tissue which closely resembles natural bone or cementum and that this capacity was

significantly enhanced by intermittent PTH administration. These results mirror the *in vitro* findings of our group, which point to a maturation state-dependent effect of intermittent PTH on nearly all major PDL cell functions (Lossdörfer et al., 2011c, 2005, 2011a) and provide proof of their physiological relevance. The anabolic effect of intermittent PTH on bone marrow stromal cells (BMSCs) transplanted in immunocompromised mice was previously demonstrated by Pettway *et al.* (Pettway et al., 2008). According to their study, 4 weeks of intermittent PTH administration increased the bone volume and bone content of implanted collagen sponges containing the implanted cells. Another proof of the anabolic potential of PTH in dentofacial applications was recently provided by Bashutski *et al*. who demonstrated the therapeutic effect of intermittent PTH on the osseous defect in the oral cavity in humans (Bashutski et al., 2010).

Taken together, our results indicate that intermittent PTH accelerates the PDL cell mediated periodontal regeneration and provide further proofs on the therapeutic potential of intermittent PTH in regenerating a functional periodontal ligament and alveolar bone.

5 REFERENCES

Abou-Samra, A. B., Jüppner, H., Force, T., Freeman, M. W., Kong, X. F., Schipani, E., Urena, P., Richards, J., Bonventre, J. V., and Potts, J. T., Jr (1992). Expression cloning of a common receptor for parathyroid hormone and parathyroid hormone-related peptide from rat osteoblast-like cells: a single receptor stimulates intracellular accumulation of both cAMP and inositol trisphosphates and increases intracellular free calcium. Proc. Natl. Acad. Sci. U.S.A *89*, 2732-2736.

Akizuki, T., Oda, S., Komaki, M., Tsuchioka, H., Kawakatsu, N., Kikuchi, A., Yamato, M., Okano, T., and Ishikawa, I. (2005). Application of periodontal ligament cell sheet for periodontal regeneration: a pilot study in beagle dogs. Journal of Periodontal Research *40*, 245-251.

Alokail, M. S., and Peddie, M. J. (2008). Quantitative comparison of PTH1R in breast cancer MCF7 and osteosarcoma SaOS□2 cell lines. Cell Biochemistry and Function *26*, 522-533.

Armamento-Villareal, R., Ziambaras, K., Abbasi-Jarhomi, S. H., Dimarogonas, A., Halstead, L., Fausto, A., Avioli, L. V., and Civitelli, R. (1997). An intact N terminus is required for the anabolic action of parathyroid hormone on adult female rats. J. Bone Miner. Res *12*, 384-392.

Arora, P. D., and McCulloch, C. A. (1994). Dependence of collagen remodelling on alpha-smooth muscle actin expression by fibroblasts. J. Cell. Physiol *159*, 161-175.

Avnet, S., Longhi, A., Salerno, M., Halleen, J. M., Perut, F., Granchi, D., Ferrari, S., Bertoni, F., Giunti, A., and Baldini, N. (2008). Increased osteoclast activity is associated with aggressiveness of osteosarcoma. Int. J. Oncol. *33*, 1231-1238.

Barros, S. P., Silva, M. A. D., Somerman, M. J., and Nociti, F. H., Jr (2003). Parathyroid hormone protects against periodontitis-associated bone loss. J. Dent. Res *82*, 791-795.

Bartold, P. M. (2006). Periodontal tissues in health and disease: introduction. Periodontol. 2000 *40*, 7-10.

Bartold, P. M., McCulloch, C. A., Narayanan, A. S., and Pitaru, S. (2000). Tissue engineering: a new paradigm for periodontal regeneration based on molecular and cell biology. Periodontol. 2000 *24*, 253-269.

Bashutski, J. D., and Wang, H.-L. (2009). Periodontal and endodontic regeneration. J Endod *35*, 321-328.

Bashutski, J. D., Eber, R. M., Kinney, J. S., Benavides, E., Maitra, S., Braun, T. M., Giannobile, W. V., and McCauley, L. K. (2010). Teriparatide and osseous regeneration in the oral cavity. N. Engl. J. Med *363*, 2396-2405.

Beck, F., Tucci, J., Russell, A., Senior, P. V., and Ferguson, M. W. (1995). The expression of the gene coding for parathyroid hormone-related protein (PTHrP) during tooth development in the rat. Cell Tissue Res. *280*, 283-290.

Becker, J., Schuppan, D., Rabanus, J. P., Rauch, R., Niechoy, U., and Gelderblom, H. R. (1991). Immunoelectron microscopic localization of collagens type I, V, VI and of procollagen type III in human periodontal ligament and cementum. J. Histochem. Cytochem *39*, 103-110.

Beertsen, W. (1975). Migration of fibroblasts in the periodontal ligament of the mouse incisor as revealed by autoradiography. Archives of Oral Biology *20*, 659-666, IN17-IN19.

Beertsen, W., McCulloch, C. A., and Sodek, J. (1997). The periodontal ligament: a unique, multifunctional connective tissue. Periodontol. 2000 *13*, 20-40.

Bellido, T., Ali, A. A., Plotkin, L. I., Fu, Q., Gubrij, I., Roberson, P. K., Weinstein, R. S., O'Brien, C. A., Manolagas, S. C., and Jilka, R. L. (2003). Proteasomal degradation of Runx2 shortens parathyroid hormone-induced anti-apoptotic signaling in osteoblasts. A putative explanation for why intermittent administration is needed for bone anabolism. J. Biol. Chem *278*, 50259-50272.

Berkovitz, B. K. (1990). The structure of the periodontal ligament: an update. Eur J Orthod *12*, 51-76.

Berkovitz, B. K. B., and Shore, R. C. (1995). The periodontal ligament in health and disease 2nd ed. (Lonodn: Mosby-Wolfe).

Beutner, E. H., and Munson, P. L. (1960). Time course of urinary excretion of inorganic phosphate by rats after parathyroidectomy and after injection of parathyroid extract. Endocrinology *66*, 610-616.

Bhattacharya, M., Peri, K., Ribeiro-da-Silva, A., Almazan, G., Shichi, H., Hou, X., Varma, D. R., and Chemtob, S. (1999). Localization of functional prostaglandin E2 receptors EP3 and EP4 in the nuclear envelope. J. Biol. Chem *274*, 15719-15724.

Billinton, N., and Knight, A. W. (2001). Seeing the wood through the trees: a review of techniques for distinguishing green fluorescent protein from endogenous autofluorescence. Anal. Biochem *291*, 175-197.

Bisello, A., Manen, D., Pierroz, D. D., Usdin, T. B., Rizzoli, R., and Ferrari, S. L. (2004). Agonist-specific regulation of parathyroid hormone (PTH) receptor type 2 activity: structural and functional analysis of PTH- and tuberoinfundibular peptide (TIP) 39-stimulated desensitization and internalization. Mol. Endocrinol *18*, 1486-1498.

Boyko, G. A., Melcher, A. H., and Brunette, D. M. (1981). Formation of new periodontal ligament by periodontal ligament cells implanted in vivo after culture in vitro. A preliminary study of transplanted roots in the dog. J. Periodont. Res *16*, 73-88.

Brixen, K. T., Christensen, P. M., Ejersted, C., and Langdahl, B. L. (2004). Teriparatide (biosynthetic human parathyroid hormone 1-34): a new paradigm in the treatment of osteoporosis. Basic Clin. Pharmacol. Toxicol *94*, 260-270.

Brown, E. M., Gamba, G., Riccardi, D., Lombardi, M., Butters, R., Kifor, O., Sun, A., Hediger, M. A., Lytton, J., and Hebert, S. C. (1993). Cloning and characterization of an extracellular Ca2+-sensing receptor from bovine parathyroid. Nature *366*, 575-580.

Carpio, L., Gladu, J., Goltzman, D., and Rabbani, S. A. (2001). Induction of osteoblast differentiation indexes by PTHrP in MG-63 cells involves multiple signaling pathways. Am. J. Physiol. Endocrinol. Metab. *281*, E489-499.

Chauvin, S., Bencsik, M., Bambino, T., and Nissenson, R. A. (2002). Parathyroid Hormone Receptor Recycling: Role of Receptor Dephosphorylation and β-Arrestin. Molecular Endocrinology *16*, 2720 -2732.

Chen, L.-P., Hsu, S.-P., Peng, Y.-S., Chiang, C.-K., and Hung, K.-Y. (2011). Periodontal disease is associated with metabolic syndrome in hemodialysis patients. Nephrol Dial Transplant. Available at: http://www.ncbi.nlm.nih.gov/pubmed/21602185 [Accessed June 9, 2011].

Cheng, Y., and Prusoff, W. H. (1973). Relationship between the inhibition constant (K1) and the concentration of inhibitor which causes 50 per cent inhibition (I50) of an enzymatic reaction. Biochem. Pharmacol *22*, 3099-3108.

Cho, M. I., Matsuda, N., Lin, W. L., Moshier, A., and Ramakrishnan, P. R. (1992). In vitro formation of mineralized nodules by periodontal ligament cells from the rat. Calcif. Tissue Int *50*, 459-467.

Cole, J. A. (1997). Down□Regulation of Protein Kinase C by Parathyroid Hormone and Mezerein Differentially Modulates cAMP Production and Phosphate Transport in Opossum Kidney Cells. Journal of Bone and Mineral Research *12*, 1223-1230.

Davidovitch, Z., Musich, D., and Doyle, M. (1972). Hormonal effects on orthodontic tooth movement in cats--a pilot study. Am J Orthod *62*, 95-96.

Demay, M., Mitchell, J., and Goltzman, D. (1985). Comparison of renal and osseous binding of parathyroid hormone and hormonal fragments. Am. J. Physiol. *249*, E437-446.

Divieti, P., Inomata, N., Chapin, K., Singh, R., Jüppner, H., and Bringhurst, F. R. (2001). Receptors for the carboxyl-terminal region of pth(1-84) are highly expressed in osteocytic cells. Endocrinology *142*, 916-925.

Dong, C., Filipeanu, C. M., Duvernay, M. T., and Wu, G. (2007). Regulation of G protein-coupled receptor export trafficking. Biochim. Biophys. Acta *1768*, 853-870.

Dublet, B., Dixon, E., de Miguel, E., and van der Rest, M. (1988). Bovine type XII collagen: amino acid sequence of a 10 kDa pepsin fragment from periodontal ligament reveals a high degree of homology with the chicken alpha 1(XII) sequence. FEBS Lett *233*, 177-180.

Duvernay, M. T., Filipeanu, C. M., and Wu, G. (2005). The regulatory mechanisms of export trafficking of G protein-coupled receptors. Cell. Signal *17*, 1457-1465.

El-Shinnawi, U. M., and El-Tantawy, S. I. (2003). The effect of alendronate sodium on alveolar bone loss in periodontitis (clinical trial). J Int Acad Periodontol *5*, 5-10.

Enomoto, M., Kinoshita, A., Pan, H. O., Suzuki, F., Yamamoto, I., and Takigawa, M. (1989). Demonstration of receptors for parathyroid hormone on cultured rabbit costal chondrocytes. Biochem. Biophys. Res. Commun. *162*, 1222-1229.

Feinstein, T. N., Wehbi, V. L., Ardura, J. A., Wheeler, D. S., Ferrandon, S., Gardella, T. J., and Vilardaga, J.-P. (2011). Retromer terminates the generation of cAMP by internalized PTH receptors. Nat. Chem. Biol. *7*, 278-284.

Ferguson, S. S. G. (2001). Evolving Concepts in G Protein-Coupled Receptor Endocytosis: The Role in Receptor Desensitization and Signaling. Pharmacological Reviews *53*, 1 -24.

Ferguson, S. S., Downey, W. E., 3rd, Colapietro, A. M., Barak, L. S., Ménard, L., and Caron, M. G. (1996). Role of beta-arrestin in mediating agonist-promoted G protein-coupled receptor internalization. Science *271*, 363-366.

Ferrari, S. L., Behar, V., Chorev, M., Rosenblatt, M., and Bisello, A. (1999). Endocytosis of ligand-human parathyroid hormone receptor 1 complexes is protein kinase C-dependent and involves beta-arrestin2. Real-time monitoring by fluorescence microscopy. J. Biol. Chem *274*, 29968-29975.

Flores, M. G., Hasegawa, M., Yamato, M., Takagi, R., Okano, T., and Ishikawa, I. (2008). Cementum-periodontal ligament complex regeneration using the cell sheet technique. J. Periodont. Res. *43*, 364-371.

Fredriksson, R., Lagerström, M. C., Lundin, L.-G., and Schiöth, H. B. (2003). The G-protein-coupled receptors in the human genome form five main families. Phylogenetic analysis, paralogon groups, and fingerprints. Mol. Pharmacol *63*, 1256-1272.

Friedman, P. A., and Goodman, W. G. (2006). PTH(1-84)/PTH(7-84): a balance of power. Am. J. Physiol. Renal Physiol *290*, F975-984.

Friedman, P. A., Gesek, F. A., Morley, P., Whitfield, J. F., and Willick, G. E. (1999). Cell-Specific Signaling and Structure-Activity Relations of Parathyroid Hormone Analogs in Mouse Kidney Cells. Endocrinology *140*, 301 -309.

Fullmer, H. M. (1958). Differential staining of connective tissue fibers in areas of stress. Science *127*, 1240.

Gardella, T. J., and Jüppner, H. (2001). Molecular properties of the PTH/PTHrP receptor. Trends Endocrinol. Metab *12*, 210-217.

Gensure, R. C., Gardella, T. J., and Jüppner, H. (2005). Parathyroid hormone and parathyroid hormone-related peptide, and their receptors. Biochem. Biophys. Res. Commun *328*, 666-678.

Gensure, R. C., Ponugoti, B., Gunes, Y., Papasani, M. R., Lanske, B., Bastepe, M., Rubin, D. A., and Jüppner, H. (2004). Identification and Characterization of Two Parathyroid Hormone-Like Molecules in Zebrafish. Endocrinology *145*, 1634 -1639.

Gentili, C., Morelli, S., and de Boland, A. R. (2003). Characterization of PTH/PTHrP receptor in rat duodenum: effects of ageing. J. Cell. Biochem. *88*, 1157-1167.

Gesty-Palmer, D., Chen, M., Reiter, E., Ahn, S., Nelson, C. D., Wang, S., Eckhardt, A. E., Cowan, C. L., Spurney, R. F., Luttrell, L. M., et al. (2006). Distinct beta-arrestin- and G protein-dependent pathways for parathyroid hormone receptor-stimulated ERK1/2 activation. J. Biol. Chem. *281*, 10856-10864.

Giannobile, W. V., and Somerman, M. J. (2003). Growth and amelogenin-like factors in periodontal wound healing. A systematic review. Ann. Periodontol *8*, 193-204.

Gonçalves, J. S., Sasso-Cerri, E., and Cerri, P. S. (2008). Cell death and quantitative reduction of rests of Malassez according to age. J. Periodont. Res. *43*, 478-481.

Goodman, O. B., Jr, Krupnick, J. G., Santini, F., Gurevich, V. V., Penn, R. B., Gagnon, A. W., Keen, J. H., and Benovic, J. L. (1996). Beta-arrestin acts as a clathrin adaptor in endocytosis of the beta2-adrenergic receptor. Nature *383*, 447-450.

Goold, C. P., Usdin, T. B., and Hoare, S. R. J. (2001). Regions in Rat and Human Parathyroid Hormone (PTH) 2 Receptors Controlling Receptor Interaction with PTH and with Antagonist Ligands. Journal of Pharmacology and Experimental Therapeutics *299*, 678 -690.

de Gortázar, A. R., Alonso, V., Alvarez-Arroyo, M. V., and Esbrit, P. (2006). Transient exposure to PTHrP (107-139) exerts anabolic effects through vascular endothelial growth factor receptor 2 in human osteoblastic cells in vitro. Calcif. Tissue Int. *79*, 360-369.

Gould, T. R., Melcher, A. H., and Brunette, D. M. (1977). Location of progenitor cells in periodontal ligament of mouse molar stimulated by wounding. Anat. Rec *188*, 133-141.

Graham, F. L., Smiley, J., Russell, W. C., and Nairn, R. (1977). Characteristics of a human cell line transformed by DNA from human adenovirus type 5. J. Gen. Virol *36*, 59-74.

Grauschopf, U., Lilie, H., Honold, K., Wozny, M., Reusch, D., Esswein, A., Schäfer, W., Rücknagel, K. P., and Rudolph, R. (2000). The N-terminal fragment of human parathyroid hormone receptor 1 constitutes a hormone binding domain and reveals a distinct disulfide pattern. Biochemistry *39*, 8878-8887.

Guerreiro, P. M., Renfro, J. L., Power, D. M., and Canario, A. V. M. (2007). The parathyroid hormone family of peptides: structure, tissue distribution, regulation, and potential functional roles in calcium and phosphate balance in fish. Am. J. Physiol. Regul. Integr. Comp. Physiol *292*, R679-696.

Habener, J. F., Kemper, B. W., Rich, A., and Potts, J. T., Jr (1976). Biosynthesis of parathyroid hormone. Recent Prog. Horm. Res *33*, 249-308.

Habener, J. F., Rosenblatt, M., Kemper, B., Kronenberg, H. M., Rich, A., and Potts, J. T., Jr (1978). Pre-proparathyroid hormone; amino acid sequence, chemical synthesis, and some biological studies of the precursor region. Proc. Natl. Acad. Sci. U.S.A *75*, 2616-2620.

Häkkinen, L., Oksala, O., Salo, T., Rahemtulla, F., and Larjava, H. (1993). Immunohistochemical localization of proteoglycans in human periodontium. J. Histochem. Cytochem *41*, 1689-1699.

Hall, R. A., and Lefkowitz, R. J. (2002). Regulation of G Protein-Coupled Receptor Signaling by Scaffold Proteins. Circ Res *91*, 672-680.

Haramoto, N., Kawane, T., and Horiuchi, N. (2007). Upregulation of PTH receptor mRNA expression by dexamethasone in UMR-106 osteoblast-like cells. Oral Dis *13*, 23-31.

Hassell, T. M. (1993). Tissues and cells of the periodontium. Periodontol. 2000 *3*, 9-38.

Heijl, L., Heden, G., Svärdström, G., and Ostgren, A. (1997). Enamel matrix derivative (EMDOGAIN) in the treatment of intrabony periodontal defects. J. Clin. Periodontol *24*, 705-714.

Hermans, E. (2003). Biochemical and pharmacological control of the multiplicity of coupling at G-protein-coupled receptors. Pharmacol. Ther *99*, 25-44.

Hoare, S. R., Bonner, T. I., and Usdin, T. B. (1999). Comparison of rat and human parathyroid hormone 2 (PTH2) receptor activation: PTH is a low potency partial agonist at the rat PTH2 receptor. Endocrinology *140*, 4419-4425.

Hoare, S. R., Clark, J. A., and Usdin, T. B. (2000). Molecular determinants of tuberoinfundibular peptide of 39 residues (TIP39) selectivity for the parathyroid hormone-2 (PTH2) receptor. N-terminal truncation of TIP39 reverses PTH2 receptor/PTH1 receptor binding selectivity. J. Biol. Chem *275*, 27274-27283.

Hodsman, A. B., Bauer, D. C., Dempster, D. W., Dian, L., Hanley, D. A., Harris, S. T., Kendler, D. L., McClung, M. R., Miller, P. D., Olszynski, W. P., et al. (2005). Parathyroid hormone and teriparatide for the treatment of osteoporosis: a review of the evidence and suggested guidelines for its use. Endocr. Rev *26*, 688-703.

Hodsman, A. B., Fraher, L. J., Ostbye, T., Adachi, J. D., and Steer, B. M. (1993). An evaluation of several biochemical markers for bone formation and resorption in a protocol utilizing cyclical parathyroid hormone and calcitonin therapy for osteoporosis. J. Clin. Invest *91*, 1138-1148.

Hodsman, A. B., Hanley, D. A., Ettinger, M. P., Bolognese, M. A., Fox, J., Metcalfe, A. J., and Lindsay, R. (2003). Efficacy and safety of human parathyroid hormone-(1-84) in increasing bone mineral density in postmenopausal osteoporosis. J. Clin. Endocrinol. Metab *88*, 5212-5220.

Hodsman, A. B., Hanley, D., Watson, P., and Fraher, L. (2002). Parathyroid hormone. In Principles of bone biology, J. P. Bilezikian and L. G. (Lawrence G. Raisz, eds. (San Diego, Calif.: Academic Press,), pp. 1305–1324.

Horiuchi, K., Amizuka, N., Takeshita, S., Takamatsu, H., Katsuura, M., Ozawa, H., Toyama, Y., Bonewald, L. F., and Kudo, A. (1999). Identification and characterization of a novel protein, periostin, with restricted expression to periosteum and periodontal ligament and increased expression by transforming growth factor beta. J. Bone Miner. Res *14*, 1239-1249.

Iida-Klein, A., Guo, J., Takemura, M., Drake, M. T., Potts, J. T., Jr, Abou-Samra, A., Bringhurst, F. R., and Segre, G. V. (1997). Mutations in the second cytoplasmic loop of the rat parathyroid hormone (PTH)/PTH-related protein receptor result in selective loss of PTH-stimulated phospholipase C activity. J. Biol. Chem. *272*, 6882-6889.

Isales, C. M., Sumpio, B., Bollag, R. J., Zhong, Q., Ding, K.-H., Du, W., Rodriguez-Commes, J., Lopez, R., Rosales, O. R., Gasalla-Herraiz, J., et al. (2000). Functional parathyroid hormone receptors are present in an umbilical vein endothelial cell line. American Journal of Physiology - Endocrinology And Metabolism *279*, E654 -E662.

Jilka, R. L. (2007). Molecular and cellular mechanisms of the anabolic effect of intermittent PTH. Bone *40*, 1434-1446.

Jilka, R. L., Weinstein, R. S., Bellido, T., Roberson, P., Parfitt, A. M., and Manolagas, S. C. (1999). Increased bone formation by prevention of osteoblast apoptosis with parathyroid hormone. J. Clin. Invest *104*, 439-446.

John, M. R., Arai, M., Rubin, D. A., Jonsson, K. B., and Jüppner, H. (2002). Identification and characterization of the murine and human gene encoding the tuberoinfundibular peptide of 39 residues. Endocrinology *143*, 1047-1057.

Johnston, S., Andrews, S., Shen, V., Cosman, F., Lindsay, R., Dempster, D. W., and Iida-Klein, A. (2007). The effects of combination of alendronate and human parathyroid hormone(1-34) on bone strength are synergistic in the lumbar vertebra and additive in the femur of C57BL/6J mice. Endocrinology *148*, 4466-4474.

Jong, Y.-J. I., Kumar, V., Kingston, A. E., Romano, C., and O'Malley, K. L. (2005). Functional metabotropic glutamate receptors on nuclei from brain and primary cultured striatal neurons. Role of transporters in delivering ligand. J. Biol. Chem *280*, 30469-30480.

Jongen, J. W., Willemstein-van Hove, E. C., van der Meer, J. M., Bos, M. P., Jüppner, H., Segre, G. V., Abou-Samra, A. B., Feyen, J. H., and Herrmann-Erlee, M. P. (1996). Down-regulation of the receptor for parathyroid hormone (PTH) and PTH-related peptide by PTH in primary fetal rat osteoblasts. J. Bone Miner. Res. *11*, 1218-1225.

Jönsson, D., Nebel, D., Bratthall, G., and Nilsson, B.-O. (2011). The human periodontal ligament cell: a fibroblast-like cell acting as an immune cell. J. Periodont. Res *46*, 153-157.

Jonsson, K. B., John, M. R., Gensure, R. C., Gardella, T. J., and Jüppner, H. (2001). Tuberoinfundibular peptide 39 binds to the parathyroid hormone (PTH)/PTH-related peptide receptor, but functions as an antagonist. Endocrinology *142*, 704-709.

Jouishomme, H., Whitfield, J. F., Gagnon, L., Maclean, S., Isaacs, R., Chakravarthy, B., Durkin, J., Neugebauer, W., Willick, G., and Rixon, R. H. (1994). Further definition of the protein kinase C activation domain of the parathyroid hormone. J. Bone Miner. Res *9*, 943-949.

Jung, R. E., Glauser, R., Schärer, P., Hämmerle, C. H. F., Sailer, H. F., and Weber, F. E. (2003). Effect of rhBMP-2 on guided bone regeneration in humans. Clin Oral Implants Res *14*, 556-568.

Juppner, H., Abou-Samra, A., Freeman, M., Kong, X., Schipani, E., Richards, J., Kolakowski, L., Hock, J., Potts, J., Kronenberg, H., et al. (1991). A G protein-linked receptor for parathyroid hormone and parathyroid hormone-related peptide. Science *254*, 1024 -1026.

Karim, Z., Gérard, B., Bakouh, N., Alili, R., Leroy, C., Beck, L., Silve, C., Planelles, G., Urena-Torres, P., Grandchamp, B., et al. (2008). NHERF1 mutations and responsiveness of renal parathyroid hormone. N. Engl. J. Med *359*, 1128-1135.

Karimbux, N. Y., Rosenblum, N. D., and Nishimura, I. (1992). Site-specific expression of collagen I and XII mRNAs in the rat periodontal ligament at two developmental stages. J. Dent. Res *71*, 1355-1362.

Kato, A., Suzuki, M., Karasawa, Y., Sugimoto, T., and Doi, K. (2005a). Immunohistochemical Detection of PTHrP and PTH/PTHrP Receptor 1 on the Odontoblastic Reparative Process after Actinomycin D Treatment in Rats. Journal of Toxicologic Pathology *18*, 33-39.

Kato, A., Suzuki, M., Karasawa, Y., Sugimoto, T., and Doi, K. (2005b). PTHrP and PTH/PTHrP receptor 1 expression in odontogenic cells of normal and HHM model rat incisors. Toxicol Pathol *33*, 456-464.

Kato, C., Kojima, T., Komaki, M., Mimori, K., Duarte, W. R., Takenaga, K., and Ishikawa, I. (2004). S100A4 inhibition by RNAi up-regulates osteoblast related genes in periodontal ligament cells. Biochemical and Biophysical Research Communications *326*, 147-153.

Kawane, T., Mimura, J., Fujii-Kuriyama, Y., and Horiuchi, N. (2001). Parathyroid hormone (PTH) suppresses rat PTH/PTH-related protein receptor gene promoter. Biochem. Biophys. Res. Commun *287*, 313-322.

Kebschull, M., Demmer, R. T., and Papapanou, P. N. (2010). “Gum bug, leave my heart alone!”--epidemiologic and mechanistic evidence linking periodontal infections and atherosclerosis. J. Dent. Res *89*, 879-902.

Kilav, R., Silver, J., and Naveh-Many, T. (1995). Parathyroid hormone gene expression in hypophosphatemic rats. J. Clin. Invest. *96*, 327-333.

King, G. L. (2008). The role of inflammatory cytokines in diabetes and its complications. J. Periodontol *79*, 1527-1534.

Kobilka, B. K. (2007). G Protein Coupled Receptor Structure and Activation. Biochim Biophys Acta *1768*, 794-807.

Laemmli, U. K. (1970). Cleavage of structural proteins during the assembly of the head of bacteriophage T4. Nature *227*, 680-685.

Langub, M. C., Monier-Faugere, M. C., Qi, Q., Geng, Z., Koszewski, N. J., and Malluche, H. H. (2001). Parathyroid hormone/parathyroid hormone-related peptide type 1 receptor in human bone. J. Bone Miner. Res *16*, 448-456.

Lawson, D. E., Fraser, D. R., Kodicek, E., Morris, H. R., and Williams, D. H. (1971). Identification of 1,25-dihydroxycholecalciferol, a new kidney hormone controlling calcium metabolism. Nature *230*, 228-230.

Lee, D. K., Lança, A. J., Cheng, R., Nguyen, T., Ji, X. D., Gobeil, F., Jr, Chemtob, S., George, S. R., and O’Dowd, B. F. (2004). Agonist-independent nuclear localization of the Apelin, angiotensin AT1, and bradykinin B2 receptors. J. Biol. Chem *279*, 7901-7908.

Lekic, P., and McCulloch, C. A. (1996). Periodontal ligament cell population: the central role of fibroblasts in creating a unique tissue. Anat. Rec *245*, 327-341.

Lekic, P., Rojas, J., Birek, C., Tenenbaum, H., and McCulloch, C. A. (2001). Phenotypic comparison of periodontal ligament cells in vivo and in vitro. J. Periodont. Res *36*, 71-79.

Li, H., Bartold, P. M., Young, W. G., Xiao, Y., and Waters, M. J. (2001). Growth hormone induces bone morphogenetic proteins and bone-related proteins in the developing rat periodontium. J. Bone Miner. Res *16*, 1068-1076.

Liu, J., Cao, Z., and Li, C. (2009). Intermittent PTH administration: a novel therapy method for periodontitis-associated alveolar bone loss. Med. Hypotheses *72*, 294-296.

Lossdörfer, S., Abuduwali, N., and Jäger, A. (2011a). Bone morphogenetic protein-7 modifies the effects of insulin-like growth factors and intermittent parathyroid hormone (1-34) on human periodontal ligament cell physiology in vitro. J. Periodontol. *82*, 900-908.

Lossdörfer, S., Götz, W., and Jäger, A. (2005). PTH(1-34) affects osteoprotegerin production in human PDL cells in vitro. J. Dent. Res. *84*, 634-638.

Lossdörfer, S., Götz, W., and Jäger, A. (2011b). PTH(1-34)-induced changes in RANKL and OPG expression by human PDL cells modify osteoclast biology in a co-culture model with RAW 264.7 cells. Clin Oral Investig *15*, 941-952.

Lossdörfer, S., Götz, W., Rath-Deschner, B., and Jäger, A. (2006a). Parathyroid hormone(1-34) mediates proliferative and apoptotic signaling in human periodontal ligament cells in vitro via protein kinase C-dependent and protein kinase A-dependent pathways. Cell Tissue Res. *325*, 469-479.

Lossdörfer, S., Götz, W., and Jäger, A. (2011b). PTH(1-34)-induced changes in RANKL and OPG expression by human PDL cells modify osteoclast biology in a co-culture model with RAW 264.7 cells. Clin Oral Investig *15*, 941-952.

Lossdörfer, S., Kraus, D., Abuduwali, N., and Jäger, A. (2011c). Intermittent administration of PTH(1-34) regulates the osteoblastic differentiation of human periodontal ligament cells via protein kinase C- and protein kinase A-dependent pathways in vitro. J. Periodont. Res. *46*, 318-326.

Lossdörfer, S., Stier, S., Götz, W., and Jäger, A. (2006b). Maturation-state dependent response of human periodontal ligament cells to an intermittent parathyroid hormone exposure in vitro. J. Periodont. Res *41*, 62-72.

Lu, B., Smock, S. L., Castleberry, T. A., and Owen, T. A. (2001). Molecular cloning and functional characterization of the canine androgen receptor. Mol. Cell. Biochem *226*, 129-140.

Lu, D., Yang, H., Shaw, G., and Raizada, M. K. (1998). Angiotensin II-induced nuclear targeting of the angiotensin type 1 (AT1) receptor in brain neurons. Endocrinology *139*, 365-375.

Luck, M. D., Carter, P. H., and Gardella, T. J. (1999). The (1-14) fragment of parathyroid hormone (PTH) activates intact and amino-terminally truncated PTH-1 receptors. Mol. Endocrinol *13*, 670-680.

Lukinmaa, P. L., and Waltimo, J. (1992). Immunohistochemical localization of types I, V, and VI collagen in human permanent teeth and periodontal ligament. J. Dent. Res *71*, 391-397.

Lutolf, M. P., and Hubbell, J. A. (2005). Synthetic biomaterials as instructive extracellular microenvironments for morphogenesis in tissue engineering. Nat Biotech *23*, 47-55.

Ma, P. X. (2008). Biomimetic Materials for Tissue Engineering. Adv Drug Deliv Rev *60*, 184-198.

Mahon, M. J., and Segre, G. V. (2004). Stimulation by parathyroid hormone of a NHERF-1-assembled complex consisting of the parathyroid hormone I receptor, phospholipase Cbeta, and actin increases intracellular calcium in opossum kidney cells. J. Biol. Chem *279*, 23550-23558.

Mahon, M. J., Bonacci, T. M., Divieti, P., and Smrcka, A. V. (2006). A docking site for G protein betagamma subunits on the parathyroid hormone 1 receptor supports signaling through multiple pathways. Mol. Endocrinol *20*, 136-146.

Mahon, M. J., Donowitz, M., Yun, C. C., and Segre, G. V. (2002). Na(+)/H(+) exchanger regulatory factor 2 directs parathyroid hormone 1 receptor signalling. Nature *417*, 858-861.

Malecz, N., Bambino, T., Bencsik, M., and Nissenson, R. A. (1998). Identification of phosphorylation sites in the G protein-coupled receptor for parathyroid hormone. Receptor phosphorylation is not required for agonist-induced internalization. Mol. Endocrinol *12*, 1846-1856.

Mannstadt, M., Jüppner, H., and Gardella, T. J. (1999). Receptors for PTH and PTHrP: their biological importance and functional properties. Am. J. Physiol *277*, F665-675.

Marchesan, J. T., Scanlon, C. S., Soehren, S., Matsuo, M., and Kapila, Y. L. (2011). Implications of cultured periodontal ligament cells for the clinical and experimental setting: A review. Arch Oral Biol. Available at: http://www.ncbi.nlm.nih.gov/pubmed/21470594 [Accessed June 11, 2011].

Marinissen, M. J., and Gutkind, J. S. (2001). G-protein-coupled receptors and signaling networks: emerging paradigms. Trends Pharmacol. Sci *22*, 368-376.

Massry, S. G., and Smogorzewski, M. (1998). PTH-PTHrP receptor in chronic renal failure. Nephrol. Dial. Transplant *13 Suppl 1*, 50-57.

McCuaig, K. A., Clarke, J. C., and White, J. H. (1994). Molecular cloning of the gene encoding the mouse parathyroid hormone/parathyroid hormone-related peptide receptor. Proc. Natl. Acad. Sci. U.S.A *91*, 5051-5055.

McCulloch, C. A., Lekic, P., and McKee, M. D. (2000). Role of physical forces in regulating the form and function of the periodontal ligament. Periodontol. 2000 *24*, 56-72.

Mosiman, V. L., Patterson, B. K., Canterero, L., and Goolsby, C. L. (1997). Reducing cellular autofluorescence in flow cytometry: an in situ method. Cytometry *30*, 151-156.

Mukai, M., Yoshimine, Y., Akamine, A., and Maeda, K. (1993). Bone-like nodules formed in vitro by rat periodontal ligament cells. Cell Tissue Res. *271*, 453-460.

Murray, T. M., Rao, L. G., Divieti, P., and Bringhurst, F. R. (2005). Parathyroid hormone secretion and action: evidence for discrete receptors for the carboxyl-terminal region and related biological actions of carboxyl- terminal ligands. Endocr. Rev *26*, 78-113.

Nanci, A., and Bosshardt, D. D. (2006). Structure of periodontal tissues in health and disease. Periodontol. 2000 *40*, 11-28.

Neer, R. M., Arnaud, C. D., Zanchetta, J. R., Prince, R., Gaich, G. A., Reginster, J. Y., Hodsman, A. B., Eriksen, E. F., Ish-Shalom, S., Genant, H. K., et al. (2001). Effect of parathyroid hormone (1-34) on fractures and bone mineral density in postmenopausal women with osteoporosis. N. Engl. J. Med *344*, 1434-1441.

Nevins, M., Giannobile, W. V., McGuire, M. K., Kao, R. T., Mellonig, J. T., Hinrichs, J. E., McAllister, B. S., Murphy, K. S., McClain, P. K., Nevins, M. L., et al. (2005). Platelet-derived growth factor stimulates bone fill and rate of attachment level gain: results of a large multicenter randomized controlled trial. J. Periodontol *76*, 2205-2215.

Nohutcu, R. M., Somerman, M. J., and McCauley, L. K. (1995). Dexamethasone enhances the effects of parathyroid hormone on human periodontal ligament cells in vitro. Calcif. Tissue Int *56*, 571-577.

Nojima, N., Kobayashi, M., Shionome, M., Takahashi, N., Suda, T., and Hasegawa, K. (1990). Fibroblastic cells derived from bovine periodontal ligaments have the phenotypes of osteoblasts. J. Periodont. Res *25*, 179-185.

Nyman, S., Lindhe, J., Karring, T., and Rylander, H. (1982). New attachment following surgical treatment of human periodontal disease. J. Clin. Periodontol *9*, 290-296.

Offenbacher, S., Katz, V., Fertik, G., Collins, J., Boyd, D., Maynor, G., McKaig, R., and Beck, J. (1996). Periodontal infection as a possible risk factor for preterm low birth weight. J. Periodontol *67*, 1103-1113.

Onyia, J. E., Bidwell, J., Herring, J., Hulman, J., and Hock, J. M. (1995). In vivo, human parathyroid hormone fragment (hPTH 1-34) transiently stimulates immediate early response gene expression, but not proliferation, in trabecular bone cells of young rats. Bone *17*, 479-484.

Ouyang, H., McCauley, L. K., Berry, J. E., D'Errico, J. A., Strayhorn, C. L., and Somerman, M. J. (2000). Response of immortalized murine cementoblasts/periodontal ligament cells to parathyroid hormone and parathyroid hormone-related protein in vitro. Arch. Oral Biol *45*, 293-303.

Pautke, C., Schieker, M., Tischer, T., Kolk, A., Neth, P., Mutschler, W., and Milz, S. (2004). Characterization of osteosarcoma cell lines MG-63, Saos-2 and U-2 OS in comparison to human osteoblasts. Anticancer Res *24*, 3743-3748.

Periodontal Ligament - Studio Dentaire Available at: http://www.studiodentaire.com/en/glossary/periodontal_ligament.php [Accessed May 18, 2011].

Periodontitis Types: Periapical and Apical, Chronic and Aggressive Periodontitis Available at: http://periodontitis.dentalbuzz.org/types/periapical-apical-chronic-aggressive-periodontitis/ [Accessed June 22, 2011].

Pettway, G. J., Meganck, J. A., Koh, A. J., Keller, E. T., Goldstein, S. A., and McCauley, L. K. (2008). Parathyroid Hormone Mediates Bone Growth through the Regulation of Osteoblast Proliferation and Differentiation. Bone *42*, 806-818.

Pettway, G. J., Schneider, A., Koh, A. J., Widjaja, E., Morris, M. D., Meganck, J. A., Goldstein, S. A., and McCauley, L. K. (2005). Anabolic actions of PTH (1-34): use of a novel tissue engineering model to investigate temporal effects on bone. Bone *36*, 959-970.

Pfaffl, M. W. (2001). A new mathematical model for relative quantification in real-time RT-PCR. Nucleic Acids Res *29*, e45.

Pihlstrom, B. L., Michalowicz, B. S., and Johnson, N. W. (2005). Periodontal diseases. Lancet *366*, 1809-1820.

Pliam, N. B., Nyiredy, K. O., and Arnaud, C. D. (1982). Parathyroid hormone receptors in avian bone cells. Proc. Natl. Acad. Sci. U.S.A. *79*, 2061-2063.

Potts, J. T., Jr, Bringhurst, F. R., Gardella, T. J., Nussbaum, S. R., Segre, G. V., and Kronenberg, H. M. (1995). Parathyroid hormone. physiology, chemistry,biosynthesis, secretion, metabolism,and mode of action. In Endocrinology, L. J. DeGroot,, ed. (Philadelphia: W.B. Saunders), pp. 920–966.

Pullman, T. N., Lavender, A. R., Aho, I., and Rasmussen, H. (1960). Direct renal action of a purified parathyroid extract. Endocrinology *67*, 570-582.

Qin, L., Li, X., Ko, J.-K., and Partridge, N. C. (2005). Parathyroid hormone uses multiple mechanisms to arrest the cell cycle progression of osteoblastic cells from G1 to S phase. J. Biol. Chem *280*, 3104-3111.

Qiu, T., Wu, X., Zhang, F., Clemens, T. L., Wan, M., and Cao, X. (2010). TGF-[beta] type II receptor phosphorylates PTH receptor to integrate bone remodelling signalling. Nat Cell Biol *12*, 224-234.

Quattrocchi, E., and Kourlas, H. (2004). Teriparatide: a review. Clin Ther *26*, 841-854.

Rao, L. G., and Murray, T. M. (1985). Binding of intact parathyroid hormone to rat osteosarcoma cells: major contribution of binding sites for the carboxyl-terminal region of the hormone. Endocrinology *117*, 1632-1638.

Rashid, G., Bernheim, J., Green, J., and Benchetrit, S. (2007). Parathyroid hormone stimulates the endothelial nitric oxide synthase through protein kinase A and C pathways. Nephrology Dialysis Transplantation *22*, 2831 -2837.

Rincon, J. C., Young, W. G., and Bartold, P. M. (2006). The epithelial cell rests of Malassez--a role in periodontal regeneration? J. Periodont. Res. *41*, 245-252.

Rios, H. F., Lin, Z., Oh, B., Park, C. H., and Giannobile, W. V. (2011). Cell- and Gene-Based Therapeutic Strategies for Periodontal Regenerative Medicine. J Periodontol. Available at: http://www.ncbi.nlm.nih.gov/pubmed/21284553 [Accessed June 9, 2011].

Rodan, S. B., Fischer, M. K., Egan, J. J., Epstein, P. M., and Rodan, G. A. (1984). The effect of dexamethasone on parathyroid hormone stimulation of adenylate cyclase in ROS 17/2.8 cells. Endocrinology *115*, 951-958.

Rubin, D. A., and Jüppner, H. (1999). Zebrafish express the common parathyroid hormone/parathyroid hormone-related peptide receptor (PTH1R) and a novel receptor (PTH3R) that is preferentially activated by mammalian and fugufish parathyroid hormone-related peptide. J. Biol. Chem *274*, 28185-28190.

Rubin, M. R., Cosman, F., Lindsay, R., and Bilezikian, J. P. (2002). The anabolic effects of parathyroid hormone. Osteoporos Int *13*, 267-277.

Schipani, E., and Provot, S. (2003). PTHrP, PTH, and the PTH/PTHrP receptor in endochondral bone development. Birth Defects Res. C Embryo Today *69*, 352-362.

Schipani, E., Karga, H., Karaplis, A. C., Potts, J. T., Jr, Kronenberg, H. M., Segre, G. V., Abou-Samra, A. B., and Jüppner, H. (1993). Identical complementary deoxyribonucleic acids encode a human renal and bone parathyroid hormone (PTH)/PTH-related peptide receptor. Endocrinology *132*, 2157-2165.

Schneider, L. C., Hollinshead, M. B., and Lizzack, L. S. (1972). Tooth eruption induced in grey lethal mice using parathyroid hormone. Arch. Oral Biol *17*, 591-594.

Seo, B.-M., Miura, M., Gronthos, S., Bartold, P. M., Batouli, S., Brahim, J., Young, M., Robey, P. G., Wang, C.-Y., and Shi, S. (2004). Investigation of multipotent postnatal stem cells from human periodontal ligament. Lancet *364*, 149-155.

Seymour, G. J., Ford, P. J., Cullinan, M. P., Leishman, S., and Yamazaki, K. (2007). Relationship between periodontal infections and systemic disease. Clin. Microbiol. Infect *13 Suppl 4*, 3-10.

Sheehan, S., Muthusamy, A., Paul, E., Sikes, R. A., and Gomes, R. R., Jr (2010). Short-term intermittent PTH 1-34 administration enhances bone formation in SCID/Beige mice. Endocr. J. *57*, 373-382.

Shenolikar, S., Voltz, J. W., Minkoff, C. M., Wade, J. B., and Weinman, E. J. (2002). Targeted disruption of the mouse NHERF-1 gene promotes internalization of proximal tubule sodium-phosphate cotransporter type IIa and renal phosphate wasting. Proceedings of the National Academy of Sciences *99*, 11470 -11475.

Shimizu, M., Carter, P. H., and Gardella, T. J. (2000a). Autoactivation of Type-1 Parathyroid Hormone Receptors Containing a Tethered Ligand. Journal of Biological Chemistry *275*, 19456 -19460.

Shimizu, M., Potts, J. T., Jr, and Gardella, T. J. (2000b). Minimization of parathyroid hormone. Novel amino-terminal parathyroid hormone fragments with enhanced potency in activating the type-1 parathyroid hormone receptor. J. Biol. Chem *275*, 21836-21843.

Shore, R. C., and Berkovitz, B. K. B. (1979). An ultrastructural study of periodontal ligament fibroblasts in relation to their possible role in tooth eruption and intracellular collagen degradation in the rat. Archives of Oral Biology *24*, 155-164.

Shvil, Y., Naveh-Many, T., Barach, P., and Silver, J. (1990). Regulation of parathyroid cell gene expression in experimental uremia. J. Am. Soc. Nephrol *1*, 99-104.

Silver, J., and Levi, R. (2005). Regulation of PTH synthesis and secretion relevant to the management of secondary hyperparathyroidism in chronic kidney disease. Kidney Int *67*, s8-s12.

Silver, J., Moallem, E., Kilav, R., Sela, A., and Naveh-Many, T. (1998). Regulation of the parathyroid hormone gene by calcium, phosphate and 1,25-dihydroxyvitamin D. Nephrol. Dial. Transplant *13 Suppl 1*, 40-44.

Silver, J., Naveh-Many, T., Mayer, H., Schmelzer, H. J., and Popovtzer, M. M. (1986). Regulation by vitamin D metabolites of parathyroid hormone gene transcription in vivo in the rat. J. Clin. Invest *78*, 1296-1301.

Silver, J., Yalcindag, C., Sela-Brown, A., Kilav, R., and Naveh-Many, T. (1999). Regulation of the parathyroid hormone gene by vitamin D, calcium and phosphate. Kidney Int *56*, 2-7.

Singh, A. T. K., Gilchrist, A., Voyno-Yasenetskaya, T., Radeff-Huang, J. M., and Stern, P. H. (2005). G alpha12/G alpha13 subunits of heterotrimeric G proteins mediate parathyroid hormone activation of phospholipase D in UMR-106 osteoblastic cells. Endocrinology *146*, 2171-2175.

Smith, D. P., Zhang, X. Y., Frolik, C. A., Harvey, A., Chandrasekhar, S., Black, E. C., and Hsiung, H. M. (1996). Structure and functional expression of a complementary DNA for porcine parathyroid hormone/parathyroid hormone-related peptide receptor. Biochim. Biophys. Acta *1307*, 339-347.

Smock, S. L., Vogt, G. A., Castleberry, T. A., Lu, B., and Owen, T. A. (2001). Molecular cloning and functional characterization of the canine parathyroid hormone/parathyroid hormone related peptide receptor (PTH1). Mol. Biol. Rep. *28*, 235-243.

Sneddon, W. B., Barry, E. L., Coutermarsh, B. A., Gesek, F. A., Liu, F., and Friedman, P. A. (1998). Regulation of renal parathyroid hormone receptor expression by 1, 25-dihydroxyvitamin D3 and retinoic acid. Cell. Physiol. Biochem. *8*, 261-277.

Somerman, M. J., Archer, S. Y., Imm, G. R., and Foster, R. A. (1988). A comparative study of human periodontal ligament cells and gingival fibroblasts in vitro. J. Dent. Res *67*, 66-70.

Songyang, Z., Fanning, A. S., Fu, C., Xu, J., Marfatia, S. M., Chishti, A. H., Crompton, A., Chan, A. C., Anderson, J. M., and Cantley, L. C. (1997). Recognition of unique carboxyl-terminal motifs by distinct PDZ domains. Science *275*, 73-77.

Stewart, A. F. (1996). PTHrP(1-36) as a skeletal anabolic agent for the treatment of osteoporosis. Bone *19*, 303-306.

Sugimoto, T., Ikeda, K., Kano, J., Yamaguchi, T., Fukase, M., and Chihara, K. (1994). Cross-talk of parathyroid hormone-responsive dual signal transduction systems in osteoblastic osteosarcoma cells: its role in PTH-induced homologous desensitization of intracellular calcium response. J. Cell. Physiol. *158*, 374-380.

Sutherland, M. K., Rao, L. G., Wylie, J. N., Gupta, A., Ly, H., Sodek, J., and Murray, T. M. (1994). Carboxyl-terminal parathyroid hormone peptide (53-84) elevates alkaline phosphatase and osteocalcin mRNA levels in SaOS-2 cells. J. Bone Miner. Res *9*, 453-458.

Takasu, H., Gardella, T. J., Luck, M. D., Potts, J. T., Jr, and Bringhurst, F. R. (1999). Amino-terminal modifications of human parathyroid hormone (PTH) selectively alter phospholipase C signaling via the type 1 PTH receptor: implications for design of signal-specific PTH ligands. Biochemistry *38*, 13453-13460.

Takayama, S., Murakami, S., Miki, Y., Ikezawa, K., Tasaka, S., Terashima, A., Asano, T., and Okada, H. (1997). Effects of basic fibroblast growth factor on human periodontal ligament cells. J. Periodont. Res *32*, 667-675.

Tawfeek, H. A. W., Qian, F., and Abou-Samra, A. B. (2002). Phosphorylation of the receptor for PTH and PTHrP is required for internalization and regulates receptor signaling. Mol. Endocrinol *16*, 1-13.

Teare, J. A., Ramoshebi, L. N., and Ripamonti, U. (2008). Periodontal tissue regeneration by recombinant human transforming growth factor-beta 3 in Papio ursinus. J. Periodont. Res *43*, 1-8.

Ten Cate, A. R. (1998). Oral Histology: Development, Structure, and Function 5th ed. (St. Louis: Mosby).

Ten Cate, A. R., Mills, C., and Solomon, G. (1971). The development of the periodontium. A transplantation and autoradiographic study. Anat. Rec *170*, 365-379.

Tenorio, D., and Hughes, F. J. (1996). An immunohistochemical investigation of the expression of parathyroid hormone receptors in rat cementoblasts. Arch. Oral Biol *41*, 299-305.

Tenta, R., Sourla, A., Lembessis, P., and Koutsilieris, M. (2006). Bone-related growth factors and zoledronic acid regulate the PTHrP/PTH.1 receptor bioregulation systems in MG-63 human osteosarcoma cells. Anticancer Res. *26*, 283-291.

Tian, J., Smogorzewski, M., Kedes, L., and Massry, S. G. (1994). PTH-PTHrP receptor mRNA is downregulated in chronic renal failure. Am. J. Nephrol *14*, 41-46.

Titus, L., Jackson, E., Nanes, M. S., Rubin, J. E., and Catherwood, B. D. (1991). 1,25-dihydroxyvitamin D reduces parathyroid hormone receptor number in ROS 17/2.8 cells and prevents the glucocorticoid-induced increase in these receptors: relationship to adenylate cyclase activation. J. Bone Miner. Res *6*, 631-637.

Tsai, B., Ye, Y., and Rapoport, T. A. (2002). Retro-translocation of proteins from the endoplasmic reticulum into the cytosol. Nat. Rev. Mol. Cell Biol *3*, 246-255.

Turner, C. H. (2002). Biomechanics of bone: determinants of skeletal fragility and bone quality. Osteoporos Int *13*, 97-104.

Ureña, P., Ferreira, A., Morieux, C., Drüeke, T., and Christine de Vernejoul, M. (1996). PTH/PTHrP receptor mRNA is down-regulated in epiphyseal cartilage growth plate of uraemic rats. Nephrology Dialysis Transplantation *11*, 2008 - 2016.

Ureña, P., Iida-Klein, A., Kong, X. F., Jüppner, H., Kronenberg, H. M., Abou-Samra, A. B., and Segre, G. V. (1994a). Regulation of parathyroid hormone (PTH)/PTH-related peptide receptor messenger ribonucleic acid by glucocorticoids and PTH in ROS 17/2.8 and OK cells. Endocrinology *134*, 451-456.

Ureña, P., Kong, X. F., Abou-Samra, A. B., Jüppner, H., Kronenberg, H. M., Potts, J. T., Jr, and Segre, G. V. (1993). Parathyroid hormone (PTH)/PTH-related peptide receptor messenger ribonucleic acids are widely distributed in rat tissues. Endocrinology *133*, 617-623.

Ureña, P., Kubrusly, M., Mannstadt, M., Hruby, M., Trinh, M. M., Silve, C., Lacour, B., Abou-Samra, A. B., Segre, G. V., and Drüeke, T. (1994b). The renal PTH/PTHrP receptor is down-regulated in rats with chronic renal failure. Kidney Int *45*, 605-611.

Usdin, T. B. (2000). The PTH2 receptor and TIP39: a new peptide-receptor system. Trends in Pharmacological Sciences *21*, 128-130.

Usdin, T. B., Bonner, T. I., and Hoare, S. R. J. (2002). The parathyroid hormone 2 (PTH2) receptor. Recept. Channels *8*, 211-218.

Usdin, T. B., Bonner, T. I., Harta, G., and Mezey, E. (1996). Distribution of parathyroid hormone-2 receptor messenger ribonucleic acid in rat. Endocrinology *137*, 4285-4297.

Usdin, T. B., Gruber, C., and Bonner, T. I. (1995). Identification and Functional Expression of a Receptor Selectively Recognizing Parathyroid Hormone, the PTH2 Receptor. Journal of Biological Chemistry *270*, 15455 -15458.

Usdin, T. B., Wang, T., Hoare, S. R., Mezey, E., and Palkovits, M. (2000). New members of the parathyroid hormone/parathyroid hormone receptor family: the parathyroid hormone 2 receptor and tuberoinfundibular peptide of 39 residues. Front Neuroendocrinol *21*, 349-383.

Vilardaga, J.-P., Romero, G., Friedman, P. A., and Gardella, T. J. (2011). Molecular basis of parathyroid hormone receptor signaling and trafficking: a family B GPCR paradigm. Cell. Mol. Life Sci *68*, 1-13.

Wada, N., Maeda, H., Tanabe, K., Tsuda, E., Yano, K., Nakamuta, H., and Akamine, A. (2001). Periodontal ligament cells secrete the factor that inhibits osteoclastic differentiation and function: the factor is osteoprotegerin/osteoclastogenesis inhibitory factor. J. Periodont. Res *36*, 56-63.

Wang, B., Bisello, A., Yang, Y., Romero, G. G., and Friedman, P. A. (2007). NHERF1 regulates parathyroid hormone receptor membrane retention without affecting recycling. J. Biol. Chem *282*, 36214-36222.

Wang, B., Yang, Y., Abou-Samra, A. B., and Friedman, P. A. (2009). NHERF1 regulates parathyroid hormone receptor desensitization: interference with beta-arrestin binding. Mol. Pharmacol *75*, 1189-1197.

Watson, P. H., Fraher, L. J., Hendy, G. N., Chung, U. I., Kisiel, M., Natale, B. V., and Hodsman, A. B. (2000). Nuclear localization of the type 1 PTH/PTHrP receptor in rat tissues. J. Bone Miner. Res *15*, 1033-1044.

Wheeler, D., Sneddon, W. B., Wang, B., Friedman, P. A., and Romero, G. (2007). NHERF-1 and the Cytoskeleton Regulate the Traffic and Membrane Dynamics of G Protein-coupled Receptors. Journal of Biological Chemistry *282*, 25076 - 25087.

Whitfield, J. F., Isaacs, R. J., Chakravarthy, B., Maclean, S., Morley, P., Willick, G., Divieti, P., and Bringhurst, F. R. (2001). Stimulation of protein kinase C activity in cells expressing human parathyroid hormone receptors by C- and N-terminally truncated fragments of parathyroid hormone 1-34. J. Bone Miner. Res *16*, 441-447.

Wong, S. K.-F. (2003). G protein selectivity is regulated by multiple intracellular regions of GPCRs. Neurosignals *12*, 1-12.

Xie, L. Y., Leung, A., Segre, G. V., Yamamoto, I., and Abou-Samra, A. B. (1996). Downregulation of the PTH/PTHrP receptor by vitamin D3 in the osteoblast-like ROS 17/2.8 cells. Am. J. Physiol *270*, E654-660.

Yaghoobian, J., and Drüeke, T. B. (1998). Regulation of the transcription of parathyroid-hormone/parathyroid-hormone-related peptide receptor mRNA by dexamethasone in ROS 17/2.8 osteosarcoma cells. Nephrol. Dial. Transplant. *13*, 580-586.

Yamamoto, I., Shigeno, C., Potts, J. T., Jr, and Segre, G. V. (1988). Characterization and agonist-induced down-regulation of parathyroid hormone receptors in clonal rat osteosarcoma cells. Endocrinology *122*, 1208-1217.

Yamashita, Y., Sato, M., and Noguchi, T. (1987). Alkaline phosphatase in the periodontal ligament of the rabbit and macaque monkey. Arch. Oral Biol *32*, 677-678.

Zhang, X., Schuppan, D., Becker, J., Reichart, P., and Gelderblom, H. R. (1993). Distribution of undulin, tenascin, and fibronectin in the human periodontal ligament and cementum: comparative immunoelectron microscopy with ultra-thin cryosections. J. Histochem. Cytochem *41*, 245-251.

Zhou, A. T., Assil, I., and Abou-Samra, A. B. (2000). Role of asparagine-linked oligosaccharides in the function of the rat PTH/PTHrP receptor. Biochemistry *39*, 6514-6520.

6 ABBREVIATIONS

℃	degrees centigrade
µg	micro grams
µl	micro litre
µM	micro molar
µm	micro meter
a.a.	amino acids
APS	ammonium per sulfate
ATP	adenosine triphosphate
BCA	bicinchonic acid
bp	base pairs
BSA	bovine serum albumin
cAMP	cyclic adenosine monophosphate
cDNA	complementary deoxyribonucleic acid
cm	centimeter
DAB	diaminobenzidine
DAPI	4', 6-Diamidino-2-phenylindole
ddH2O	double distilled water
dNTP	deoxynucleotide triphosphate
DMEM	dulbecco´s modified Eagle’s medium
DMSO	dimethyl sulphoxide
DNA	deoxyribonucleic acid
ECL	enhanced chemiluminescence
EDTA	ethylene diamine tetra acetic acid
ELISA	enzyme linked immunosorbant assay
FACS	fluorescence actovated cell sorter
FBS	fetal bovine serum
FITC	fluorescein isothiocyanate
gm	grams
GPCR	G-protein coupled receptors
GTP	guanosine triphosphate
HRP	horse radish peroxide
h	hour

IBMX	3-isobutyl-1-methylxanthine
kb	kilo bases
K_d	dissociation constant
kDa	kilodalton
kg	kilogram
kV	kilovolts
L	litre
M	molar
mg	milligrams
min	minute(s)
ml	milliliter
mM	millimolar
mm	millimeter
ng	nanograms
nm	nanometer
mRNA	messenger ribonucleic acid
O.D	optical density
PCR	polymerase chian reaction
pM	picomolar
PKA	protein kinase A
PKC	protein kinase C
PTH	parathyroid hormone
PTH1R	parathyroid hormone receptor 1
PLC	phospholipase C
RT	room temperature
rpm	rounds per minute
TBE	tris-borate-EDTA
TBS	tris-buffered saline
TRITC	tetramethylrhodamine isothiocyanate

7 LIST OF FIGURES

8 LIST OF TABLES